OPTIMIZATION OF THE LEAD-ACID BATTERY DISCHARGE CAPACITY USING ALTERNATIVE ELECTROLYTES FROM NATURAL PLANT EXTRACTS

BY

VITUMBIKO NUNDWE

A Thesis Submitted to the School of Engineering, Department of Energy Engineering in Partial Fulfilment of the Requirements for the Degree of Master of Science in Energy Studies

Moi University

2023

DECLARATION

Declaration by Candidate

This thesis is my original work and has not been presented for a degree in any other University. No part of this thesis may be reproduced without the prior written permission of the author and/or Moi University.

Sign:_____ Date:_____

Vitumbiko Nundwe:

MS/MES/5510/21

Declaration by Supervisors

This thesis has been submitted for examination with our approval as university supervisors.

Sign:_____ Date:_____

Prof. Eng Augustine Makokha

(Moi University, Eldoret, Kenya)

Sign:_____ Date:_____

Prof. Josphat Igadwa Mwasiagi

(Moi University, Eldoret, Kenya)

DEDICATION

I, therefore, dedicate this work to myself, to the dream, sleepless nights, labours, the loneliness and endless hunger to learn new things – I wrote this thesis for myself and all the things that inspired me to embark on this journey.

ACKNOWLEDGEMENTS

I would like to extend my profound gratitude to my supervisors, Eng. Prof. Augustine B. Makokha and Prof. Josphat Igadwa Mwasiagi whose invaluable guidance and research expertise guided me to the completion of this thesis, I shall forever remain indebted. I am also thankful to friends and family for the academic and moral support throughout the entire journey.

ABSTRACT

Lead-acid batteries present an innovative strategy to aid the integration and adoption of renewable energy sources. The build-up of inert lead compounds on the negative electrode is the main obstacle to a longer life span for these batteries. The main objective of this study was to optimize the discharge capacity of the flooded lead-acid battery using electrolyte additive from natural plant extracts. The specific objectives were to; develop electrolyte additive from natural plant extracts; evaluate the electrochemical potential of the electrolyte solutions; evaluate and compare the battery discharge capacity of electrolyte with plant derived additive versus conventional electrolyte; and determine optimum additive amount. Extracts from Calyces of *Hibiscus Sabdariffa* and leaves of *Bidens Pilosa* were obtained by a decoction procedure using distilled water. The aqueous plant extracts were mixed with conventional dilute battery sulfuric acid in concentrations of 15.86% (w/v), 10% (w/v), 44% (w/v) and 30% (w/v) while one electrolyte solution was maintained with 100 percent dilute battery sulfuric acid. Evaluation of the electrochemical potential of the electrolyte solutions was done using a floating hydrometer to measure the specific gravity of the electrolyte solutions and results varied between a maxima of 1170 kg/m^3 to 1220 kg/m^3 and the minima varied between 1140 kg/m^3 and 1160 kg/m^3 within which the highest electrochemical activity was achieved. The evaluation of the discharge capacity was done by comparing discharge cycles, coulombic efficiency, and energy efficiency. The highest recorded discharge duration was 4.63 hours in the 15.86% (w/v) Roselle additive-electrolyte solution, 0.13 hours longer than the conventional electrolyte. The highest coulombic efficiency in 44.14% (w/v) *Hibiscus Sabdariffa* additive electrolyte solution was 97.3% and 94.6% in 15.86% (w/v) *Bidens Pilosa* electrolyte compared to 87.3% in conventional electrolyte. In terms of energy efficiency, the highest value in 44.14% (w/v) *Hibiscus Sabdariffa* additive electrolyte solution was 83.8% and 81.3% for 15.86% (w/v) *Bidens Pilosa* electrolyte compared to 74.9% in conventional electrolyte. Optimal additive parameters, 44.14%(w/v) *Bidens Pilosa*, 15.86% (w/v) *Bidens Pilosa*, 15.86% (w/v) *Hibiscus Sabdariffa*, were determined by a numerical optimization procedure using the experimental data. The results from this study show that bio-active compounds present in *Hibiscus Sabdariffa* and *Bidens Pilosa* aqueous extracts can be used as electrolyte additive to influence the discharge capacity of the lead-acid battery without altering the chemical composition of the battery active materials. In conclusion, the phytochemicals present in the extracts from *Bidens Pilosa* and *Hibiscus Sabdariffa* can be used to enhance the discharge capacity of lead-acid battery. It is recommended that plant extracts should be incorporated in lead-acid battery technology as alternative electrolytes to improve the battery discharge capacity whilst minimizing usage of chemical based conventional electrolytes.

TABLE OF CONTENTS

LIST OF TABLES

LIST OF FIGURES

ABBREVIATIONS AND ACRONYMS

BES	Battery Energy Storage
Blackjack	*Bidens Pilosa*
EES	Electrochemical Energy Storage
$H_3 PO_4$	Phosphoric acid
NAM	Negative Active Material
PAM	Positive Active Material
Pb	Lead
PbO_2	Lead Dioxide
$PbSO_4$	Lead Sulfate
PV	Photovoltaic
Roselle	*Hibiscus Sabdariffa L.*
VRLA	Valve Regulated Lead-Acid

CHAPTER 1: INTRODUCTION

1.1 Background

Energy storage is considered a key enabling technology to ensure wide adoption of renewable energy sources and therefore demands dependable backup sources. It is also preferable that the backup facility is not of further primary generation but rather of storage type (Leahy et al., 2010). Battery storage presents a mature technology with a market presence consisting of a variety of suppliers providing reliable systems to aid the integration of renewable energy (IRENA, 2015). The electricity industry has yet to fully integrate battery storage as a mainstream alternative due to a few performance and safety-related concerns, many of which can be resolved.

There are several uses for lead acid batteries, including in PV off-grid systems, which typically include a PV generator, charge controller, and battery (Vetter & Rohr, 2014). Because lead-acid battery technology is advanced, they are known for their simple production process and affordable prices. Lead acid batteries also have low cost per watt hour, high specific power, the ability to withstand large discharge currents, and there is no requirement for a cell-wise battery management system (*BU-201*, 2010). However, a comparison of important battery parameters which influence important performance elements for various batteries technologies shows that lead-acid rank poorly in against the criterion which includes energy density; round trip efficiency; life span and eco-friendliness. Such performance elements as life span has the biggest impact in reviewing economic efficiency (Asian Development Bank, 2018).

Despite the fact that electrochemical energy storage systems like the lead-acid battery have been around for a while, there are still significant gaps in our understanding of the intricate and often interlinked mechanisms that control how they work. (Goodenough et al., 2007). The lead-acid battery's performance and design have seen numerous

changes over the years, yet the battery still has issues that need to be resolved. One strategy that has improved key battery properties is the incorporation of additives to active battery components. Additives are substances that are added in varying amounts to a specific product in a bid to have significant positive effects on the qualities of the final product. Various studies have investigated the use of additives in Lead-acid batteries; however, none have accomplished significant results to warrant wide adoption. The ultimate goal is to choose an appropriate addition that is chemically, electrochemically, and thermally stable in an environment that is susceptible to corrosion. (Bhattacharya & Basumallick, 2003; Paglietti, 2016; Pavlov, 2017a).

Sustainable energy sources are considered vital in efforts to curtail effects of fossil fuels on the environment as can be observed in the increased consideration of renewable resources in the design of battery active materials that could potentially enable achievement of green batteries(Liedel, 2020). Whether the lead acid battery can be made completely sustainable is a question that can only be answered with extensive research, Armand and Tarascon (Armand & Tarascon, 2008) envisioned batteries made from renewable resources and such the quest to achieve this feat continues.

1.2 Problem Statement

Wet cell batteries are predominantly used for providing back-up to variable renewable energy sources but are constrained by longevity and costs issues(Asian Development Bank, 2018; Denholm et al., 2010). The dominant issue limiting lead-acid batteries from having a longer life span is the accumulation of inert lead compounds on the negative electrode, which results in the formation of a coating that results in lower battery discharge amp-hour capacity.(Pavlov, 2017a; Zhang et al., 2010). The structure of the active materials undergoes partial disintegration during discharge and are restored when charging, however, formation of inert lead compounds ($PbSO_4$) crystals

also proceeds slowly, an irreversible process resulting in the passivation of the electrode which affects the cycle life of the battery (Pavlov, 2017a). To speed up the dissolution of the lead compounds ($PbSO_4$) and facilitate electron transport on the negative plates during charge and discharge of the lead-acid cell, additives can be added to the electrolyte.

There is still a lot of room to increase the performance of the lead acid battery despite the application and usage of numerous and different additives (Asian Development Bank, 2018; Goodenough et al., 2007; Pavlov, 2017c). Therefore, this study aims to utilize natural plants extracts as additive material to optimize the discharge capacity of the lead-acid battery.

1.3 Research Objectives

The main objective of this study is to optimize the discharge capacity of the flooded lead-acid battery using electrolyte additive from natural plant extracts.

1.4 Specific Objectives

The study has the following specific objectives.

1. To develop electrolyte additive from natural plant extracts
2. To evaluate the electrochemical potential of the electrolyte solutions
3. To evaluate and compare the battery discharge capacity of electrolyte with plant derived additive versus conventional electrolyte.
4. Determine optimum additive amounts.

1.5 Justification of the Study

Incorporating additives into the battery's active components has been one approach to sulfation, the most prevalent issue with lead acid batteries that causes lead compounds to crystallize on the negative electrode (Posada et al., 2017). Certain additives have

been recorded to improve certain characteristics for the lead acid battery, nonetheless, there remains a huge gap that needs innovative solutions in order to achieve high efficiency electrochemical storage. Modern storage facilities require longer life spans with multiple charge-discharge cycles with minimal loss of performance (Goodenough et al., 2007), and as such incorporating biomass derived battery components as well as building organic batteries from biomass is a promising alternative towards truly sustainable storage (Liedel, 2020). The future battery storage facility must not only ensure long life spans but should also ensure practical approaches in the fabrication of components that guarantee minimal environmental effects and are realized at reasonable costs.

CHAPTER 2: LITERATURE REVIEW

2.1 Overview

In 1859, Gaston Planté was credited with developing the first practical rechargeable battery by fusing a Pb|$PbSO_4$ electrode with a $PbO_2|PbSO_4$ electrode in a sulfuric acid electrolyte to create an electrochemical power source. (Kurzweil, 2010). When a lead-acid battery's electrodes are connected to an electrical load, chemical energy is transformed into electrical energy, which causes an electric current to flow through the conductor (Pavlov, 2017b). The lead lead-acid cell operates by using the processes of lead oxidation at the anode and lead dioxide reduction at the cathode. The electrochemical reactions processes occur as indicated by equation (1) during discharge, lead oxide is reduced to Pb^{2+} (Posada et al., 2017);

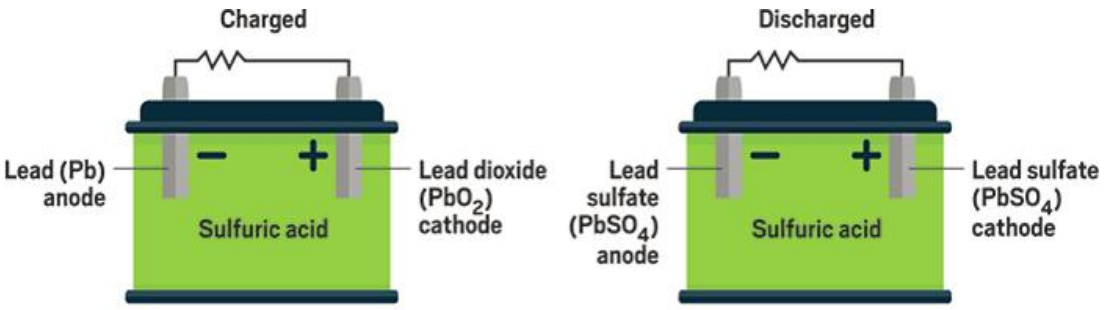

Figure 2.1: Schematic of the Lead-acid battery(KITARONKA, Sefu, 2022)

$$PbO_2 + 4H^+ + 2e^- \leftrightarrow Pb^{2+} + H_2O \qquad E^0 = 1.46V \ \ldots\ldots\ldots\ldots\ldots \textit{Equation 1}$$

The Pb^{2+} ions then precipitate in the form lead sulfate,$PbSO_4$, as shown in equation (2);

$$Pb^{2+} + {SO_4}^{2+} \leftrightarrow PbSO_4 \ \ldots\ldots\ldots\ldots\ldots\ldots\ldots \textit{Equation 2}$$

According to equation (3), the metallic lead at the anode undergoes oxidation as shown;

$$Pb \leftrightarrow Pb^{2+} + 2e^- \qquad E^0 = -0.13V \ \ldots\ldots\ldots\ldots \textit{Equation 3}$$

2.2 Fundamental processes during charge/ discharge of the lead-acid battery

The transfer of electrons at the electrodes causes the basic electrochemical reactions that ultimately result in the creation of a layer of lead sulfate compounds (Pavlov, 2011) .These phenomena are discussed in detail below;

2.2.1 Fundamental processes during cell discharge

The lead-acid cell goes through the following processes when it is connected to a load;

2.2.1.1 Reactions at the cathode

The oxidation of lead (Pb) commences as a result of anodic polarization at the cathode surface;

$$Pb \rightarrow Pb^{2+} + 2e^{-} \quad \text{.....Equation 4}$$

The Pb^{2+} ions then react with the HSO_4 ions from the H_2SO_4 to form $PbSO_4$ molecules:

$$Pb^{2+} + H_2SO_4 \rightarrow PbSO_4 + 2H^{+} \quad \text{..... Equation 5}$$

The reaction depicted in *equation 1* releases electrons, which travel in the direction of the positive electrode via an external electric circuit. The H^{+} ions released by reaction (equation 2) drift through the electrolyte towards the anode. The lead-sulfate molecules that are obtained in equation 2 accumulate and grow into lead sulphate crystals on the lead surface. These electrochemical processes are summarized and expressed by equation 6:

$$Pb + H_2SO_4 \rightarrow PbSO_4 + 2H^{+} + 2e^{-} \quad \text{..... Equation 6}$$

The reactions at the cathode releases electrons that travel along the electric circuit to reach the anode. The potential difference between the anode and the cathode drives the H^{+} ions towards the positive electrode.

2.2.1.2 Electrochemical reactions at the anode.

The lead dioxide particles that are in contact with the dilute sulfuric acid electrolyte at the anode undergo partial hydration as shown by the following expression:

$$PbO_2 \cdot PbO_2 + H_2O \rightarrow PbO_2 \cdot PbO(OH)_2 \quad \ldots\ldots\ldots\ldots \textit{Equation 7}$$

Lead dioxide particles comprise crystal zones (PbO_2) and hydrated zones ($PbO(OH)_2$) which are in equilibrium. The electrochemical reactions proceed in the hydrated zones. The processes of PbO_2 reduction take place in the hydrated zones of the lead dioxide particles under the influence of electrons from the negative electrode.

At the anode, there are partially hydrated lead dioxide zones $PbO(OH)_2$ which are in equilibrium with crystal regions of PbO_2. Electrochemical reactions in the hydrated zones result in the reduction of the PbO_2 to form PbO. This reaction involves electrons migrating from the cathode and the H+ moving from the same electrode.

$$PbO_2 \cdot PbO(OH)_2 + e^- + H^+ \rightarrow PbO_2 \cdot PbO(OH)_2 + H20 \ldots\ldots\ldots\ldots \textit{Equation 8}$$

$$PbO_2 \cdot PbO(OH)_2 + e^- + H^+ \rightarrow PbO_2 \cdot PbO + H_2O \ldots\ldots\ldots\ldots\ldots \textit{Equation 9}$$

Lead sulfate ($PbSO_{4)}$ is formed because of the reaction of PbO and the sulfuric acid electrolyte according to the following

$$PbO_2 \cdot PbO + H_2SO_4 \rightarrow PbO_2 + PbSO_4 + H2O \ldots\ldots\ldots\ldots\ldots\ldots \textit{Equation 10}$$

These processes result in the generation of in the lead-acid cell along with water. The water is formed as result of the reaction of H^+ions shown in *equation 2* and O^{2-}ions which are obtained from the reduction of PbO_2.

As electrochemical reactions proceed, the size of the lead sulphate crystals also grows. The lead sulphate crystals are inert compounds which reduce the active surface area of

the anode and cathode resulting in the decrease of the cell voltage and consequently the end of discharge of the cell.

The lead electrodes are semi-solid structures whose pores allow the flow of H_2SO_4 and H_2O. The growth of the crystal lead sulphate layer reduces the diameters of the pores thereby impeding the transportation of the dilute sulfuric acid within the active material (Catherino et al., 2004; Pavlov, 2011).

2.2.2 Fundamental processes during charge cycle

To charge the lead-acid cell, a power source with an output voltage of 0.3 – 0.5 V higher than the voltage of the cell in the discharged state is connected to the terminals. This results in the reversal of the electrochemical reactions during the discharge cycle.

2.2.2.1 Reactions at the anode

The following equations represent the chemical reactions at the anode during the charge cycle.

$$PbSO_4 + 2H_2O \rightarrow PbO_2 + H_2SO_4 + 2H^+ + 2e^- \quad \text{Equation 11}$$

$$PbSO_4 \rightarrow Pb^{2+} + SO_4^{2-} \quad \text{Equation 12}$$

During charge, the Pb^{2+} ions are adsorbed at the positive electrode and as such proceeds the process of electron transfer:

$$Pb^{2+} \rightarrow Pb^{4+} + 2e^- \quad \text{Equation 13}$$

The Pb^{4+} ions are unstable, they react with water to form $Pb(OH)_4$ as shown in *equation 14*.

$$Pb^{4+} + 4H_2O \rightarrow Pb(OH)_4 + 4H^+ \quad \text{Equation 14}$$

Subsequent reactions are presented below by *equation 15* and *16*:

$$Pb(OH)_4 \rightarrow Pb(OH)_2 + H_2O \quad \text{Equation 15}$$

$$Pb(OH)_2 \rightarrow PbO_2 + H_2O \quad \ldots\ldots\ldots\ldots\ldots\ldots\ldots\ldots \quad \textit{Equation 16}$$

The SO_4^{2-} ions which remain in the electrolyte (see equation 9), react with H^+ions to form H_2SO_4 thus neatralizing the charge of the SO_4^{2-}.

$$SO_4^{2-} + 4H^+ \rightarrow H_2SO_4 \quad \ldots\ldots\ldots\ldots\ldots\ldots\ldots\ldots \quad \textit{Equation 17}$$

2.2.2.2 Reactions at the cathode

During the charging of the lead-acid cell, electrochemical processes at the negative electrode proceed and result in the formation of Pb atoms which combine with the lead crystals on the surface of the electrode;

$$Pb^{2+} + 2e^- \rightarrow Pb \quad \ldots\ldots\ldots\ldots\ldots\ldots\ldots \quad \textit{Equation 18}$$

Sulfuric acid (H_2SO_4) is formed by the neutralization of sulphate ions by H^+ions migrating from the anode as shown by the following reaction.

$$SO_4^{2-} + 2H^+ \rightarrow H_2SO_4 \quad \ldots\ldots\ldots\ldots\ldots\ldots \quad \textit{Equation 19}$$

As the charge process continues, new quantities of the lead sulfate are dissolved until the entire amount is consumed. The capacity of the cell is thus restored as the concentration of the dilute sulfuric acid increases along with the other active materials.(Pavlov, 2011).

2.3 Battery Classification, Specification, and Parameters

A common method of classifying lead-acid batteries depends on the amount and condition of the electrolyte. The classes of lead-acid batteries include: Flooded electrolyte batteries; low-maintenance batteries; absorptive glass mat (AGM) batteries; gel electrolyte batteries (Pavlov, 2017b). These batteries are defined by variables that characterize operating conditions and describe specifications set by manufacturers and

the ones pertinent to this study include basic concepts such as the C and E rates, battery condition and technical specifications (MIT, 2008).

2.3.1 Basic terms and technical specifications

2.3.1.1 C and E rates

The C rate is a method for indicating the charge/discharge current of the battery. It is however often used to measure the rate of discharge of a battery relative to its maximum capacity(Linden & Reddy, 2002; MIT, 2008). The C rate can be expressed as

$$I = M \times C_n$$

Where I = current in amperes

$C_n =$ Rated capacity (ampere-hours)

$n =$ is the time base (h) for rated capacity.

$M =$ Fraction of C

E rate on the other hand is used to express charge/discharge rate in terms of power. The E rate can be expressed as

$$P = M \times E_n$$

Where $P = power\ (W)$

$E = rated\ energy\ (Wh)$

$n = time\ in\ hours$

$M = fraction\ of\ E$

2.3.2 Battery condition

2.3.2.1 The depth of discharge

The depth of discharge is an expression for defining the amount of charge removed from the battery at a particular state (Q_d) relative to the total amount of charge which the battery is capable to store and is expressed as a percentage (Waag & Sauer, 2009):

$$DoD = \frac{removed\ amount\ of\ charge\ Q_d}{maximum\ available\ amount\ of\ charge\ (C)} \times 100\%$$

2.3.2.2 State of charge

The state of charge indicates the battery capacity as a percentage of the maximum capacity and is expressed as;

$$SOC = \frac{Available\ capacity\ (Ah)}{Rated\ capacity\ (Ah)} \times 100\ \%$$

It is of vital importance that the true indication of this parameter is known in order to maximize the utilization of the battery. Various techniques are used to determine the electrochemical potential of the lead acid battery are discussed by Deepti & Ramanarayanan (Deepti & Ramanarayanan, 2006) and include: measurement of specific gravity; Measurement of open circuit voltage; current integration method and; impedance measurement method. However, for this study we will only discuss the first two methods because of their simplicity and reliability.

2.3.2.2.1 Specific gravity method

In order to achieve optimum performance, the lead-acid battery operates with dilute H_2SO_4 solutions of concentrations between 1.11 gcm^{-3} on deep discharge and 1.28 gcm^{-3} when fully charged which results in an open circuit cell voltage range of 2.15 V – 1.95 (Pavlov, 2017b). The specific gravity measurement is an electrochemical method used to model the performance of the lead acid battery by measuring the

concentration of sulfuric acid in the electrolyte (Deepti & Ramanarayanan, 2006; Megateli et al., 2015). The state of charge can therefore be determined using a float hydrometer.

Variations in specific gravity are caused by chemical reactions that occur in charge/discharge cycles of the battery. As shown by works done by several researchers, sulfuric acid is consumed during discharge and the electrolyte solution becomes more dilute up to 16 wt% and relative density of 1.11 gcm^{-3}, the regeneration of the acid then occurs during charge and the concentration rises up to 38 wt% and relative density of 1.28 gcm^{-3} (Linden et al., 2019; Pavlov, 2017b; Perry & Green, 2008).

Megateli et al., studied the evolution of electrolyte specific gravity using a charge/discharge protocol and showed that successive charge/discharge cycles results in the variation of the maxima and minima of specific gravity. This is attributed to the physio-chemical mechanisms during the battery operation.

2.3.2.2.2 Open circuit voltage method

The voltage difference between the terminals of the lead-acid battery when no load is connected is what is known as the open circuit voltage. It is a parameter used to estimate the state of charge of the lead acid battery. This expression defines the concentration of sulfuric acid near the electrodes of the battery. It is a simple to use method with the major disadvantage being that it is hard to implement for practical use since it is done offline (Al Hadi et al., 2019; Deepti & Ramanarayanan, 2006; MIT, 2008).

2.3.3 Modes Failure in Lead acid batteries

2.3.3.1 Positive-plate expansion

Repetitive discharge and recharging of the lead-acid battery may lead to the expansion of the anode. The anode's expansion in the plane can be recovered after recharge, but

not to its initial volume. The negative plate does not show the same tendency to expand. The increase in charge/discharge cycles escalates the expansion of the positive plate and consequently affects the current-collection process. The electrical performance of the battery is lowered and disintegration of the active material structure slowly occurs (Rand & Moseley, 2015).

2.3.3.2 Water loss

Water loss is defined expressed as a function of the condition of the electrolyte from a flooded state to an insufficient state. It can be caused by factors such as leakage of water through the battery housing, inefficiencies in the recombination of oxygen, and corrosion in the grid of the positive plate (Chalasani, 1998).

In addition, overcharging the lead-acid cell leads to the overproduction of hydrogen and oxygen. This has the potential of causing excessive heating because of the reduction in the volume of the electrolyte and consequently results in increased rate of water loss. The presence of impurities also strongly influences the propensity of a battery to gas (Rand & Moseley, 2015).

2.3.3.3 Acid stratification

This refers to the collection of acid at the base of the lead-acid cell. A vertical concentration gradient of acid can be created during recharge, such that it results in sulfuric acid of higher concentration and greater relative density in and around the plates. As a result, there is a non-uniform usage of the battery active materials which leads to the formation of irreversible $PbSO_4$. Acid stratification also leads corrosion on the positive grid of the lead-acid cell (Rand & Moseley, 2015).

2.3.3.4 Corrosion

Corrosion occurs when lead intermingles with oxygen which has diffused through the thick oxide layer. For the positive grid, corrosion is influenced by the arrangement and structure of the grid material, potential of the plate, composition of the electrolyte, and temperature. The corrosion gives rise to an electrically resistive product by comparison to the grid which causes a decrease in the output of the lead-acid cell. In some instances, the grid breaks down and can also result in collapse of the plate (Rand & Moseley, 2015). Terminals corrosion can also be caused by addition of excessive topping water to the cells, poor sealing of batteries, loose vent caps or float guide, spillage of electrolyte, direct connection of bare wires to battery terminals, terminals that are loosely connected and lack of application of petroleum jelly for protection (Exide Industries, 2022).

2.3.3.5 Sulfation

Chemical reactions in lead-acid battery occurring at the electrodes surfaces result in formation of Lead (Pb^{2+}) ions and a $PbSO_4$ layer which covers the surface of the lead-acid cell active materials. Because the lead sulfate precipitate is inert, it passivates the anode and the cathode, making them unreactive. The performance of the battery hence its characteristics are therefore determined by the size of contact area on the surface of the active materials where the reactions occur (Pavlov, 2017a).

The lead-acid battery has three active materials namely, lead (Pb), lead oxide (PbO_2), and sulfuric acid (H_2SO_4). On discharge, the capacity of the lead-acid cell is most often affected by the active material with the biggest usage coefficient. During the discharge process, sulfuric acid (H_2SO_4) reacts with the other active materials (Pb and PbO_2) and is therefore consumed to form lead sulfate ($PbSO_4$) precipitate on both the electrodes (Pavlov, 2017c), a process which should be reversible during charge.

However, irreversible processes which compromise the electrodes also proceed at a slower rate, one of which is a phenomenon widely known as sulfation.

The occurrence and concept of sulfation is described in various ways by Catherino et al . (Catherino et al., 2004); First, it is defined as the general cause of lead-acid battery performance collapse, which is manifested by capacity loss, voltage loss, an increase in internal resistance, and a reduction in sulfuric acid concentration. it is further defined as the re-crystallization e-crystallization of lead sulfate into an inert form that doesn't participate in the charge/discharge process. Finally, sulfation is defined as the chemical reaction that produces sulfates.

The overall energy storage reaction of the lead-acid cell is shown below.

Discharge process $\Rightarrow Pb$(s) + PbO_2(s) + $2H_2SO_4$ (aq)

$\leftrightarrow$ 2 $PbSO_4$(s) + 2 H_2O (liq) $\Leftarrow$ charge process…… *Equation 20*

The oxidation reaction at the lead alloys material results in the generation of the inert and insoluble $PbSO_4$ which causes the electrode surfaces to become unreactive, an inevitable occurrence and a phase which can be temporary or result in the formation of a final product (Yu & O'Keefe, 2002).

2.4 Use of additives and Influence on Battery Performance

Important battery performance characteristics such as the capacity, energy, and power output depend on the rate at which electrical energy is converted into chemical energy and vice versa. Since electrochemical reactions occur at the interface of the lead electrode surface and the electrolyte solution, the amount of contact surface area therefore determines the performance of the lead-acid battery (Pavlov, 2017a).

The performance characteristics of the battery can be improved by making sure that the electrochemical reactions of the lead-acid cell advance into the inner depth of the lead

electrodes. It is therefore desirable that the inert lead sulfate layer that accumulates on the surface of the electrodes should be highly porous to involve a thick layer of electrode active in the chemical reaction process.

The use of additives in the lead acid battery has been attempted by various researchers as a possible method to improve the specific energy by attempting to enhance the usage of the active materials. Various attempts have introduced additives to the electrolyte in order to improve the reversal of the lead sulfate compounds, their main goal is to increase the dissolution rate of lead sulfate ($PbSO_4$) and improve charge acceptance at the negative electrode by accelerating transfer of electrons (Pavlov, 2017a).

Additives are known to adsorb to the battery active components which either alters their morphology, chemical activity or consequently affects certain parameters of the lead acid battery. Various studies have shown that the specific adsorption of certain additives results in surface coverage of the electrode and thus alters the activity of the solid Pb. The chemical activity of the ${SO_4}^{2-}$ ions may also be altered because of the presence of additives in the electrolyte. Finally, the presence of additives may also change the morphology and activity of the $PbSO_4$ precipitate on the electrode surface (Bhattacharya & Basumallick, 2003; Pavlov, 2017a, 2017c). The quantity of additives in the product's formulation should be in the range of 0.02% to 2% of the total weight of the initial material but can in some cases exceed this range depending on obtained experimental results.

2.4.1 Additives to the pastes of battery plates

Materials called expanders were shown to be useful in preventing formation of an unreactive layer on the surface of the active materials and as resulted in improvement of the life and performance of the lead-acid battery. The main principal ingredients of

expanders are barium sulfate, lignosulfonate and carbon black. Each of these ingredients performs a specific function in the operation of the negative plate. The expander components increase the surface area by means of adsorption on the lead surface which results in the formation of a porous sulfate layer. This action stabilizes the structure of the negative active material (Boden, 2004; Pavlov, 2017a).

Addition of expanders to the negative paste material can be accomplished in several ways which may involve the separate components being mixed with the paste during preparation or by pre-mixing before addition. The battery manufacturer is responsible for pre-mixing these components. Manufacturers of expanders also perform this activity.

2.4.1.1 Effect of expander organic component on the electrochemical Processes

A comprehensive account of expander technology is given by Boden and Pavlov (Boden, 2004; Pavlov, 2017a) and define lignosulfate, the organic consituent of the expander material, as chemically treated lignins and its derivatives. They contain active structural groups which influence in different ways the processes involved in the formation and fragmentation of the negative active material structure. Phenolic groups showed a positive effect on the characteristics of the negative plate, by changing the behavior of the second hydroxyl group and enhancing their effect in the order ortho, meta, and para. Other structural groups such as carboxylic and ketonic groups showed little benefit on the behavior of the expander. It terms of battery efficiency; aldehyde groups were shown to significantly improve this parameter for the lead-acid battery.

Quinones and their derivatives have also been investigated for their well-pronounced expander properties. The pyrocatechol structural groups, which are a constitutive part

of the lignin structure, have been shown to have a beneficial effect on battery performance.

However, although the capacity of the Pb|$PbSO_4$ in lead-acid cells is improved, the organic expander slows down the reduction of $PbSO_4$ to Pb. The properties that have an effect of expander behavior include its molecular weight, chemical structure, components purity, and chemical stability.

When discharging a lead-acid battery, some of the active groups in the expander are adsorbed on the surface of Pb or $PbSO_4$, while other groups are in direct contact with the solution. In this way they can thus dissociate and/or interact with the water molecules of the solvent. The expander structural groups do not form strong chemical bonds with the lead particles.

2.4.2 Classes of electrolyte additives

It is of vital importance that additives should possess stable chemical, thermal and electrochemical properties to withstand the acidic effect of H_2SO_4 if they are to improve the technological process of the product. Pavlov's book (Pavlov, 2017c) classifies electrolyte additives as inorganic compounds; carbons and; polymer emulsions.

2.4.2.1 Inorganic compounds

Examples of inorganic compounds used as additives include phosphoric acid, boric acid, citric acid, and other types of soluble metal sulfates. Phosphoric acid (H_3PO_4) is widely considered as a prominent additive and is claimed to reduce irreversible sulfation of the positive electrode along with lessening of shedding, prevent early capacity loss and yields stable capacity performance (El-Rahman et al., 2011; Wagner & Sauer, 2001), however, incorporation of this additive also facilitates the formation a

modified lead oxide (PbO_2) and of fine lead sulfate ($PbSO_4$) reduces the capacity of the positive plates (Garche et al., 1991; Meissner, 1997).

Variations of mixed additives have shown to improve the properties of phosphoric acid as an additive, for instance adding stannous sulfate ($SnSO_4$) and picric acid is known to slow down corrosion of the positive grid (Bhattacharya & Basumallick, 2003). An additive formula that contains phosphoric acid and colloidal silica improves the life cycle of the battery (Torcheux & Lailler, 2001).

Studies investigating the role of boric acid as an electrolyte additive in lead acid batteries, show that boric acid is beneficial as it prolongs battery life by hindering corrosion of the lead grids which is due to the formation of a dense structure of ${BO_3}^{3-}$. Results of their experiment also show that adding boric acid to the electrolyte increases the hydrogen evolution and oxygen evolution overpotential which in turn reduces water loss(Wu et al., 2020).

2.4.2.2 Carbons

The use of additive material constituting ultrafine carbon (UFC) and polyvinyl alcohol (PVA) was found to reduce the size of inactive $PbSO_4$ that accumulates on the cathode and converts it into its active form. It was also observed that an oxidized graphite aqueous solution improves the discharge capacity, charge acceptance and prolongs the life cycle of the battery by enhancing electrical contact of lead oxide (PbO_2) particles in the positive electrode (Kimura et al., 2000).

2.4.2.3 Polymer emulsions

Several substances have been shown to act as inhibitors of hydrogen evolution (Dietz et al., 1992) They are known to reduce water loss during cycling. These are organic substances and include by-products of benzaldehyde, benzoic acid and benzene.

Polymer materials have been studied and shown to influence the battery characteristics, these include; FORAFAC 1033D (polyfluoroalkyl sulfonic acid) which improves cycle life ,poly(N-vinylpyrrolidone) polymers (PVPs) which rather shows effective results when added to the electrodes rather than electrolytes (Karimi et al., 2006) and polyaspartate (PASP) which modifies the structure of the lead sulfate crystals (Petkova et al., 2006).

2.4.2.4 Mixed additives and others

2.4.2.4.1 Mixed additives

The impact of mixed additives to the electrolyte of the lead acid battery is discussed by Bhattacharya & Basumallick (Bhattacharya & Basumallick, 2003). Significant reduction of corrosion of the battery plates was discovered by using mixed additives of $H_3PO_4 + H_3BO_3$ and $H_3PO_4 + SnSO_4$. This conclusion was made by examining Tafel polarization curves, double layer capacitance and percentage inhibition efficiency. It was observed that the additives were adsorbed on the surface of electrodes and altered the structure of $PbSO_4$ layer.

2.4.2.4.2 Sulfates

Studies to determine the influence of sulfate compounds as additives to the electrolyte of the lead acid battery have shown a variety of results. Musei et al (Musei et al., 2021) explored the effect of lithium sulfate and zinc sulfate used as additives on the efficiency and cycle life of a 2V/20Ah lead acid battery. Unlike zinc sulfate whose contribution was insignificant to the performance of the battery, the lithium sulfate showed distinctive improvement in terms of the voltage efficiency. In a study by Onu et al (Onu et al., 2021) where they explored the effect of the use of aluminium sulphate and potassium sulphate in enhancing the charge cycle of a lead acid battery and concluded that these additives had no positive impact on the performance of the battery, however

in another study by Chen et al. (Chen et al., 2022) they discovered that aluminium sulfate significantly reduced sulfation and could also repair spent batteries effectively.

2.5 Biomass Based Battery Materials

Attempts have been made to introduce as well as increase the role of sustainable materials in battery construction, a concept to build batteries from renewable resources was previously envisioned by Armand & Tarascon, 2008 .Various approaches have since been described to tackle aspects such as composition; recycling ; and implementation (Lecce et al., 2017; Liedel, 2020; Mauger & Julien, 2017; Ordoñez et al., 2016).

2.5.1 Renewable carbon materials

Application of carbonized biomass based materials as electrodes for various battery technologies which include; Lithium-sulfur, lithium- serenium, lithium ion,lithium oxygen, and sodium ion batteries has been reviewed by Liedel (Liedel, 2020). Such materials have been derived from biomass wastes such as rice husks, corn/wheat straw, soybean residues, nutshells, wood chips, shrimp shells and many others. Apart from being used as the major composition of the electrodes, these materials can also be synthesized and used as additives and have shown to improve charge storage.

2.5.2 Non-carbon-based materials

Non-carbonized biomass-based organic electrodes have been used in construction of battery active materials from various biomass materials by researchers. Redox active biomolecules that are capable of participating in reversible oxidation and reduction reactions are described as promising electrode materials without undergoing any carbonization (Liedel, 2020).

2.5.2.1 Carboxylates

Sustainable biomass-based materials that have been investigated for their potential include carboxylates. Armand et al.(Armand et al., 2009) reported the use of terephthalates in the anode of lithium ion batteries. Use of other conjugated multi-carboxylates has been reported in potassium ion half-cell experiments (Deng et al., 2017).

2.5.2.2 Quinones and related carbonyls

Other naturally occurring compounds that are reported as promising electrode materials because of their redox potential are Quinones(B. Lee et al., 2018; Son et al., 2016; H. Wang et al., 2017). Catechols, for instance, which are found in many fruits may be oxidized to form o-benzoquinones according to Hammerstone et al. (Hammerstone et al., 2000) and can be used in organic redox flow batteries as electrolytes (Mukhopadhyay et al., 2018).

Naphthoquinones have reportedly been used for various electrochemical applications in sodium-ion batteries, as supercapacitors and in lithium ion batteries(J. Lee & Park, 2017; Miroshnikov et al., 2019; H. Wang et al., 2016).

2.5.2.3 Flavins and more pteridines

Flavins are a group of redox-active materials which have found application in redox flow batteries and as electrodes for bio-organic batteries (Tan & Webster, 2012). Pteridines have also been used and investigated for energy storage applications (Hong et al., 2014).

Eftekhari & Kim (Eftekhari & Kim, 2017) discuss some of the stability problems that arise from the usage of non-carbonized biomass- based organic electrode materials

despite their potential of redox-active biomolecules in lithium-ion and sodium ion batteries.

2.6 Taxonomy, Botanical properties and Adsorptive Properties of *Hibiscus Sabdariffa* and *Bidens Pilosa*

2.6.1 *Hibiscus Sabdariffa*

Hibiscus Sabdariffa is a widely grown plant in many countries and belongs to the *Malvaceae* family. It is known for its medicinal properties, as a delicacy and for its industrial applications. The different parts of the plant are rich in phytochemical compounds that are used in various applications, for instance, the leaves are utilized in traditional medicinal and therapeutic applications and are known for being diuretic, antiscorbutic and sedative among the many observed effects. Similarly, the calyces which are rich in carbohydrates, dietary fiber, minerals, proteins and bioactive compounds have variety of culinary, medicinal and therapeutic and industrial applications and benefits which include production of drinks, wines, jams, food coloring and food preservation (Pacôme et al., 2014; Riaz & Chopra, 2018).

2.6.1.1 Phytochemistry

Identification of plant compounds provides valuable insight into the composition and significance of the phytochemical components. Several researchers have investigated the chemical composition of the different parts (leaves, calyces, stems) of Roselle. The calyces (petals) yield a variety of bio active compounds after being extracted using water (Pacôme et al., 2014). The main phytochemicals with biological activity were detected as follows; alkaloids, anthocynanins, flavonoids, tannins, steroids, sterols and saponins. In the summary table below, positive (+) indicates presence and negative (-) indicates absence.

Table 1: Bio active compounds in *Hibiscus Sabdariffa*

No	Test	Result
1	Alkaloids	+
2	Anthocyanins	+
3	Flavonoids	+
4	Phenols	+
5	Quinones	-
6	Saponins	+
7	Steroids and sterols	-
8	Tannins	+
9	Terpenoids	-

2.6.2 *Bidens Pilosa*

Bidens Pilosa is a herb which is widely distributed all over the world particularly across tropical regions. It has a variety of uses mainly as a source of food and as medicine for animals and human beings. The plant has leaves that are lobed, dissected, or serrate and can either be glabrous or hairy. The flowers are either black or yellow and has long ribbed blacked achenes that are narrow (Bartolome et al., 2013).

Many studies have reported the utilization of *Bidens Pilosa* in America, Asia, Africa and Oceania where it is used as an ingredient in teas and medicines and as a herb (Chiang et al., 2003; Oliveira et al., 2004). All parts of the plant have been reported as a useful ingredient in folk medicines either as tinctures or dry powder (Oluyele et al., 2020; Redl et al., 1994).

2.6.2.1 Phytochemistry

A lot of studies have considered *Bidens Pilosa* to be an extraordinary source of bio-active compounds circa 300, with comprehensive information presented in assorted reviews (Silva et al., 2011; Xuan & Khanh, 2016). Among the many records available, qualitative phytochemical screening of *Bidens Pilosa* aqueous extracts tested positive

for tannins, flavonoids, phlobatannins, terpenoids, saponins and cardiac glycosides (Ajayi et al., 2019; Ezeonwumelu et al., 2011; Owoyemi & Oladunmoye, 2017).

2.6.3 Plant material preparation and extraction

2.6.3.1 Preparation

Plant material to be used for extraction of bioactive compounds should be dried as quickly as possible to avoid enzymatic degradation after collection. Choice of drying procedure depends on the nature of indicated and desired constituents. Common drying methods include drying at room temperature with ample air circulation, electric ovens and freeze driers especially for volatile compounds(Stéphane et al., 2021).

Homogenization is another important aspect of the preparation process and as discussed by Stéphane et al and Tiwari et al (Stéphane et al., 2021; Tiwari et al., 2011) it involves grinding or powdering the plant material in order to achieve a homogenous sample with low particle size. It is considered essential to lower the particle size so as to increase extraction efficiency. Methods used to grind plant material include the use of electric blender or the conventional mortar and pestle.

2.6.4 Extraction techniques

Extraction is the process of separating secondary metabolites using selective solvents by following standard procedures (Abubakar & Haque, 2020). The purpose of extraction is to obtain soluble plant metabolites, a complex mixture of bioactive materials obtained in either liquid or solid form. Some of the conventional techniques used in extraction are as follows.

2.6.4.1 Maceration

Maceration is the simplest of the extraction techniques. This process is conducted by soaking whole or coarsely powdered plant materials in a solvent. This is done in an

enclosed container and left to stand for a defined period at room temperature. During this period, it is stirred frequently to obtain plant extracts. Soaking softens the plant and facilitates disintegration of the plant's cell walls to release the soluble phytochemicals (Stéphane et al., 2021; Tiwari et al., 2011).

2.6.4.2 Decoction

This method involves boiling the plant sample in water to obtain heat stable and water-soluble plant extracts. The sample is boiled in a specific volume of water for a fixed time which usually ranges between 10 to 60 minutes After cooling and filtering, cold water is passed through the drug to obtain the required volume(Stéphane et al., 2021; Tiwari et al., 2011). However another form of water decoction is described by Liu et al (Liu et al., 2017) where the plant material is macerated for 1 hour followed by application of heat to boil for 5 – 10 minutes and then put on a low simmer for 2 hours in order to achieve the first part of the decoction. After filtration, water is added to the residue to obtain the second decoction by repeating the procedure.

2.6.4.3 Infusion

This is process is used to extract volatile components which are readily soluble. Infusions are prepared by soaking the plant material in boiled or cold water and allowing it to steep in the liquid for a short time. The maceration time is shorter than normal and the resulting liquid can be concentrated under vacuum using a rotary evaporator (Abubakar & Haque, 2020; Stéphane et al., 2021; Tiwari et al., 2011)

2.6.5 Plant bio-active compounds adsorptive properties and technological applications

Bioactive compounds derived from natural sources such as plants and animals' in usually small quantities and varying concentrations and can be classified as essential or

non-essential depending on their biological significance. The biologically significant chemicals referred to as being essential include compounds such as vitamins while examples of the non-essential compounds include polyphenols, alkaloids, etc. The bioactive compounds present in parts of plant such as leaves, roots, barks and gums can be obtained through various extraction techniques (Stéphane et al., 2021)

2.6.5.1 Adsorptive properties

2.6.5.1.1 Tannins

Tannins are a heterogeneous group of polyphenols that belong to a vast family of secondary metabolites stored in vegetal cells. They can be classified as either hydrolysable or condensed tannins (Fraga-Corral et al., 2020). These natural plant products have provideant amount of adjacent phenolic hydroxyls which provides them with the ability to create stable bonds within themselves and with other compounds. It is this property that ensures that they have a strong chelating ability towards heavy metal ions such as Cr (III), Pb (II), Hg (II), Cd (II) and Au (II) (Meethale Kunnambath & Thirumalaisamy, 2015).

2.6.5.1.2 Saponins

Saponins are glycosides and a highly amphipathic compound, a diverse group of natural products found in abundance (Mugford & Osbourn, 2012). The name ‘Saponins’ derives from the latin word ‘Sapo’ which means soap due to the soap-like properties of these natural products. They have a rigid skeleton consisting of hydrocarbons to which sugars are attached (Kregiel et al., 2017). They are a naturally surface-active substance present whose diverse amphiphilic structures of the molecules influences their rich physicochemical properties and biological activity (Stanimirova et al., 2011).

2.6.5.2 Technological applications

2.6.5.2.1 Anti-Corrosion and inhibitive effects

Adsorptive studies are used to evaluate surface coverage of the plant extracts on selected surfaces and their effect. Various methods are used to facilitate the analyses of surface coverage and include the gasometric and potentiodynamic polarization techniques, the Temkin, Freundlich, Langmuir and Frumkim isotherms and the correlation coefficient (R2) are applied to efficiently decide on the best fitted isotherm (Ajayi et al., 2019; Oguzie, 2008).

A series of experiments designed to ascertain the inhibitive properties of *Bidens Pilosa* plant extract on mild steel in 1.75 M HCl acid were conducted at room temperature by Ajayi et al (Ajayi et al., 2019). Varied concentrations of acidic *Bidens Pilosa* extracts were used and showed that studying the corrosion of the mild steel resulted in a reduction in release of hydrogen indicative of an increase in inhibition efficiency with 50% v/v concentration showing highest inhibition while 10% v/v showed the lowest inhibition. In addition, the study showed chemisorption of the *Bidens Pilosa* extracts since they obeyed the Langmuir adsorption isotherm.

Extracts in 2M HCl and 1M H_2SO_4 of selected plant extracts which included extracts from *Hibiscus Sabdariffa* were used to investigate corrosion inhibition of mild steel by Oguzie (Oguzie, 2008). The results indicated that inhibition efficiency of anti-corrosion properties improved with increased concentration by adsorption of extract organic matter in both acid media. The major components that for the inhibitory anti-corrosion properties of *Hibiscus Sabdariffa* were found to be ascorbic and amino acids, flavonoids, and β-carotene.

2.6.5.2.2 Coagulation - Environmental Application

Coagulation is an important method for treating surface water and industrial wastewater as it promotes the bundling of colloids and other suspended substances (Yin, 2010). Coagulants sourced from plant extracts are seen by researchers as a substitute for metallic-based inorganic ones. Application of tannin-based coagulants obtained from renewable resources in the treatment of different waters and better results have been observed in comparison to the conventional ones (Graham et al., 2008).

2.6.5.2.3 Fabric manufacture: Leather Industry

Owing to the structural makeup of leather, it is susceptible to deterioration over time, which lowers its durability and, in turn, its economic value, directly hurting leather goods. Tannins are utilized in a process known as tanning to prevent skin breakdown and to provide it inalterability and resistance by binding to proteins and stabilizing their structure. It is one of the earliest methods of treating leather. (Fraga-Corral et al., 2020).

2.6.5.2.4 Floatation

The industrial processing method of flotation allows for the separation of materials by adjusting the hydrophobicity of their surfaces to increase or decrease their attraction to water or polar solvents. Metallurgy utilizes this method frequently to concentrate ores.

The capacity of tannins to form complexes with metal ions like iron, copper, or noble metal salts is a crucial characteristic. Their depressive and dispersion properties make them valuable as a selective modifying agent in flotation. This kind of substance enables the use of plant-derived materials as flotation agents in place of highly harmful substances. (Fraga-Corral et al., 2020).

CHAPTER 3: MATERIALS AND METHODS

3.1 Methodology and Research Design

Qualitative and quantitative methods were used throughout the research process. Qualitative techniques that were used included phytochemical screening of plant extracts. Further experimental work involved gathering of data through measurements, monitoring, and control of battery parameters such as specific gravity of electrolytes, open circuit voltage and analyzing charge/discharge cycle data for different battery electrolyte solutions.

3.1.1 Chemicals and Reagents

Analytical grade chemicals and reagents including 10% Ferric chloride solution (light yellow); 10% Ferric chloride solution, distilled water; 99.5% sodium hydrogen carbonate, Olive oil, battery grade sulfuric acid, distilled water were obtained from the chemistry laboratory of Moi University.

3.1.2 Instruments and Equipment

Oven (LabTech, make: LDO-150F, serial number 2018070203), Blender (Nutribullet 600 series, 600W, Capbran Holdings, LLC Los Angeles, CA 90025, USA), Hotplate (Pro-Scientific HPS-7), analytical balancing scale (Mettler- Toledo, XS2002S, Delta Range, Switzerland), beakers, measuring cylinders, IMAX B6 v2 professional balance charger/discharger (skyrc, serial number SN: 003243990), 300W power inverter, 100W incandescent lamp, solar batteries (Chloride Exide N50, 50Ah C20), AC power adapter (SUDER, 240V/12V, 4A output).

3.2 Procedure

3.2.1 Collection, authentication and sample preparation

Solar dried calyces of *Hibiscus Sabdariffa (Figure 3.1)* were bought from the market in Eldoret town (Uasin Gishu County, Kenya). Leaves of *Bidens Pilosa* (Blackjack) were obtained from Kesses constituency in Uasin Gishu County, Kenya. The *Bidens Pilosa* leaf samples were washed under tap water and later dried for 4 hours at 60 degrees Celsius in a laboratory oven (LabTech, make: LDO-150F, serial number 2018070203).

The samples were ground into a fine homogenous powder using an electric grinder (Nutribullet 600 series). The samples were weighed using an analytical balance (Metler-Toledo XS2002S).

Figure 3.1: Calyces of *Hibiscus Sabdariffa*

3.2.2 Extraction

The weighed samples were then transferred into separate conical flasks measuring 250 ml. A decoction procedure adopted from Liu et al. (Liu et al., 2017) was used to extract phytochemicals from the samples. 10 grams of raw powdered plant material was soaked for 1 hour in a beaker (500ml) of distilled water. Then, the beaker was transferred onto a hotplate-stirrer (Pro-Scientific HPS-7) and heat was applied until the water boiled for 15 minutes as shown in Figure 3.2. The mixture was later allowed to simmer for 2 hours. The solution was filtered using Whatman No.1 filter paper. The filtered decoction was then heated using low simmer while being stirred slowly until concentrations of 10%(w/v), 15.86%(w/v), 30%(w/v) and 44.14%(w/v) were achieved.

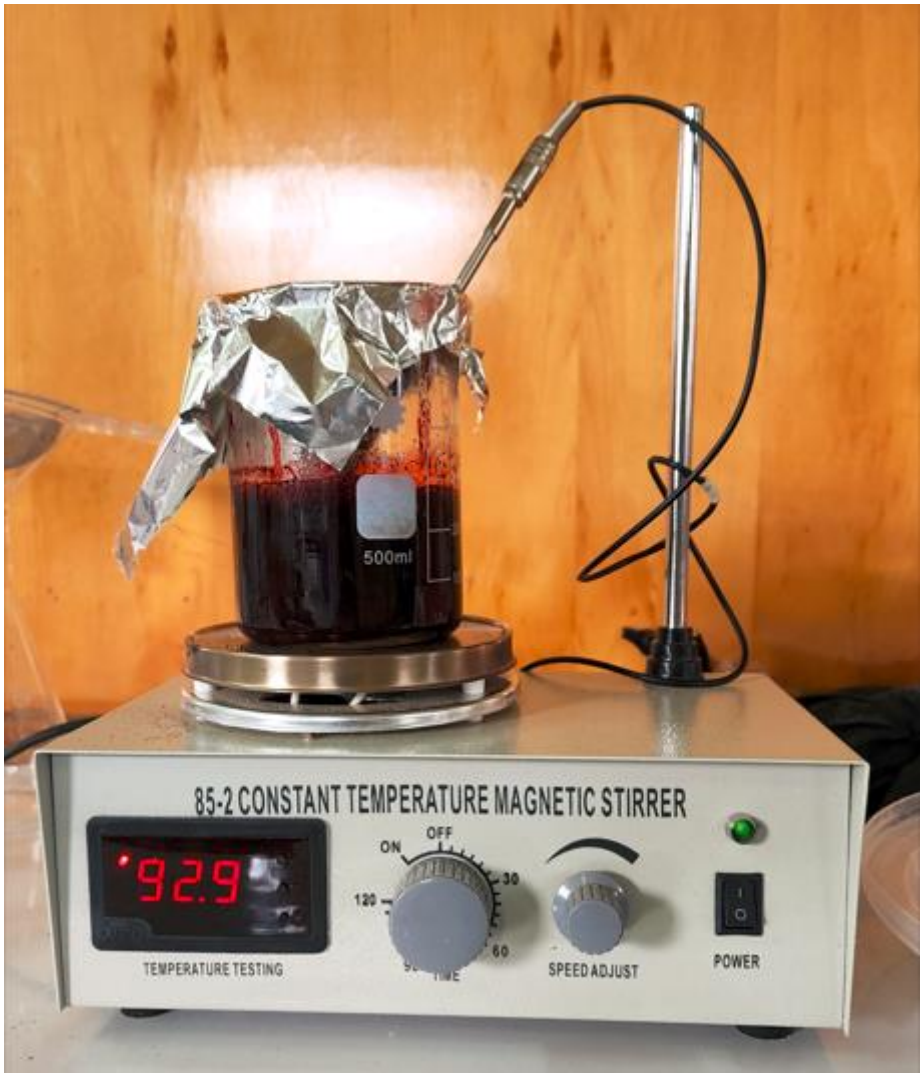

Figure 3.2: Decoction process of Roselle

3.2.2.1 Phytochemical screening

Standard qualitative phytochemical tests (Auwal et al., 2014; Owoyemi & Oladunmoye, 2017; Shaikh & Patil, 2020) were performed on the aqueous extract solution for saponins, tannins, carboxylic acids and flavonoids. The results were recorded either positive for presence or negative for absence with all the tests.

3.2.2.1.1 Test for Saponins

3 milliliters (3 mL) of the extract aqueous solution were added to 5 milliliters (5 mL) of distilled water in a test-tube. A stopper was placed on the test-tube and the sample

was shaken vigorously for 5 minutes. Persistent appearance of honeycomb froth lasting for at least 15 minutes is indicative of saponins presence (Auwal et al., 2014; Kareru et al., 2007).

3.2.2.1.2 Test for Tannins

a) Ferric Chloride Test

A few drops of 10% Ferric chloride solution (light yellow) were added to two Milliliters (2mL) of the aqueous solution of the plant extract. Presence of gallic tannins is shown by the occurrence of a blackish blue color while occurrence of green-blackish colour indicate the presence of catechol tannins (Auwal et al., 2014).

b) Braymer's test

One Milliliter (I mL) of plant extract filtrate was added to three milliliters (3 mL) of distilled water and three drops of 10% Ferric chloride solution. Appearance of a blue-green color is indicative of the presence of tannins(Shaikh & Patil, 2020).

3.2.2.1.3 Test for Carboxylic acid

0.1 grams of 99.5% Sodium Hydrogen carbonate was added to one milliliter (1mL) of plant extract solution. Appearance of effervescence is indicative of the presence of carboxylic acid (Shaikh & Patil, 2020).

3.2.3 Evaluation of electrochemical potential

Prior to commencement of the charge/discharge cycles the following initial requirements were checked and verified; correctness of battery connections and all resistances, a record of float current and terminal float voltage and specific gravity (IEEE, 2020).

3.2.3.1 Battery with dilute sulfuric acid electrolyte (conventional electrolyte)

3.2.3.1.1 Initial filling and charging

The batteries were checked for physical integrity and cleaned prior to filling of acid. Sufficient quantity of battery grade sulfuric acid of 1.245 g/cm³ specific gravity at room temperature was used to fill to the maximum level of each of the 6 cells of the battery. 900ml was used per cell.

The voltage of all the cells was used to evaluate the polarity of the cells just after acid filling. After that, the battery was given a 6-hour break so that the plates and separators could soak up the electrolyte solution.

A constant current charger, IMAX b6 balance charger/discharger was used for the initial charging at a constant current at 0.07C (3.5A) till a constant maximum rated charge voltage of 14.4V was observed for 3 consecutive hourly readings at the end of the charge procedure using the IMAX B6 balance charger/discharger. The initial charge was taken as the test run after which the battery was discharged by a connected load of a recorded current draw of 11.5A comprising a power inverter, incandescent lamp, and the IMAX B6 discharger. The cutoff voltage was set at 10.8V as specified by the battery manufacturer data sheet.

3.2.3.1.2 Specific gravity measurement

Specific gravity of dilute sulfuric acid solution in the conventional lead acid battery was measured using a portable floating hydrometer prior to the first charge cycle at the discharged state cutoff voltage of 10.8V (10.86V as determined by IMAX B6 V2 charger) and at for every 2 hour interval until full charge voltage of 14.4V was reached, a method adopted from Megateli et al (Megateli et al., 2015). A rest period of 5 hours was observed after full charge was achieved before commencement of the discharge

procedure. The specific gravity on discharge was measured at 2-hour intervals until cutoff voltage was reached.

Figure 3.3: Specific gravity measurement using a float hydrometer.

3.2.3.1.3 Open circuit voltage measurement

Open circuit voltage of battery with dilute sulfuric acid solution was measured using a digital voltmeter and the IMAX B6 V2 charger at 0 hours in the discharged state and at full charge respectively.

3.2.3.2 Battery with electrolyte solution with plant extracts additive

Plant extract were added to the batteries in the following variations by volume percentage to dilute battery sulfuric acid ;0.3% v/v, 1.005% v/v, 1.7% v/v and 2 % v/v, a method adopted from Pavlov (Pavlov, 2011) and Wu et al. (Wu et al., 2020). An experiment design in Table 2 was used to determine concentration corresponding to

additive volume. The plant extract solution concentration was measured as percentage of the ratio of the weight of crude plant sample to volume of distilled water (w/v %).

3.2.3.2.1 Specific gravity (Relative density)

Specific gravity of electrolyte with plant extract additive was measured using a portable floating hydrometer prior to the first charge cycle at the discharged state cutoff voltage of 10.8V (10.86V as determined by IMAX B6 V2 charger) and at for every 2-hour interval until full charge voltage of 14.4V was reached, a method adopted from Megateli et al (Megateli et al., 2015). A rest period of 5 hours was observed after full charge was achieved before commencement of the discharge procedure. The specific gravity on discharge was measured at 2-hour intervals until cutoff voltage of 10.8 V was reached.

3.2.3.2.2 Open circuit Voltage

Open circuit voltage of battery with dilute sulfuric acid solution was measured using a digital voltmeter and the IMAX B6 V2 charger at 0 hours in the discharged state and at full charge respectively.

3.2.4 Evaluation and comparison of battery discharge capacity

This procedure whose setup is shown in 3.4 was run concurrently with the electrochemical approach of assessing the different battery experiments and therefore a constant current charger (the IMAX B6 balance charger/discharger) , as per methods adopted from Exide Industries, Ghufron et al., and Kore et al., (Exide Industries, 2022; Ghufron et al., 2020; Kore et al., 2021), was used for the initial charging at a constant current at 0.07C (3.5A) till a constant maximum rated charge voltage of 14.4V was observed for 3 consecutive hours at the end of the charge procedure. Hourly readings

using the IMAX B6 balance charger/discharger and a digital multimeter were recorded for each of the 3 replicated charge cycles for each battery chemistry experiment.

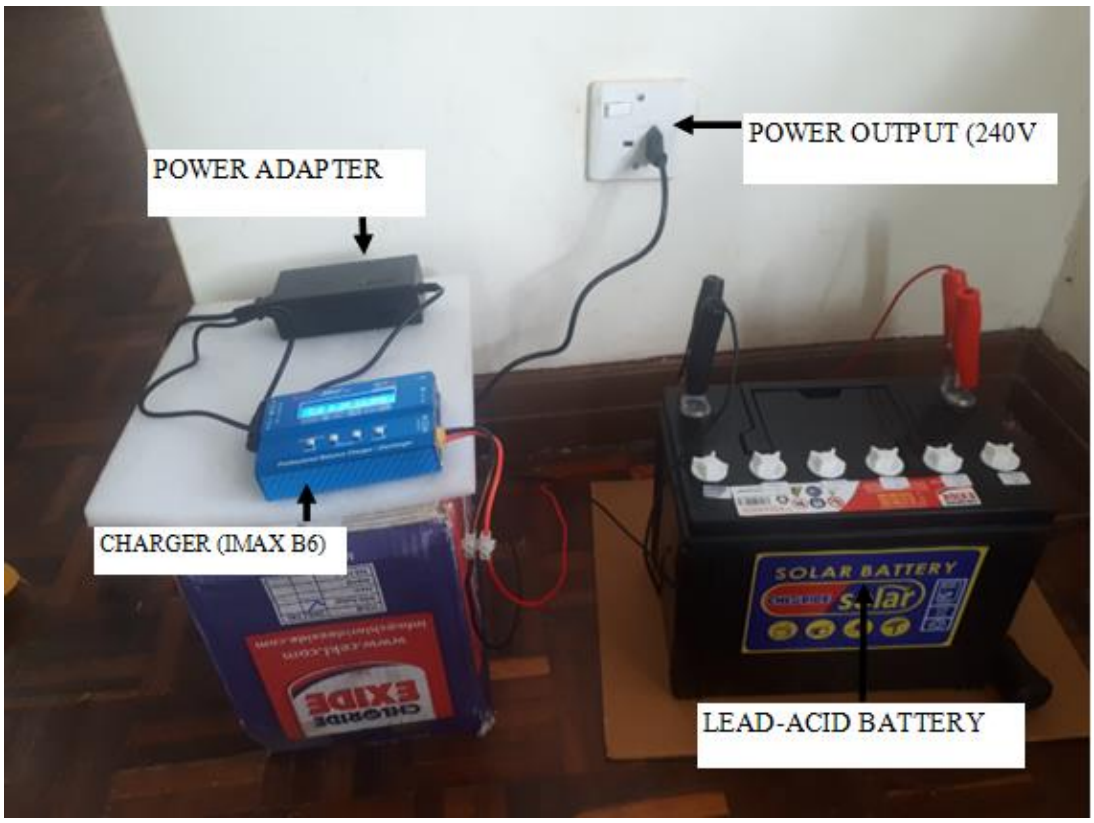

Figure 3.4: Charge cycle setup

The discharge current was maintained at a value of 11.5A determined by total current drawn by the applied load until the battery terminal voltage decreased to 10.8V, a value equal to the minimum average voltage per cell (specified by manufacturer) times the number of cells. Voltage was measured by the IMAX B6 V2 discharger and validated by a digital multimeter. Recordings were done at hourly intervals for each of the 3 replicated discharge cycles for each battery chemistry experiment.

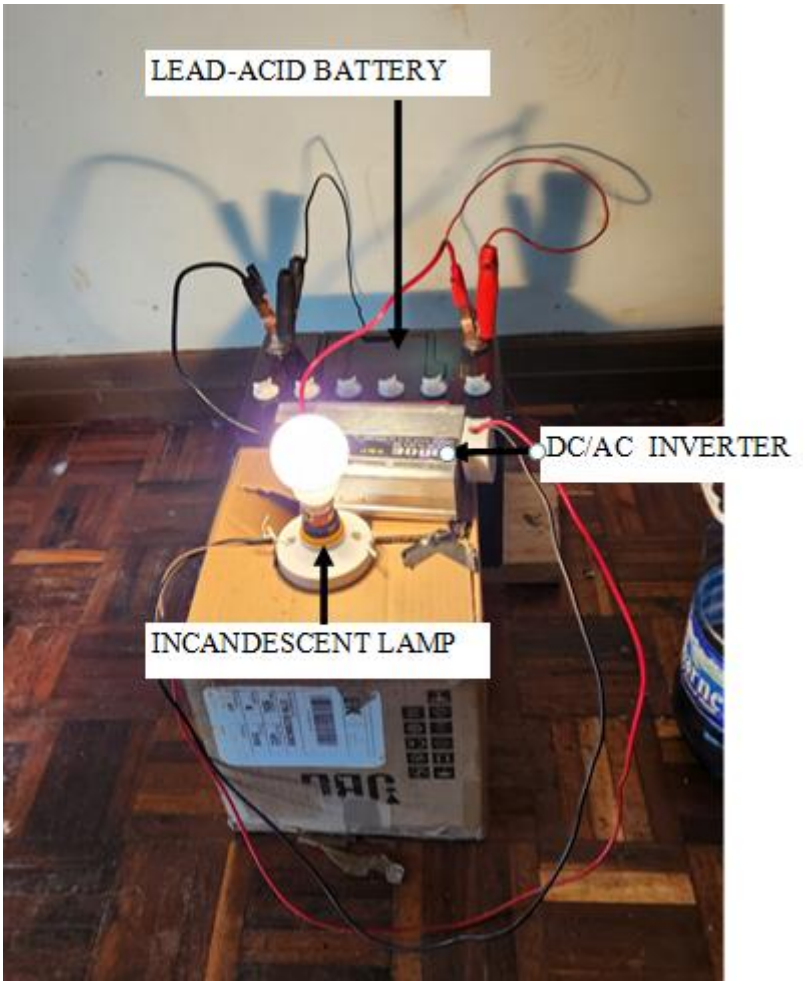

Figure 3.5: Discharge cycle setup

3.2.5 Determining Optimum additive amounts

Design of the experiments was done using Design Expert 11 statistical software for windows (Stat-Ease, Inc, United States). All experiments were replicated three times. Quantitative data analysis and optimization was done by Design-Expert 11. All graphical illustrations and comparisons were done in OriginPRO 2021 software for windows.

The experimental runs examined, their factor combinations, and the conversion of the coded level to the experimental units used in the investigation are all summarized in Table 2.

Table 2: Factor combinations

Factor	Name	Units	Minimum	Maximum	Coded Low	Coded High
A	Volume	(ml)	0.01	2	-1 ↔ 0.30	+1 ↔ 1.71
b	Conc	(g/ml) %	10	50	-1 ↔ 15.86	+1 ↔ 44.14

For the responses (charge duration and discharge duration) to be assigned criteria, models were created by checking the design evaluation, ANOVA statistics and diagnostic graphs in Design Expert. These tools provided the best estimate of the response surface. Using the numerical optimization tool, a range of the minimum and maximum was specified for the factors as per values set in the design of experiments in Table 3. In a similar manner, goals were specified for the responses by selecting to minimize charge duration and maximize discharge duration.

Table 3: Randomized Design Table

Std	Group	Run	Volume	Concentration
18	1	1	0	0
17	1	2	0	0
19	1	3	0	0
2	2	4	1	-1
1	2	5	-1	-1
8	3	6	0	-1.41421356
9	3	7	0	-1.41421356
4	4	8	1	1
3	4	9	-1	1
6	5	10	0	0
7	5	11	0	0
5	5	12	0	0
12	6	13	-1.414214	0
13	6	14	1.4142136	0
10	7	15	0	1.414213562
11	7	16	0	1.414213562
15	8	17	0	0
16	8	18	0	0
14	8	19	0	0

CHAPTER 4: RESULTS AND DISCUSSIONS

4.1 Development of Electrolyte Additive

4.1.1 Extraction of plant material bio-active compounds

Water was used as a solvent for extraction of active compounds from the plant material sample. It is a universal solvent that dissolves several compounds which include tannins; saponins; terpenoids; polypeptides; lectins. The polarity of the solvent used significantly determines the solubility of the phytochemicals (Abd Aziz et al., 2021; Tiwari et al., 2011).

4.1.2 Phytochemical screening results

Screening of the extract from calyces of *Hibiscus Sabdariffa* revealed the presence of several bioactive compounds which include: saponins; tannins; carboxylic acids; flavonoids. Screening of leaf extract of *Bidens Pilosa* also revealed the presence of several secondary metabolites which include saponins and tannins. The results are summarized in the tables below.

Table 4: Phytochemicals identified in calyces of *Hibiscus Sabdariffa*

Phytochemicals	Type of test	Result
Saponins	Frothing	+
		+
Tannins	Ferric Chloride	+
	Braymer's	+
Carboxylic acid	Effervescence	+
Flavonoids	Conc. Sulfuric acid	-
	Ferric Chloride	+

Table 5: Phytochemicals identified in the leaves of *Bidens Pilosa*

Phytochemicals	Type of test	Result
Saponins	Frothing	+
		+
Tannins	Ferric Chloride	+
	Braymer's	+
Carboxylic acid	Effervescence	-
Flavonoids	Conc. Sulfuric acid	-
	Ferric Chloride	-

Figure 4.1: Test for Tannins in Roselle

Figure 4.2: Test for Saponins in Roselle (Frothing test)

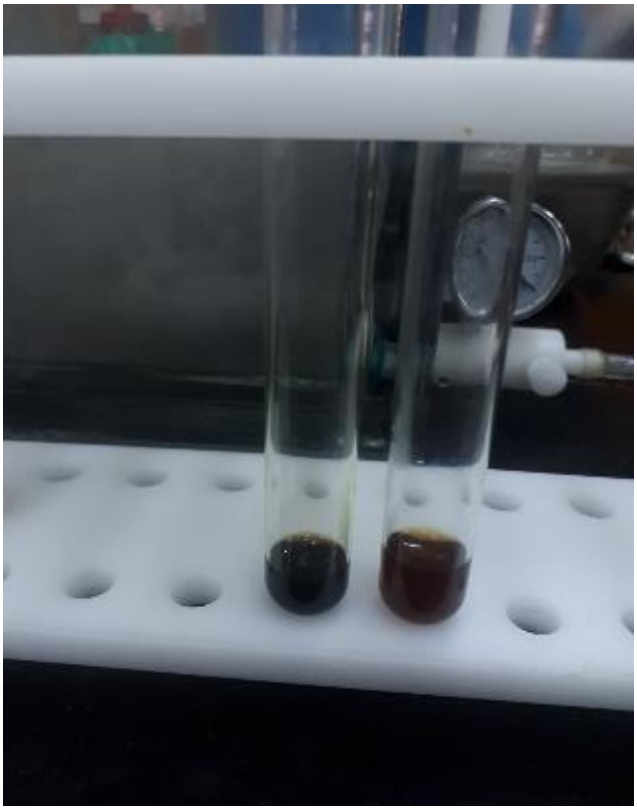

Figure 4.3: Test for Tannins in Blackjack (Ferric Chloride test)

4.2 Evaluation of Electrochemical Potential

Monitoring the evolution of the specific gravity of the electrolyte during the charge/discharge cycle was done over 3 cycles for each battery electrolyte chemistry. The fluctuating specific gravity maxima and minima show the use of active materials in the electrochemical processes, underlying irreversible reactions as well as effect of the additives on the standard electrolyte. Earlier studies found that the electrochemical activity of lead and lead oxide active materials is dependent on the concentration of H_2SO_4, where the highest activity being achieved in solutions with concentrations from 1.10 g/cm³ to 1.28 g/cm³ result in batteries with lower initial capacity, longer cycle life and higher charge efficiency (Pavlov et al., 2006, 2008).

4.2.1 Specific gravity of conventional electrolyte Lead-acid battery

And as captured in the results of this study it is observed that data collected from all electrochemical cells reveal variation of the specific gravity between the 1.10 g/cm³ to 1.28 g/cm³ range described as optimum by Petkova et al(Petkova et al., 2006) and Pavlov(Pavlov, 2017c). In the initial cycling of the battery with conventional electrolyte, the change in specific gravity during the charging cycle is shown in Figure 4.4, Figure 4.5 and Figure 4.6, the comparable discharge cycle plots are shown in Figure 4.7, Figure 4.8 and Figure 4.9. These plots reveal the variation of the specific gravity from a range of 1.200 g/cm³ to 1.210 g/cm³ in the maxima while the minima varied between 1.120 g/cm³ and 1.150 g/cm³. The similarity in the profile of per cell relative density was indicative of uniform electrochemical activity in the different cells.

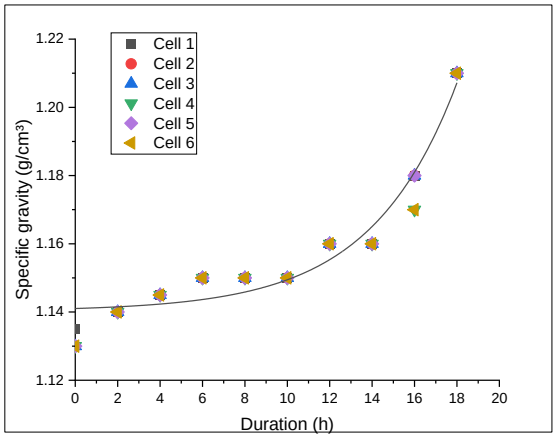

Figure 4.4: Specific Gravity of Standard electrolyte battery during first charge cycle

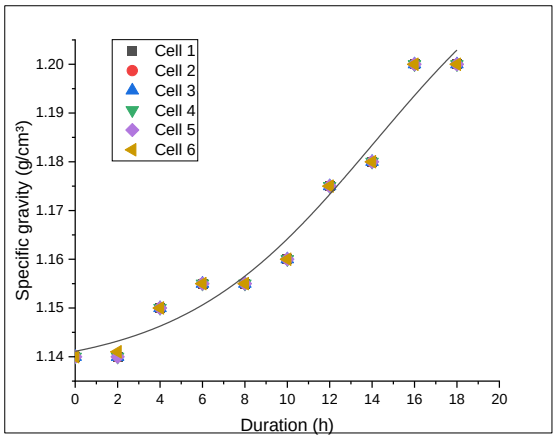

Figure 4.5: Specific Gravity of Standard electrolyte battery during second charge cycle

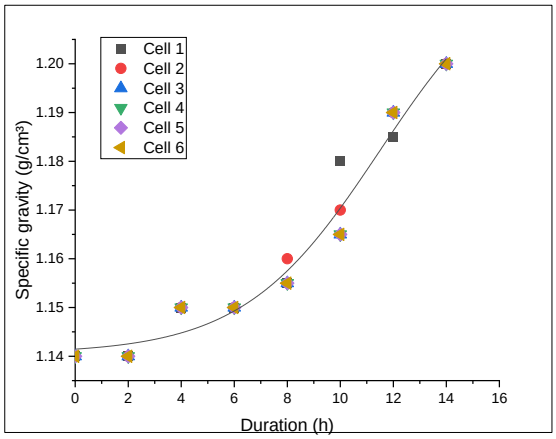

Figure 4.6: Specific Gravity of Standard electrolyte battery during third charge cycle

The explanation for the variations in specific gravity is described by various researchers as being a result of the electrochemical mechanisms during charge and discharge (Megateli et al., 2015; Pavlov, 2017b, 2017c; Pavlov et al., 2006; Petkova et al., 2006). During discharge the sulfuric acid (H_2SO_4) in the electrolyte is consumed and water is produced and as a result makes the solution more dilute. The sulfuric acid (H_2SO_4) is then regenerated during the charging process.

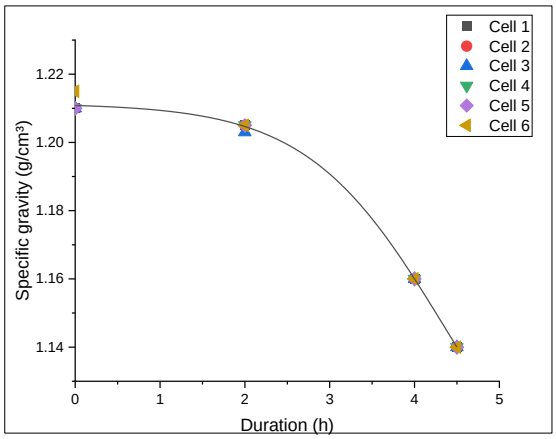

Figure 4.7: Standard electrolyte battery during first discharge

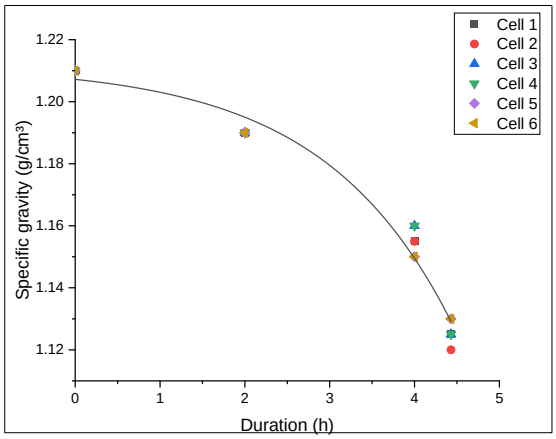

Figure 4.8: Standard electrolyte battery during second discharge

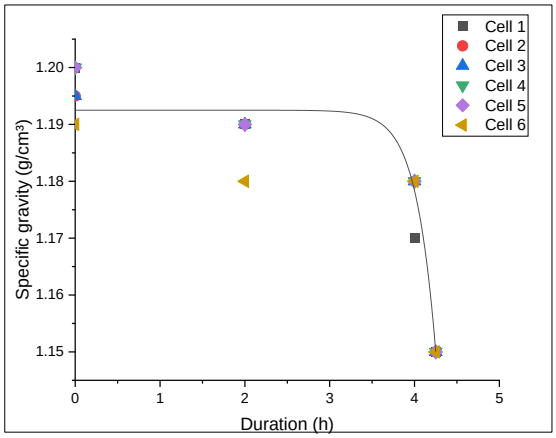

Figure 4.9: Standard electrolyte battery during third discharge

4.2.2 Specific gravity of Roselle electrolyte lead-acid battery

Similar to the conventional electrolyte specific gravity for battery electrolyte with Roselle additive varied over a maxima and minima within which the electrolyte provides condition for optimum battery performance as described by Pavlov and Petkova (Pavlov, 2017c; Petkova et al., 2006). However, the electrochemical profile of the battery cells is not as uniform, a phenomenon which can be attributed to the presence and effect of plant extract additives in the electrolyte solution.

4.2.2.1 10% (w/v) *Hibiscus Sabdariffa* extract solution.

The specific gravity for the battery with 10% (w/v) Roselle extract solution varied in the maxima range of 1.200 g/cm³ to 1.220 g/cm³ while the minima varied between 1.14 g/cm³ and 1.15 g/cm³ during the charge cycle.

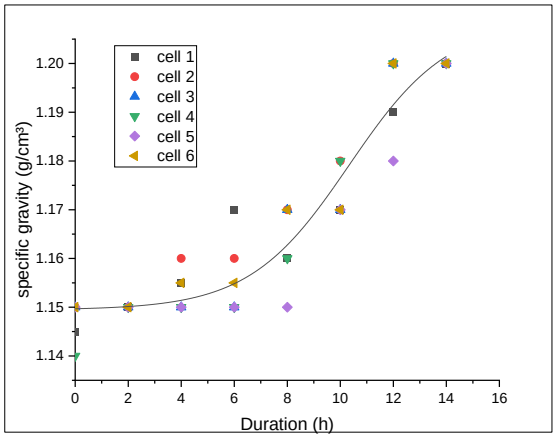

Figure 4.10: Electrolyte with 1% (v/v) Roselle additive first charge.

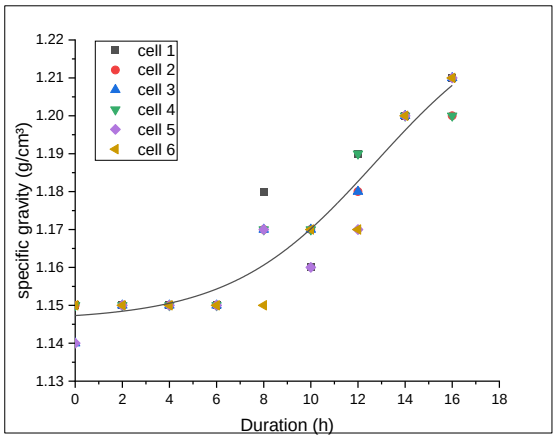

Figure 4.11: Electrolyte with 1% (v/v) Roselle additive second charge

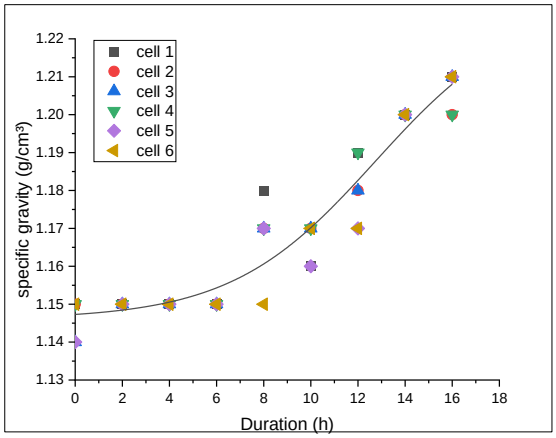

Figure 4.12: Electrolyte with 1% (v/v) Roselle additive third charge

Similarly, on discharge the specific gravity varies in descending manner due to the same factors that influence the change in the charge cycle. The following graphs illustrate the behavior of the specific gravity on discharge.

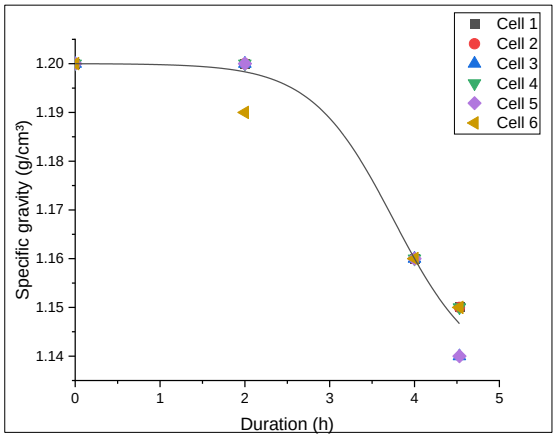

Figure 4.13: Electrolyte with 1% (v/v) Roselle additive first discharge

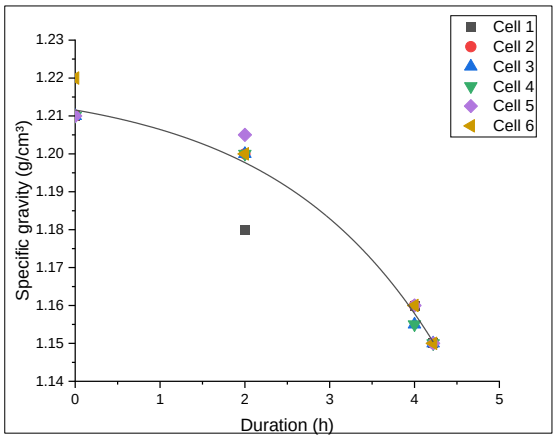

Figure 4.14: Electrolyte with 1% (v/v) Roselle additive second discharge

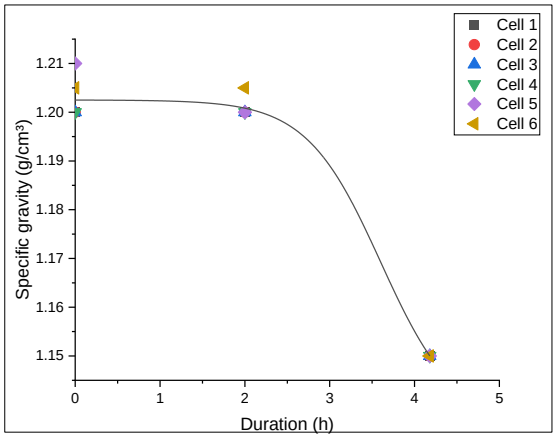

Figure 4.15: Electrolyte with 1% (v/v) Roselle additive third discharge

4.2.2.2 15.86% (w/v) *Hibiscus Sabdariffa* extract solution.

The maxima specific gravity for the battery with 2ml of 15.86% (w/v) Roselle additive per cell varied between 1.200 g/cm³ to 1.21 g/cm³ at full charge, illustrated in Figure 4.16, Figure 4.17 and Figure 4.18 for the first, second and third charge cycles respectively.

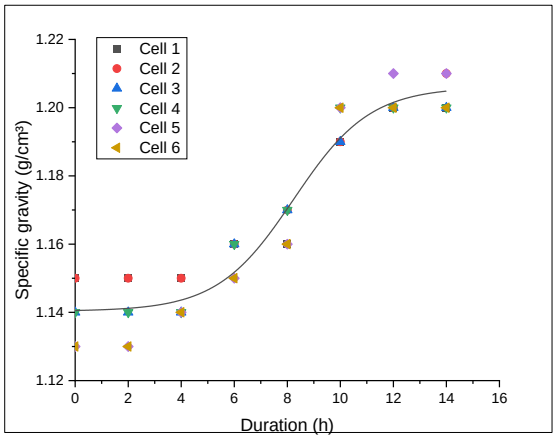

Figure 4.16: Electrolyte with 0.3% (v/v) Roselle additive first charge cycle

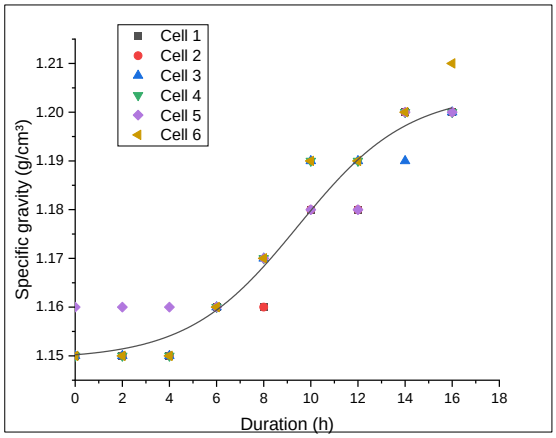

Figure 4.17: Electrolyte with 0.3% (v/v) Roselle second charge cycle

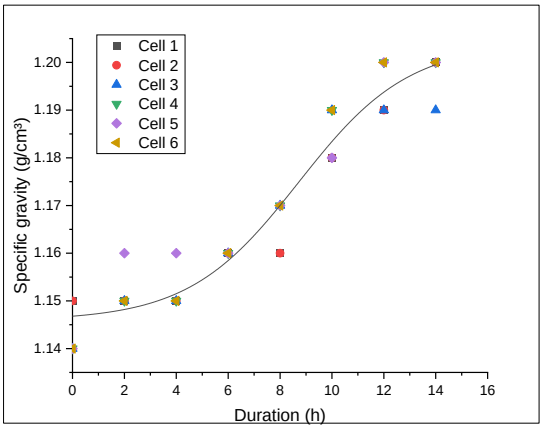

Figure 4.18: Electrolyte with 0.3% (v/v) Roselle additive third charge cycle

At the voltage cut-off point the minima varied between 1.13 g/cm³ and 1.16 g/cm³.

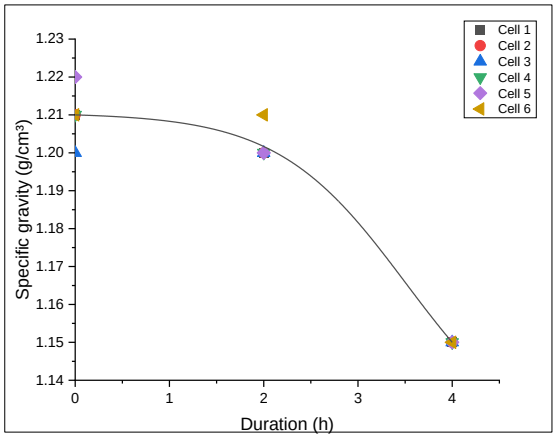

Figure 4.19: Electrolyte with 15.86% (w/v) Roselle extract first discharge cycle

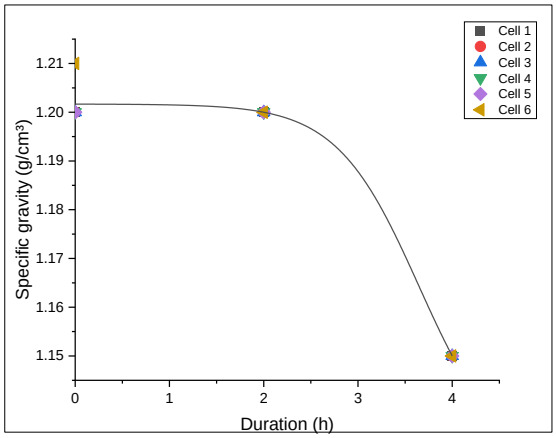

Figure 4.20: Electrolyte with 15.86% (w/v) Roselle extract second discharge cycle

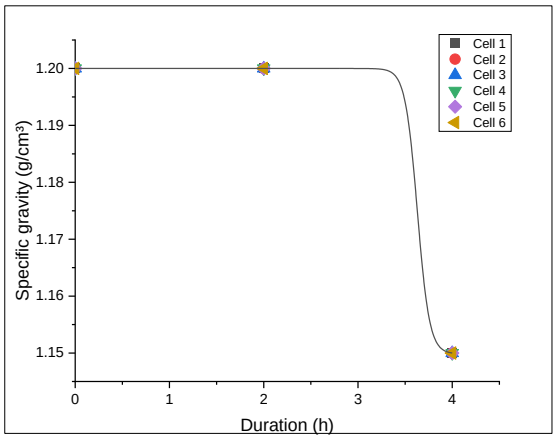

Figure 4.21: Electrolyte with 15.86% (w/v) Roselle extract third discharge cycle

4.2.2.3 30% (w/v) *Hibiscus Sabdariffa* extract solution.

For the electrolyte solution with 30% (w/v) *Hibiscus Sabdariffa* L. (2% (v/v) additive, specific gravity values varied for the maxima from 1.170 g/cm³ to 1.210 g/cm³ while the minima varied between 1.13 g/cm³ and 1.15 g/cm³ over 3 cycles.

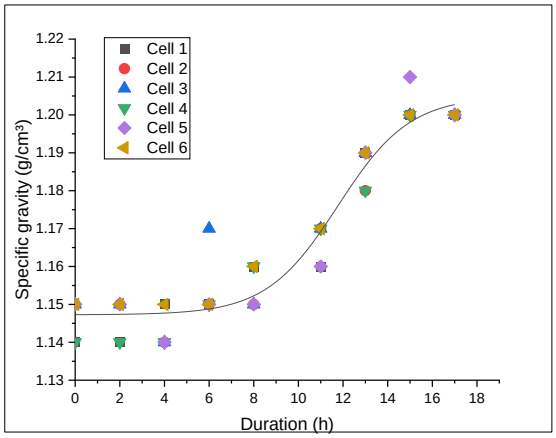

Figure 4.22: Electrolyte with 2% (v/v) Roselle additive first charge cycle

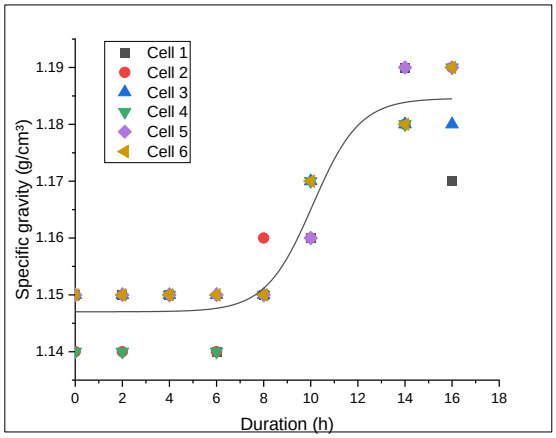

Figure 4.23: Electrolyte with 2% (v/v) Roselle additive second charge cycle

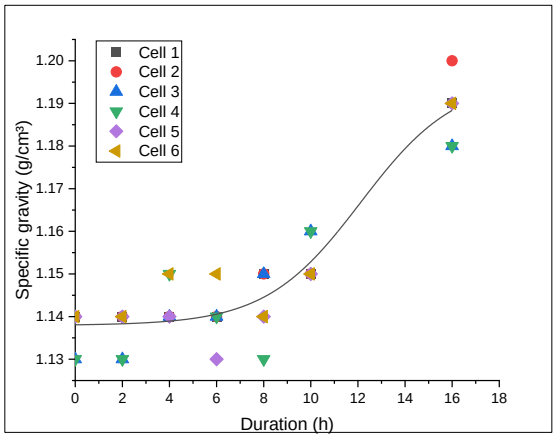

Figure 4.24: Electrolyte with 2% (v/v) Roselle additive third charge cycle

Similarly, on discharge the specific gravity varies in descending manner due to the same factors that influence the change in the charge cycle. The following graphs illustrate the behavior of the specific gravity on discharge.

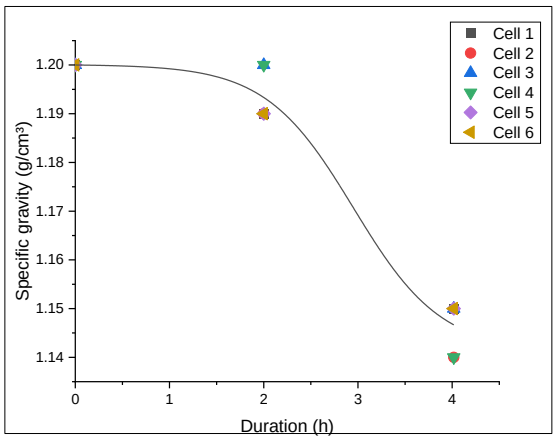

Figure 4.25: Electrolyte with 2% (v/v) Roselle additive first discharge cycle

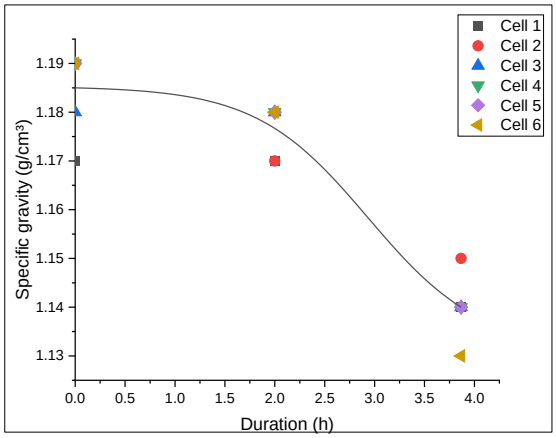

Figure 4.26: Electrolyte with 2% (v/v) Roselle additive second discharge cycle.

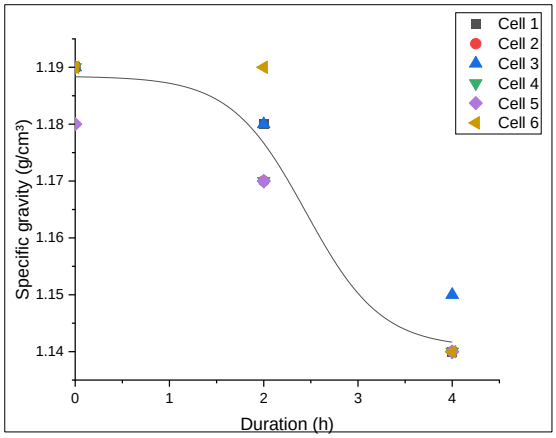

Figure 4.27: Electrolyte with 2% (v/v) Roselle additive third discharge cycle.

4.2.2.4 44.14% (w/v) *Hibiscus Sabdariffa* extract solution.

The maxima specific gravity per cell for the battery with 44.14% (w/v) Roselle additive varied between 1.170 g/cm³ to 1.200 g/cm³ at full charge as illustrated in Figure 4.28, Figure 4.29 and Figure 4.30.

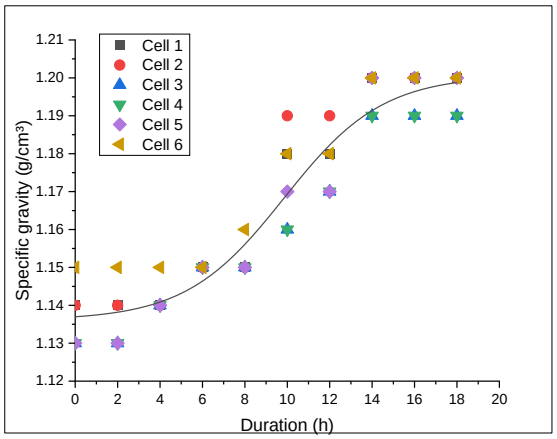

Figure 4.28: 1.7% (v/v) Roselle additive first charge cycle

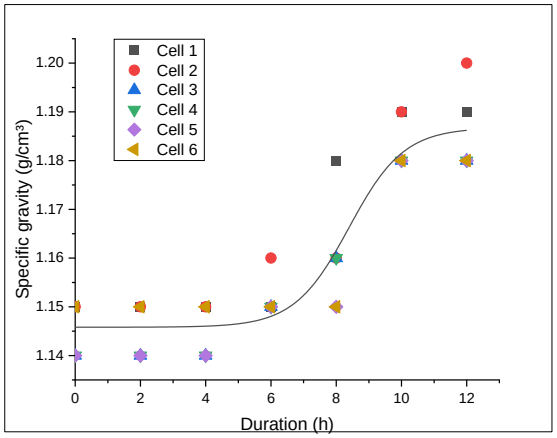

Figure 4.29: 0.3% (v/v) Roselle additive second charge cycle

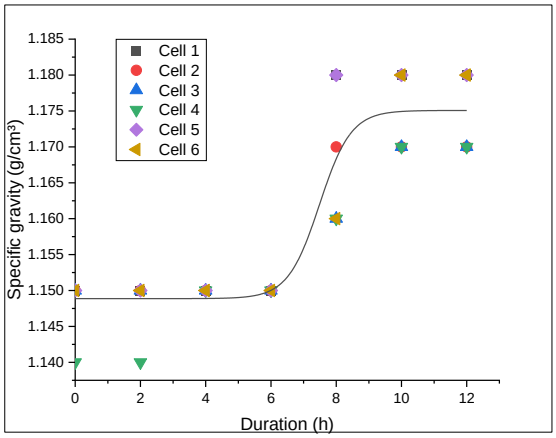

Figure 4.30: 1.7% (v/v) Roselle additive third charge cycle

At the voltage cut-off point the minima of the specific gravity, illustrated in Figure 4.31, Figure 4.32 and Figure 4.33, varied between 1.13 g/cm³ and 1.15 g/cm³.

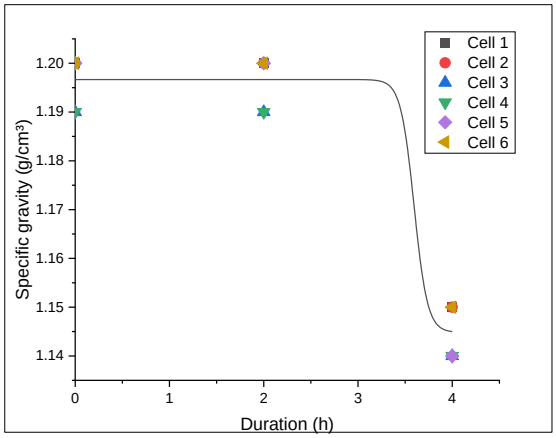

Figure 4.31: 44.14% (w/v) Roselle additive first discharge cycle

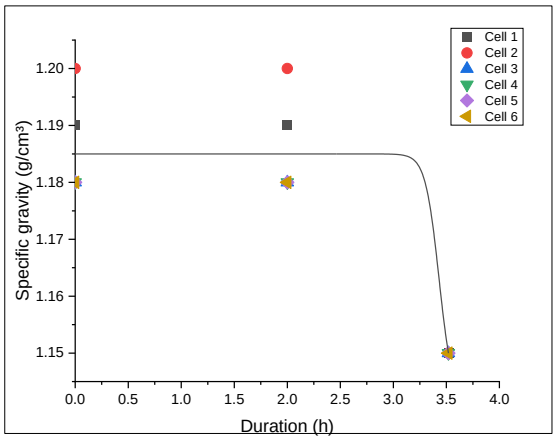

Figure 4.32: 44.14% (w/v) Roselle additive second discharge cycle

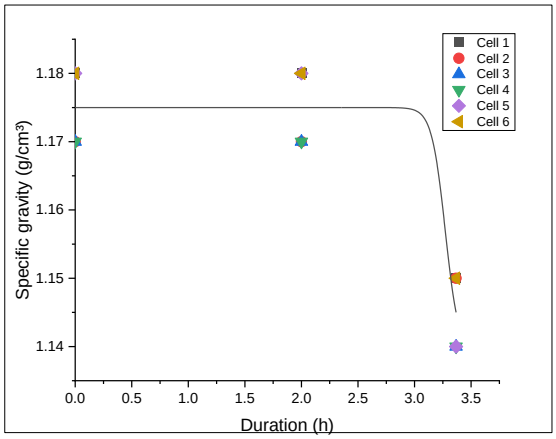

Figure 4.33: 44.14% (w/v) Roselle additive third discharge cycle

4.2.3 Specific gravity of *Bidens Pilosa* extract electrolyte solution.

4.2.3.1 10% (w/v) *Bidens Pilosa* extract solution.

Specific gravity measurement during cycling of the battery with electrolyte solution with 10% (w/v) *Bidens Pilosa* extract reveal the variation of the maxima from 1.180 g/cm³ to 1.210 g/cm³ while the minima varied between 1.120 g/cm³ and 1.160 g/cm³. The variation in specific gravity per cell as illustrated in Figure 4.34, Figure 4.35 and Figure 4.36 for the charge cycles can be attributed to the differences in the physical adsorption variation of the additive on the electrode surface.

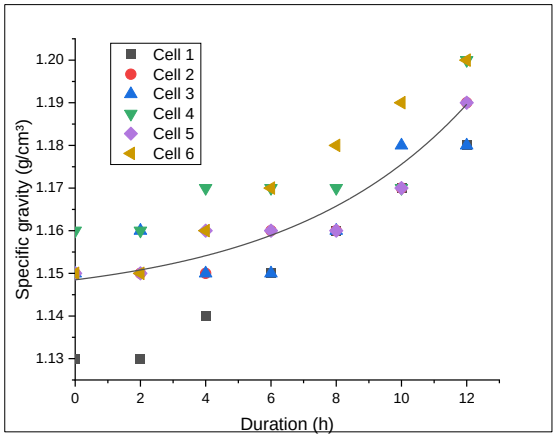

Figure 4.34: Electrolyte with 10% (w/v) *Bidens Pilosa* additive first charge.

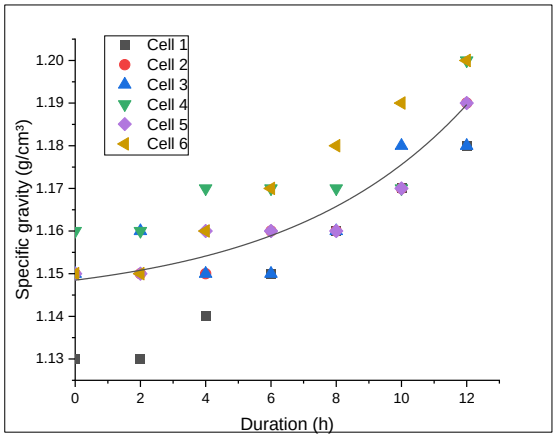

Figure 4.35: Electrolyte with 10% (w/v) *Bidens Pilosa* additive second charge.

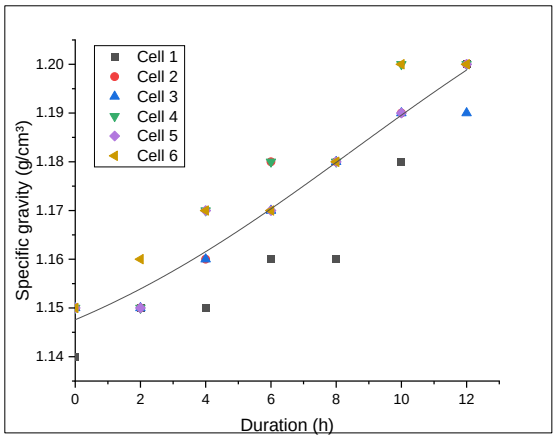

Figure 4.36: Electrolyte with 10% (w/v) *Bidens Pilosa* additive third charge

Similarly, on discharge the specific gravity varies in descending manner due to the same factors that influence the change in the charge cycle. The following graphs illustrate the behavior of the specific gravity on discharge.

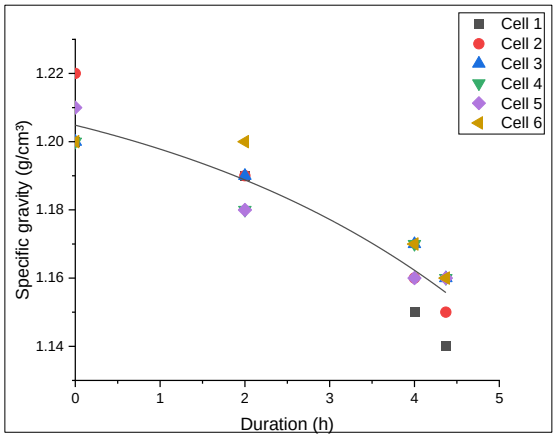

Figure 4.37: Electrolyte with 1.005% (v/v) *Bidens Pilosa* additive first discharge.

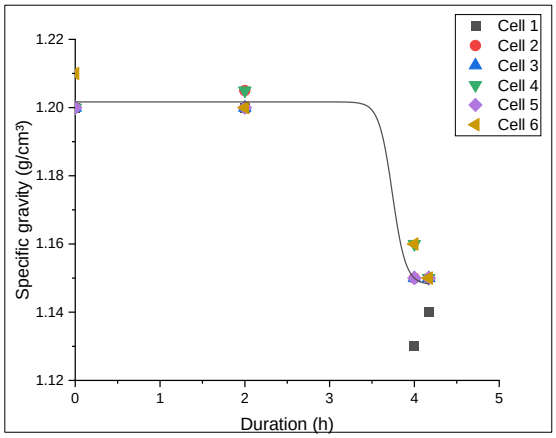

Figure 4.38: Electrolyte with 10% (w/v) *Bidens Pilosa* additive second discharge.

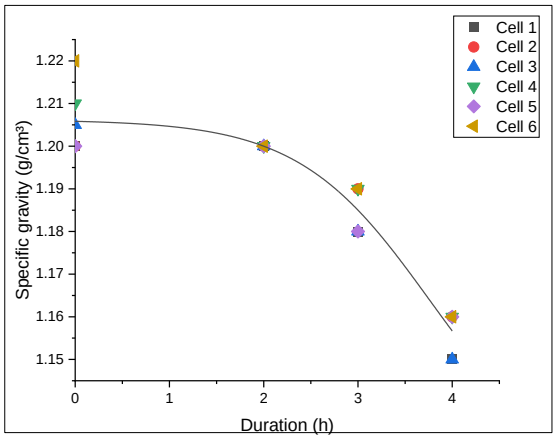

Figure 4.39: Electrolyte with 10% (w/v) *Bidens Pilosa* additive third discharge.

4.2.3.2 15.86% (w/v) *Bidens Pilosa* extract solution.

The maxima for the specific gravity of the six cells in the lead-acid battery containing 15.86% (w/v) *Bidens Pilosa* additive varied between 1.220g/cm³ to 1.180g/cm³ while the minima varied between 1.160 g/cm³ and 1.140 g/cm³ over the 3 charge/discharge cycles. The first charge cycle is illustrated in Figure 4.40, Figure 4.41 for the second charge cycle and Figure 4.42 for the third charge cycle.

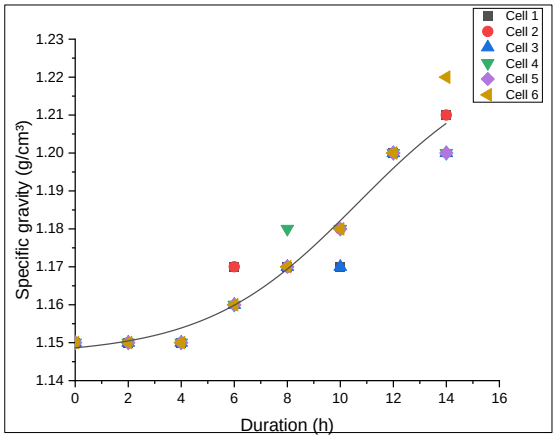

Figure 4.40: Electrolyte with15.86% (w/v) *Bidens Pilosa* extract first charge.

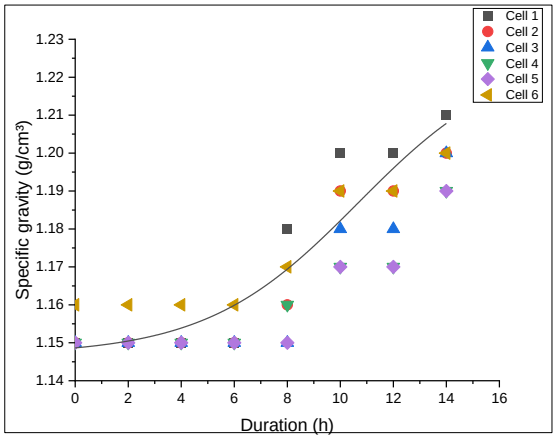

Figure 4.41: Electrolyte with15.86% (w/v) *Bidens Pilosa* extract second charge.

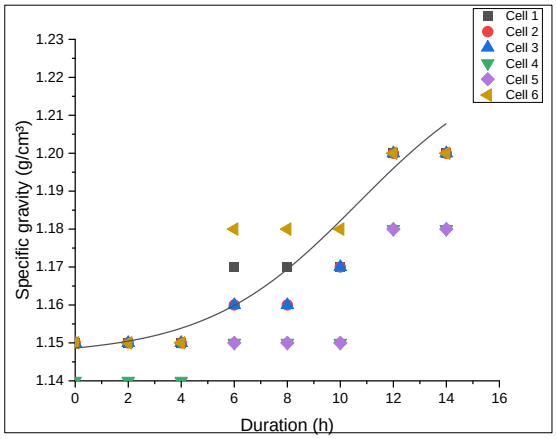

Figure 4.42: Electrolyte with15.86% (w/v) *Bidens Pilosa* extract third charge.

On discharge the relative density variation is represented in Figure 4.43, Figure 4.44 and Figure 4.45 for the first, second and third charge cycles respectively.

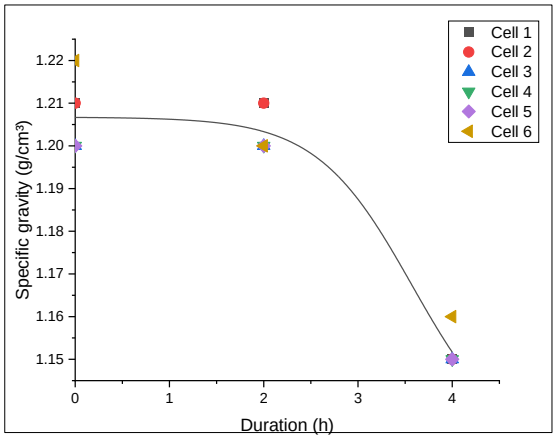

Figure 4.43: Electrolyte with 15.86% (w/v) *Bidens Pilosa* additive first discharge.

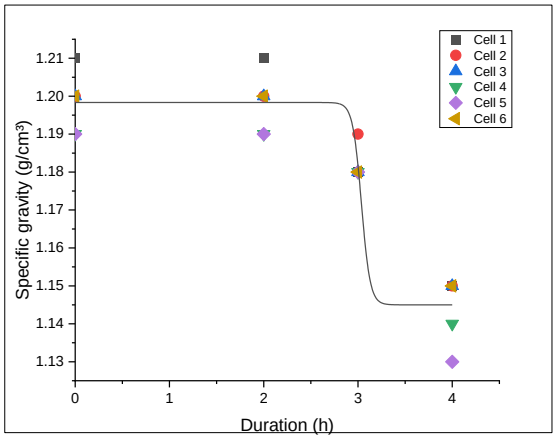

Figure 4.44: Electrolyte with 15.86% (w/v) *Bidens Pilosa* additive second discharge

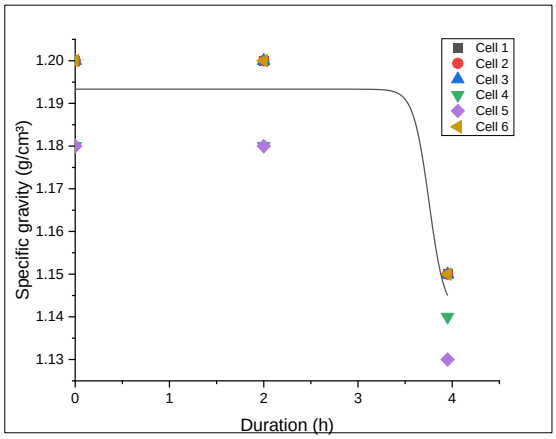

Figure 4.45: Electrolyte with 15.86% (w/v) *Bidens Pilosa* additive third discharge

4.2.3.3 30% (w/v) *Bidens Pilosa* extract solution.

For the electrolyte solution with 30% (w/v) *Bidens Pilosa* extract additive, specific gravity values varied for the maxima of 1.180 g/cm³ to 1.210 g/cm³ while the minima varied between 1.14 g/cm³ and 1.16 g/cm³ over the 3 charge/discharge cycles.

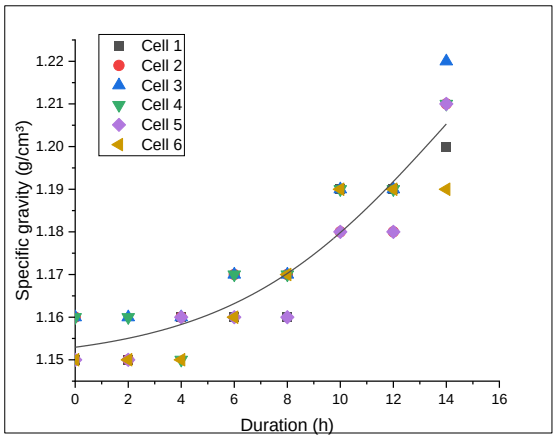

Figure 4.46: Electrolyte with 30% (w/v) *Bidens Pilosa* additive first charge

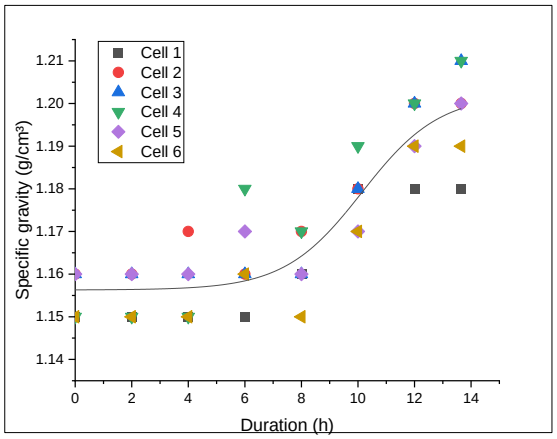

Figure 4.47: Electrolyte with 30% (w/v) *Bidens Pilosa* additive second charge.

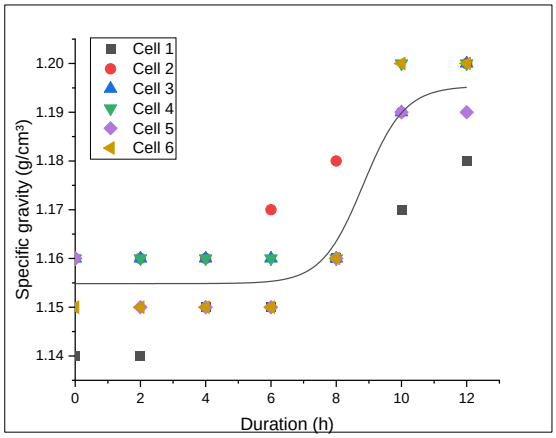

Figure 4.48: Electrolyte with 30% (w/v) *Bidens Pilosa* additive third charge cycle

Similarly, on discharge the specific gravity varies in descending manner due to the same factors that influence the change in the charge cycle. The following graphs illustrate the behavior of the specific gravity on discharge.

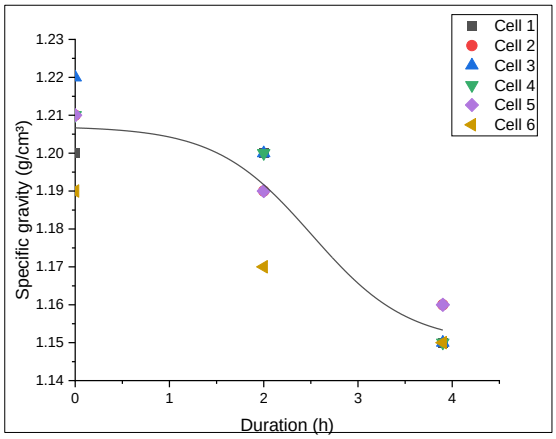

Figure 4.49: Electrolyte with 30% (w/v) *Bidens Pilosa* additive first discharge cycle.

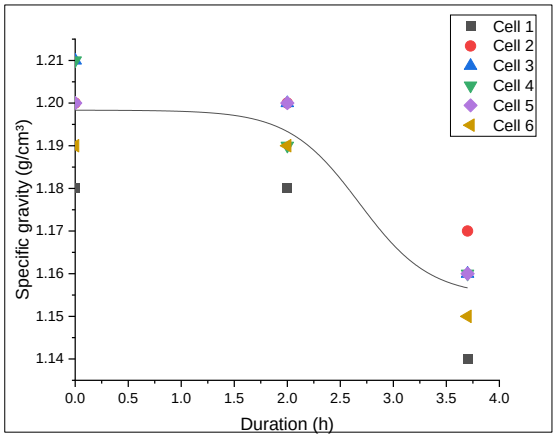

Figure 4.50: Electrolyte with 30% (w/v) *Bidens Pilosa* additive second discharge cycle.

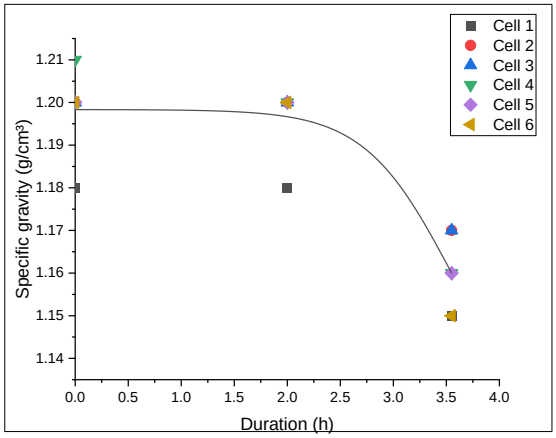

Figure 4.51: Electrolyte with 30% (w/v) *Bidens Pilosa* additive third discharge cycle

4.2.3.4 44.14% (w/v) *Bidens Pilosa* extract solution.

The maxima specific gravity for the battery with 44.14% (w/v) *Bidens Pilosa* additive per cell varied between 1.170 g/cm³ to 1.230 g/cm³ at full charge as illustrated in Figure 4.52, Figure 4.53 and Figure 4.54 while at the voltage cut-off point the minima varied between 1.50 g/cm³ and 1.230 g/cm³.

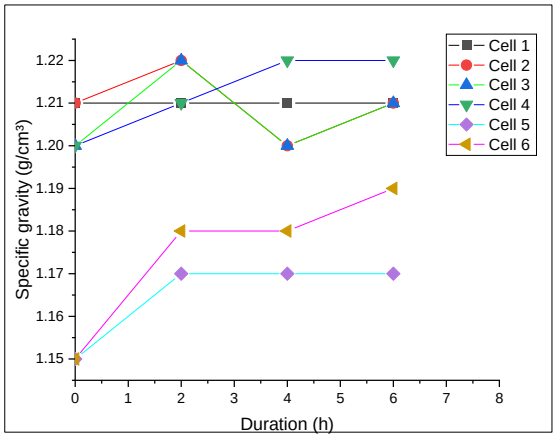

Figure 4.52: 44.14% (w/v) *Bidens Pilosa* additive first charge cycle.

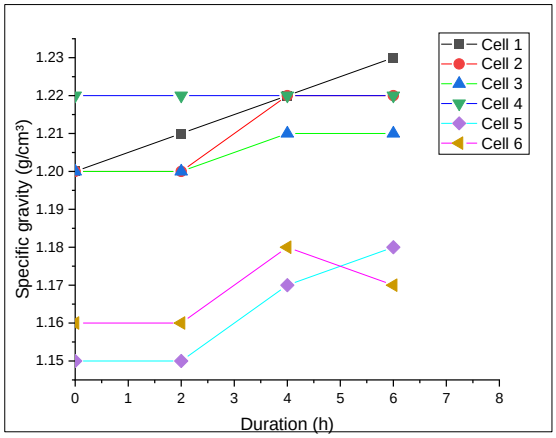

Figure 4.53: 44.14% (w/v) *Bidens Pilosa* additive second charge cycle

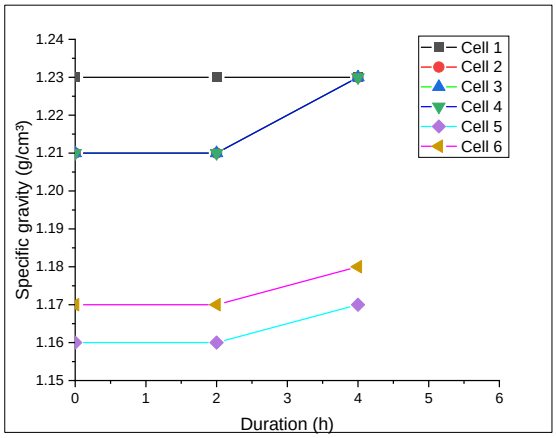

Figure 4.54: 44.14% (w/v) *Bidens Pilosa* additive third charge cycle

On discharge the specific gravity varies in descending manner due to the same factors that influence the change in the charge cycle. The following graphs illustrate the behavior of the specific gravity on discharge.

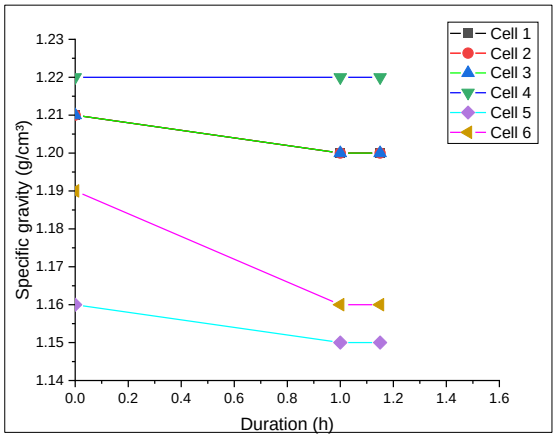

Figure 4.55: 44.14% (w/v) *Bidens Pilosa* additive first discharge cycle

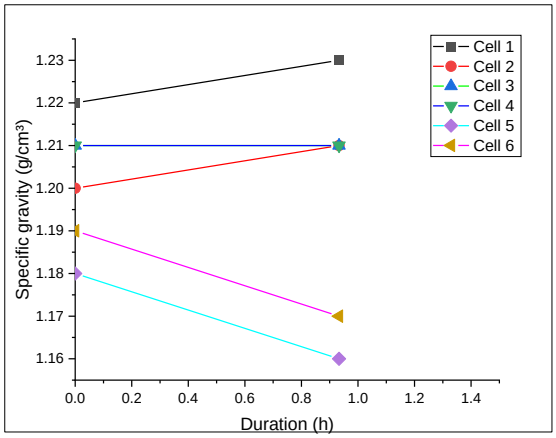

Figure 4.56: 44.14% (w/v) *Bidens Pilosa* additive second discharge cycle.

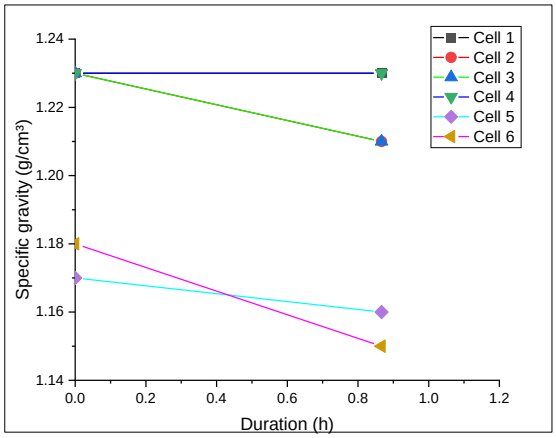

Figure 4.57: 1.7% (v/v) *Bidens Pilosa* additive third discharge cycle.

4.3 Evaluation and Comparison of Battery Discharge Capacity

Lead sulfate is formed when lead acid cells are discharged because of chemical processes that liberate electrons and hydrogen ions at the negative electrode. These electrons travel, diffuse, and migrate to the positive electrode. The potential difference between the two electrodes is decreased during this process and electric energy is produced as a result of these activities. During the charging process, lead sulfate produced at the negative electrode is reduced back to lead, whereas that at the positive electrode is oxidized to lead dioxide, resulting in the generation of electric energy (Pavlov, 2017b). The action of these elementary processes and the corresponding effect of the plant extract additive in the electrolyte solution is discussed below.

4.3.1 Charge cycle

Lead sulfate, which forms at the negative electrode of a lead acid cell, is converted back into lead during charge, while lead dioxide, which forms at the positive electrode, is converted into lead sulfate. As a result, the active materials at the two electrodes are recovered, and electric energy is accumulated. Voltage rises between the two electrodes. The foregoing charge processes at the two electrodes result in the formation of sulfuric acid, which raises the acid content in the electrolyte. (Pavlov, 2011) .

4.3.1.1 Charge cycle for *Hibiscus Sabdariffa* extract electrolyte solutions.

The difference in duration of charge duration as shown in indicates the varying effect of additive material on charge acceptance. As further evidenced by Pavlov (Pavlov, 2017c), as the amount of additives in the electrolyte solution increases, the charge acceptance accelerates. The diffusion rate of Pb^{2+} ions through the porous $PbSO_4$ layer is influenced by the difference in concentration of Pb^{2+} ions in the pores of the $PbSO_4$ and the additive layer adsorbed on the electrode surface. This diffusion rate determines the rate of charge processes.

However, during battery discharge, the active surface of the electrode is reduced due to the thickness of the active groups in the adsorbed additive layer, which suppresses oxidation and restricts the participation of active materials in the electrochemical reactions, lowering the voltage that is available. Since the concentration is substantially lower, it appears that the reduction of Pb^{2+}ions during the charge process is expedited.

Table 6: Roselle additive charge cycle.

Electrolyte solution	Standard	10% (w/v)	15.86% (w/v)	30% (w/v)	44% (w/v)
Cycle 1	18	17.63	16.67	17.35	18.5
Cycle 2	17	16.5	16.03	15.6	12.5
Cycle 3	16	15.52	15.42	15.87	12.38

The reason for the decrease in electrode charge acceptance hence extended charge duration in the first cycle of the 44.14% (w/v) Roselle that could explain the margin with the second and third charge cycles is that cathodic process of reduction of Pb^{2+} ions is retarded because of their slow diffusion through the adsorbed additive layer and $PbSO_4$ layer which is also a result in the thickness of a non- porous additive layer.

The cathodic process of Pb^{2+} ion reduction is delayed because of their slow diffusion through the adsorbed additive layer and $PbSO_4$ layer, which is also a result of the thickness of a non-porous additive layer. The result is a decrease in electrode charge acceptance hence extended charge duration as can be interpreted from the difference in the obtained values (Figure 4.58) for first charge cycle of the 44.14% (w/v) Roselle by comparison to the second and third charge cycles.

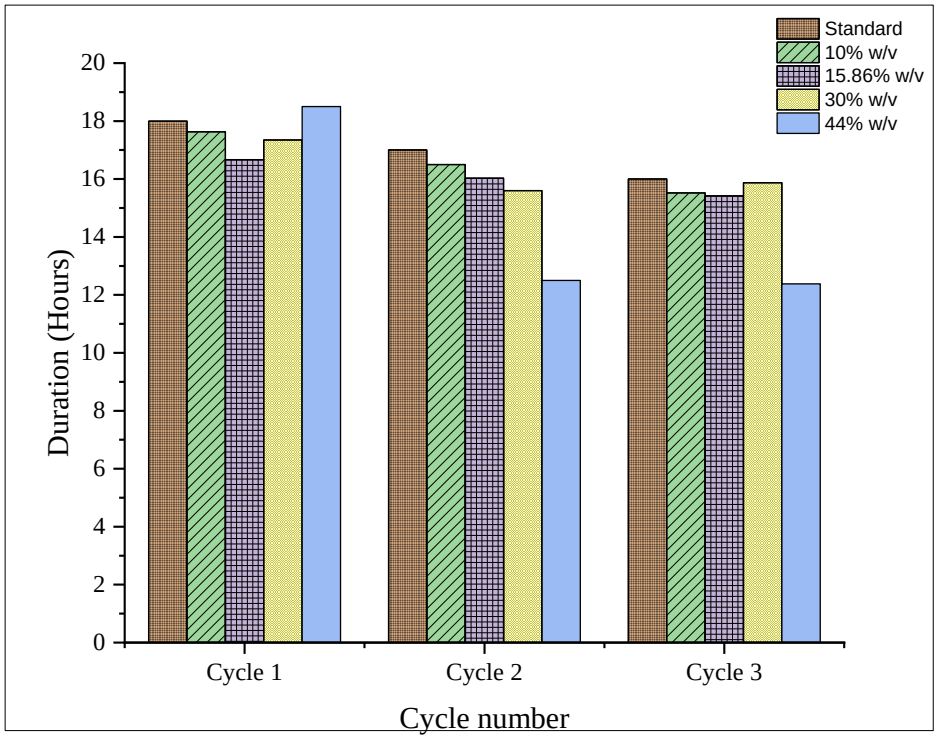

Figure 4.58: Roselle extracts additive charge cycle.

4.3.1.2 Charge cycle for Blackjack additive electrolyte solutions

As shown in Table 7, the presence of these additives also had an impact on charge acceptance in the electrolyte containing various amounts of *Bidens Pilosa* extracts. Compared to the conventional electrolyte solution, blackjack additive-electrolyte solutions consistently displayed superior charge profiles throughout all charge cycles. The effectiveness of the additions is further depicted in Figure 4.59, it can be seen that

the lead-acid battery became more effective at maintaining excellent charge acceptance due to the presence of the blackjack additives.

Table 7: Black additive electrolyte solution charge cycle.

Electrolyte solution	Standard	10% (w/v)	15.86%(w/v)	30% (w/v)	44.14%(w/v)
Cycle 1	18	17.18	15.05	14.92	6.75
Cycle 2	17	14.98	14.35	13.65	6.32
Cycle 3	16	15.05	14.08	13.13	5.45

Comparing the charge cycles in Table 6 and Table 7 will show the difference in activity between the Roselle and Blackjack additives. The time required to charge the *Hibiscus Sabdariffa* additive electrolyte solutions ranged from 17.63 - 12.38 hours compared to 17.18 – 5.45 hours for the blackjack additive electrolyte solutions. These variations imply that a variety of variables, such as molecular weight, chemical structure, component purity, and chemical stability, affect the activity of additives in the electrolyte solution.

It was discovered that phenolic groups improve negative plate properties (Pavlov, 2017a). The phenolic content of *Hibiscus Sabdariffa* aqueous extract was 72.22 mg/g (Al-Hashimi, 2012). Saponin content in *Bidens Pilosa* aqueous extract was 10 ±0.01 mg/g and the quantity tannin was 13-14 mg/g (Owoyemi & Oladunmoye, 2017). Such differences in the yield of these phytochemicals determines the interaction behavior of the plant extracts solution with battery active materials during the charge/discharge cycles.

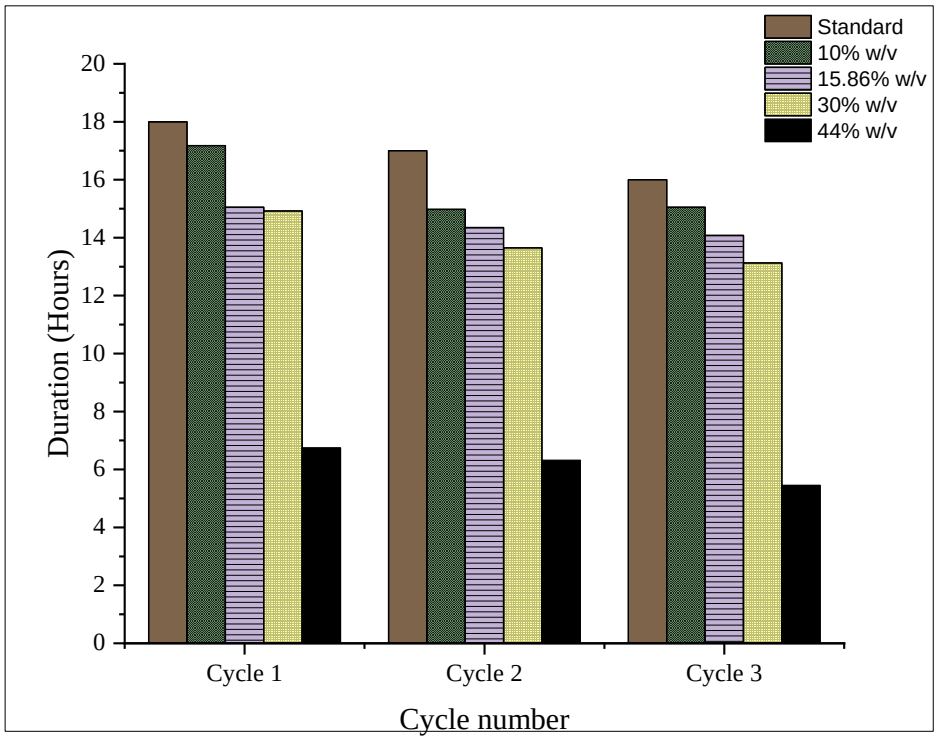

Figure 4.59: Blackjack additive charge cycle.

The results obtained from these experiments suggest that the cathodic process of the reduction of Pb^{2+} ions is accelerated due to their rapid diffusion through the combination of the $PbSO_4$ layer and adsorbed plant extract layers. The implication is that charging time improves with a corresponding increase in plant extracts additive volume and concentration thus electrode charge acceptance improves on the electrode surface. The improvements that are shown during charging whereas the inverse is true during discharge. Similar observations are made by Pavlov and Boden when they discussed the impact of organic components present in expander material used in lead-acid battery (Boden, 2004; Pavlov, 2017a)

4.3.2 Discharge cycle.

Variations in the time taken to discharge the batteries containing different plant extract additives was indicative of the effect of the interaction of the additives and the battery active materials and shall be discussed.

4.3.2.1 Results - *Hibiscus Sabdariffa* extract additive solution.

A significant result was obtained in the Roselle additive electrolyte solution with an additive concentration of 15.86% (w/v) with an observed improvement in the discharge duration by 0.13 hours relative to the conventional electrolyte over the first cycle and 0.03 hours during the second discharge cycle. Other improvements in discharge duration were observed in the first and third cycles of the 10% (w/v) Roselle extract electrolyte mixture. As shown in Figure 4.60, a decrease in discharge capacity is observed with increase in additive concentration of 30% and 44.14%.

Table 8: Roselle electrolyte solution discharge duration.

Electrolyte solution	Conventional	10% (w/v)	15.86%(w/v)	30% (w/v)	44.14%(w/v)
Cycle 1	4.5	4.53	4.63	4.017	3.72
Cycle 2	4.4	4.37	4.43	3.87	3.85
Cycle 3	4.25	4.3	4.18	4	3.37

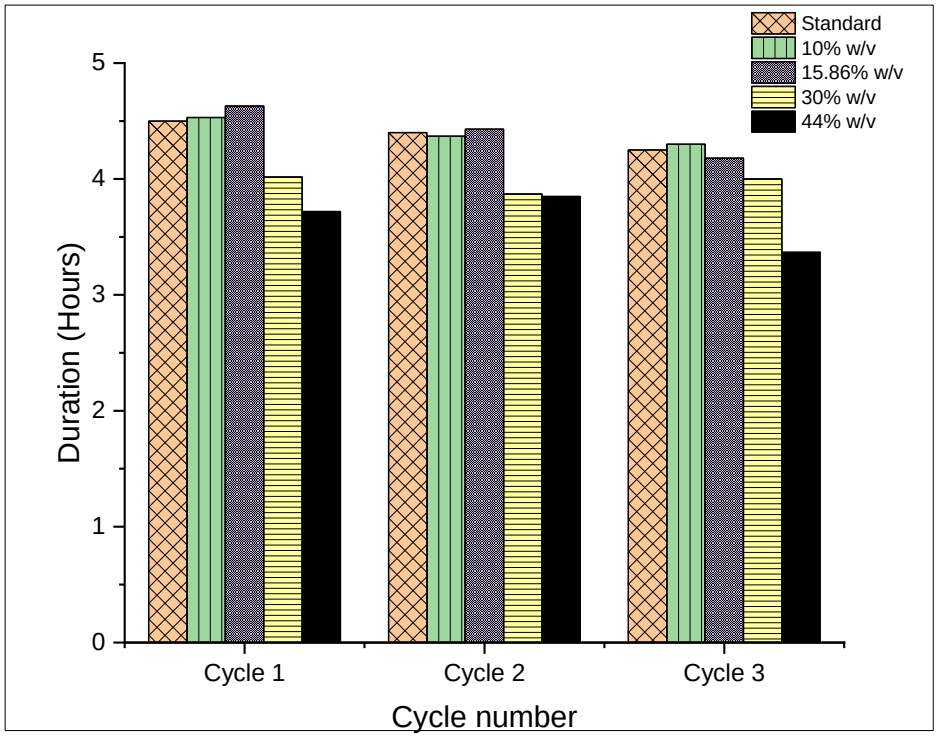

Figure 4.60: Roselle additive discharge duration plot.

4.3.2.2 Results - *Bidens Pilosa* extract additive electrolyte solution.

The electrolyte solutions with *Bidens Pilosa* additive did not achieve any improvement in the discharge capacity by comparison with the standard (conventional) electrolyte solution over three charge/ discharge cycles as indicated in Table 9 below. The highest discharge duration for the additive electrolyte solutions was achieved in the first discharge cycle of 10% (w/v) *Bidens Pilosa* extract electrolyte solution. This, however, was less than the relative duration to the standard electrolyte solution over the same cycle. Similarly, as illustrated in Figure 4.61, an increase in concentration resulted in further reduction in discharge capacity of the lead-acid acid battery, with a 52-minute discharge duration at 44% concentration being the least achieved.

Table 9: Blackjack electrolyte solution discharge duration

Electrolyte solution	Standard	10% (w/v)	15.86% (w/v)	30% (w/v)	44.14%(w/v)
Cycle 1	4.5	4.37	4.32	3.9	1.15
Cycle 2	4.4	4.17	4.13	3.7	0.933
Cycle 3	4.25	4	3.95	3.55	0.867

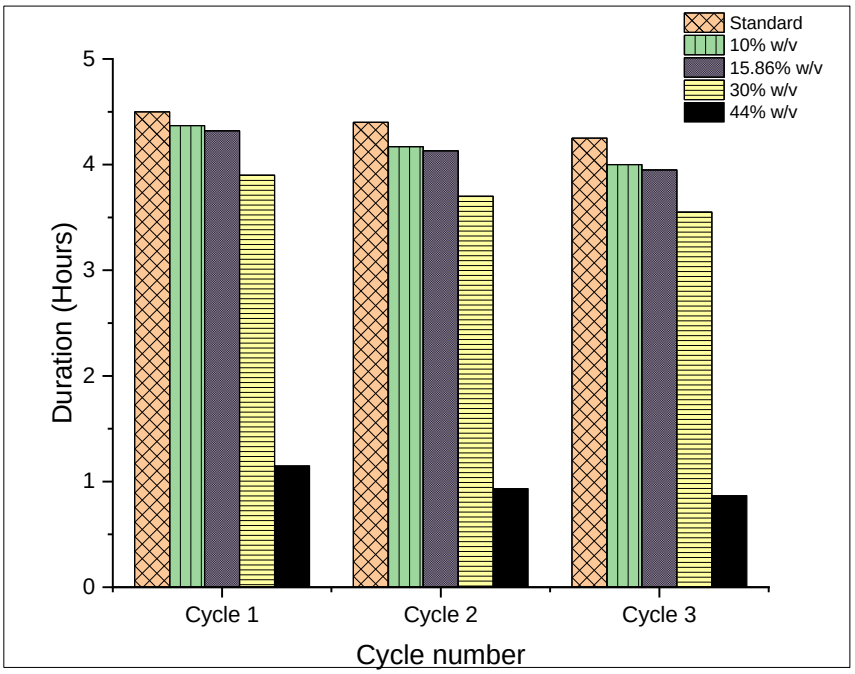

Figure 4.61: Blackjack additive discharge duration plot.

4.3.2.3 Discussion of results – Discharge cycle

Electrons and hydrogen ions are released at the cathode during the discharge of the lead-acid cell because of electrochemical reactions within the cell. The electrons and hydrogen ions disperse and migrate to the anode where they create lead sulfate. As a result of these electrochemical activities, the potential difference between the anode and the cathode is decreased and electric energy is produced (Pavlov, 2017b).

For this study, the natural plant extracts additives were used with the intention of enhancing the utilization of the active negative active material and extending battery discharge capacity. As shown in the results obtained from the experiments, a variation in the discharge duration seems to be influenced by the action of adsorbed additive substances on the lead surface which agrees with observations made by other researchers (Bhattacharya & Basumallick, 2003; Pavlov, 2011) on the behavior and interaction of battery active components and additives. There is an increase in the surface area of the electrode as result of the adsorption of the additive, thus the lead sulfate layer on the electrode becomes more porous making it easier for the ions to enter the negative active material's inner structure in the electrolyte solutions. This led to an improvement in discharge capacity. On the other hand, early passivation of the electrodes is evidenced by the loss of discharge capacity for some Roselle additive electrolyte solutions and in all Blackjack additive battery electrolyte suggesting that the sulfate + additive layer suppresses the flow of electrons and hydrogen ions.

In similar studies, it was discovered that the electrode potentials may be altered in various ways. The activity of solid Pb may change due to the specific additives that adsorb to it, modifying the surface coverage of the reaction-active surface; the activity of the SO_4^{2-} ion may change due to the presence of the additive in the electrolyte; and

the activity of the $PbSO_4$ layer may also change over time due to changes in the morphological features (Bhattacharya & Basumallick, 2003).

Lignosulfonates, a few humic acids, and tannic products were used to evaluate how organic components affected the inhibition of the passivation of the lead electrode (Pavlov, 2017a). It was discovered that while battery life, when limited by the negative plates, improves with an increase in the concentration of carboxylic and phenolic groups and of lignin purity, their charge acceptance decreases, and their self-discharge increases.

Being natural plant products, tannins have an excess of nearby phenolic hydroxyls, which enables them to form stable connections with heavy metal ions such as lead (Pb (II)) (Meethale Kunnambath & Thirumalaisamy, 2015). They also interact with adhesins, obstruct membranes, impair substrate availability, and complex metal ions (Tiwari et al., 2011). In contrast, saponins are a naturally occurring surface-active substance whose varied amphiphilic molecule configurations affect their extensive physicochemical properties and biological activity (Stanimirova et al., 2011).

As observed by Pavlov (Pavlov, 2017a), the chemical makeup and arrangement of the adsorbed expander layer, its affinity to Pb or $PbSO_4$ surfaces, and its electric charge were shown to impede the passivation phenomena caused by the $PbSO_4$ layer. Hence, in this study, it can be said that the active plant extracts' influence is what causes the observed change in discharge regimes compared to the lead-acid battery with standard electrolyte.

4.3.3 Coulombic efficiency

Studying the charging and discharging regimes across a number of operation cycles, a determination of the battery's coulombic efficiency can be made. According to the expression below, it is the ratio of the discharged Ah divided by the charged Ah.

$$\eta_{Ah} = \frac{Discharged\ Ah}{Charged\ Ah} = \frac{\int_0^t I\,dt}{\int_0^t I\,dt} \quad \ldots\ldots\ldots\ldots\ldots\ldots\ldots\ldots\ldots\ldots\ldots\ldots\ldots\ldots\ldots\ldots\ldots\ldots \textit{Equation 21}$$

Below is an illustration of the variability in coulombic efficiency with relation to the number of cycles.

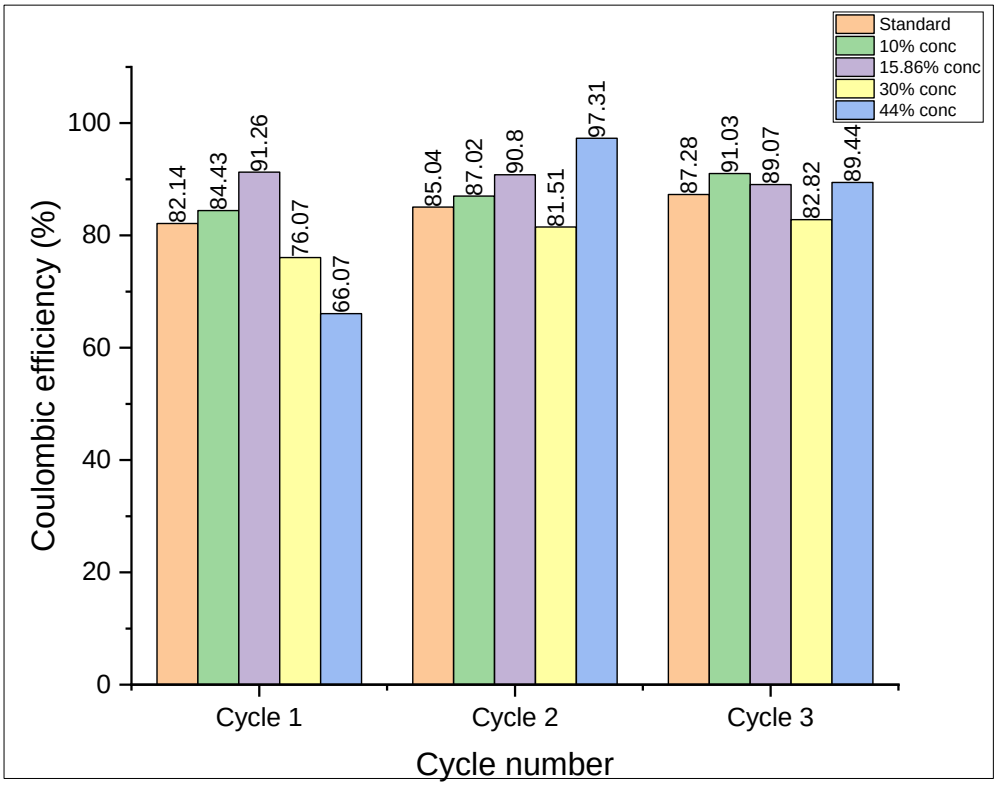

Figure 4.62: Coulombic efficiency of Roselle additive electrolyte solution.

It is frequently used as a measurable indicator for the reversibility of batteries and is the most used metric for measuring internal reactions that affect battery life. The Coulomb efficiency is typically less than 1, as the total electrical energy discharged from the battery is almost always less than the total electrical energy charged. Some of

the causes are electrolyte degradation, material aging, ambient temperature, and various charge-discharge current rates. The battery's internal resistance also consumes some electrical discharge energy (S. Wang et al., 2021).

Table 10: Coulombic efficiency of *Hibiscus Sabdariffa* additive.

Additive	Conventional	10% (w/v)	15.86%(w/v)	30% (w/v)	44.14% (w/v)
Cycle 1 (Ah %)	82.1	84.4	91.3	76.1	66.1
Cycle 2 (Ah %)	85.0	87.0	90.8	81.5	97.3
Cycle 3 (Ah %)	87.3	91.0	89.1	82.8	89.4

Lead acid batteries have a coulombic efficiency of about 90 percent (*BU-201*, 2010), 98 percent (Sauer, 2009), 85 percent (Rand & Moseley, 2015). It can be seen from the results of the experiment that in terms of the efficacy in the transfer of the electrons, the battery with Roselle 2% additive has a relatively lower coulombic efficiency value over the three charge cycles while the battery with 44.14% (w/v) Roselle extract achieved the least efficiency for the first charge/discharge cycle.

Table 11: Coulombic efficiency *Bidens Pilosa* additive.

Additive	Conventional	1.005% v/v	0.3% v/v	2% v/v	1.7% v/v
Cycle 1 (Ah %)	82.1	83.6	94.3	85.9	56.0
Cycle 2 (Ah %)	85.0	91.5	94.6	89.1	48.5
Cycle 3 (Ah %)	87.3	87.3	92.2	88.8	52.3

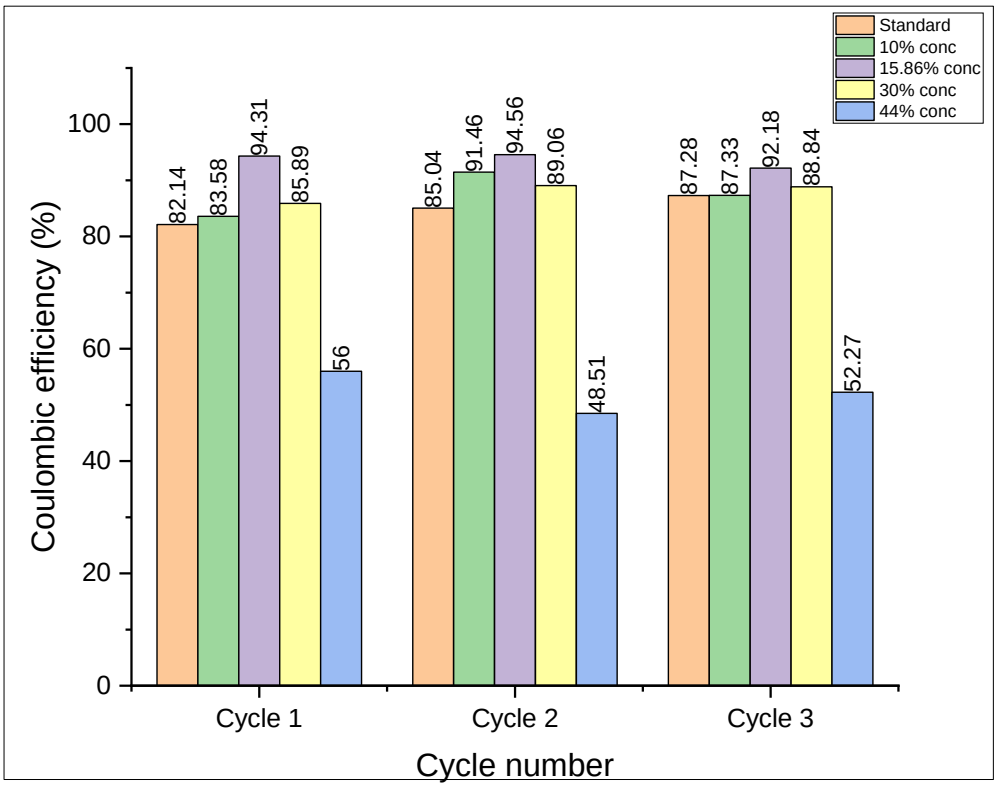

Figure 4.63: Coulombic efficiency of Blackjack additive electrolyte solution.

4.3.4 Energy efficiency

Energy efficiency is regarded as being of the utmost importance since it significantly affects the economics of battery operation and determines whether additional energy must be obtained to make up for losses. (Sauer, 2009). Lead-acid batteries have an energy efficiency of 80 – 85 percent (Sauer, 2009), 70 percent (Rand & Moseley, 2015), 75-90 percent (KITARONKA, Sefu, 2022). This measurement is determined by *equation 20*, which compares the quantity of energy (Watt-hours) that can be extracted from the battery to the amount of energy that was charged into the battery.

$$\eta_{Wh} = \frac{Discharged\ Wh}{Charged\ Wh} = \frac{\int_0^t I.U_{battery}\,dt}{\int_0^t I.U_{battery}\,dt} \quad \ldots\ldots\ldots\ldots\ldots\ldots\ldots\ldots\ldots\ldots \textit{equation 22}$$

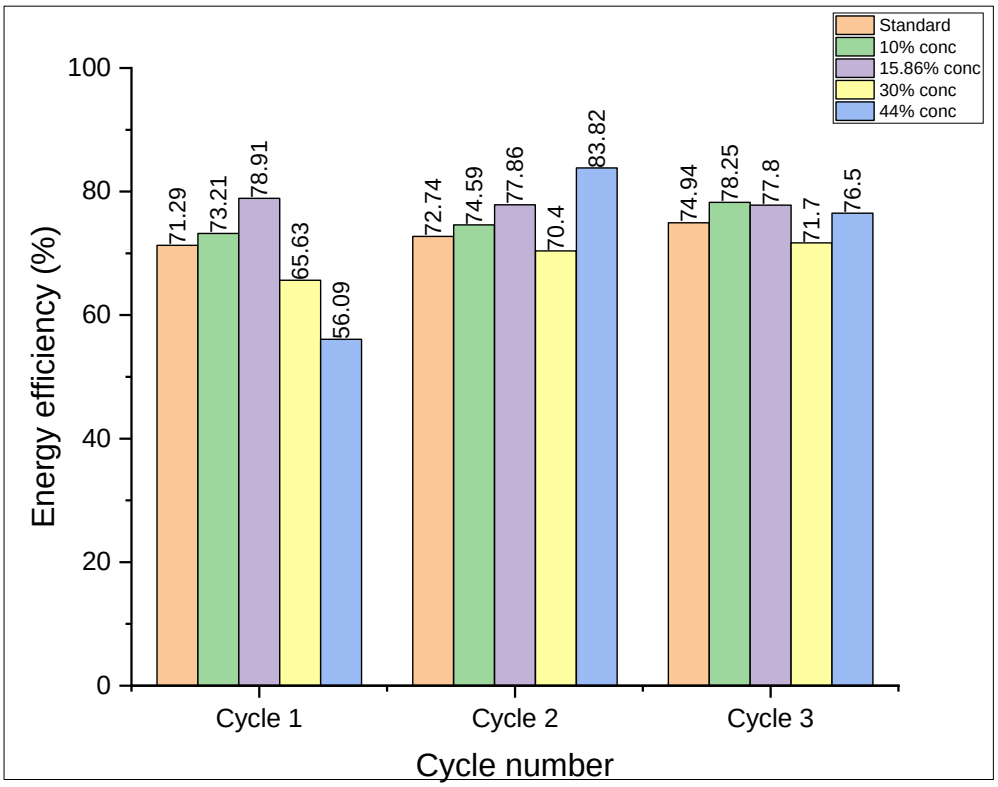

Figure 4.64: Energy efficiency of Roselle additive electrolyte solution

Table 12: Energy efficiency of Roselle additive electrolyte solution.

Additive	Standard	1.005% v/v	0.3%v/v	2%v/v	1.7% v/v
Cycle 1 (Wh %)	71.3	73.2	78.9	65.6	56.1
Cycle 2 (Wh %)	72.7	74.6	77.9	70.4	83.8
Cycle 3 (Wh %)	74.9	78.2	77.8	71.7	76.5

As can be seen in Figure 4.65, the battery with conventional electrolyte achieved efficiency of 71.29%, 72.74% and 74.94% over the first, second and third charge-discharge cycles respectively. Relative upward efficiency profiles were observed for the electrolyte with *Bidens Pilosa* additive as well as 1.005% (v/v) Roselle which indicate an improvement of the energy efficiency mainly as a result of the improvement in charge acceptance and charging time as was also observed by Hamed et al., 2018 (H. Hamed et al., 2018). The energy efficiency for the 1.005% (v/v) blackjack additive was

72.62%, 79.11% and 76.16%, the 1.005% (v/v) Roselle was 73.21%, 74.59% and 78.25% for the triplicated charge/discharge cycles respectively.

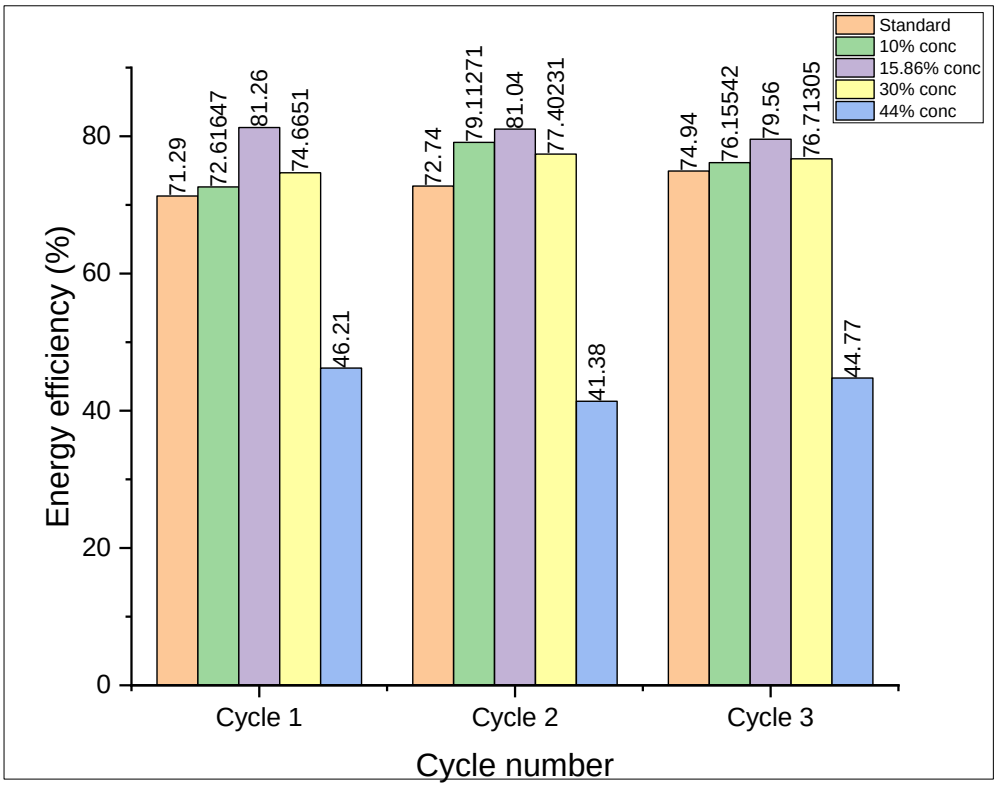

Figure 4.65: Energy efficiency of Blackjack additive electrolyte solution.

Table 13: Energy efficiency of Blackjack additive electrolyte solution.

Additive	Standard	1.005% v/v	0.3% v/v	2% v/v	1.7% v/v
Cycle 1 (Wh %)	71.3	72.6	81.3	74.7	46.2
Cycle 2 (Wh %)	72.7	79.1	81.0	77.4	41.4
Cycle 3 (Wh %)	74.9	76.2	79.6	76.7	44.8

4.4 Analysis and Optimization

The relationship between the battery discharge capacity and two controllable factors namely concentration and volume of additive was studied. From Table 14, a mathematical equation that evaluates the response variable as a function of controllable variables was created using a central composite design (CCD). The CCD is a frequently

used statistical technique for determining the regression model equations, optimizing process variables, and analyzing how different process factors interact. (Sadhukhan et al., 2016).

In this work, the CCD was utilized to identify the ideal process variables to increase the lead-acid battery's discharge capacity.

Table 14: Factor settings for improving discharge capacity of lead-acid battery.

Factor	Units	Minimum	Maximum	Coded Low	Coded High
Volume	ml	0.01	2	-1 ↔ 0.30	+1 ↔ 1.71
Concentration	g/ml %	10	50	+1 ↔ 44.14	+1 ↔ 44.14

4.4.1 *Bidens Pilosa* additive experiments.

4.4.1.1 Charge cycle

4.4.1.1.1 Analysis

Table 15 displays the results of a one-way analysis of variance (ANOVA) for the charge cycle. The model is not significant in comparison to the noise, according to the model's F-value of 6.82. The likelihood of noise causing an F-value this large is 26.14%. With a P-value of 0.2614, no meaningful model terms are present.

Table 15: ANOVA for linear model for *Bidens Pilosa* Charge cycle.

Source	Sum of Squares	df	Mean Square	F-value	p-value	
Model	59.18	2	29.59	6.82	0.2614	not significant
A-volume	6.8	1	6.8	1.57	0.4291	
B-concentration	48	1	48	11.05	0.186	
Residual	4.34	1	4.34			
Cor Total	63.52	3				

According to the predicted R^2, a negative value, the overall mean might be a more accurate predictor of the charge duration response than the existing model. The signal to noise ratio is a measure of adequate precision, with a ratio greater than 4 being preferred. Since the ratio of 5.975 in Table 16 suggests a sufficient signal and as such this model can be utilized to explore the design space.

Table 16: Fit statistic for *Bidens Pilosa* Charge cycle

Std. Dev.	2.08		R^2	0.9317
Mean	13.47		Adjusted R^2	0.795
C.V. %	15.46		Predicted R^2	-0.2303
			Adeq Precision	5.9753

The following linear model reveals how the individual variables affected the battery electrochemical processes during the first charge cycle, where X_1 represents volume and X_2 represents concentration; $Y = 10.9 + 1.99\,X_1 - 5.29\,X_2$

In Figure 4.66 shows a response surface model plot for the first charge cycle of the electrolyte solution with Blackjack additive shows a linear relationship between concentration and charge duration.

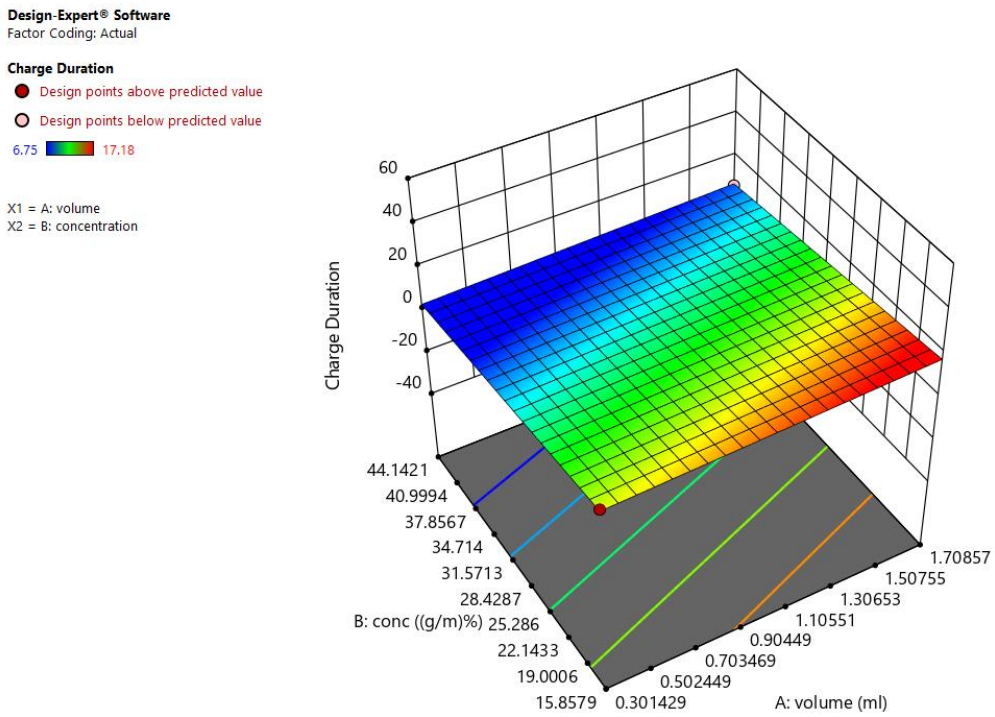

Figure 4.66: Surface model plot for the first charge cycle of the electrolyte solution with Blackjack additive.

4.4.1.1.2 Numerical optimization

A numerical optimization procedure using desirability function was done using Design expert software with the objective of maximizing utilization of battery active components in order to reduce charge duration by maintaining the dependent variables of volume and concentration within the specified ranges of the experiment design in Table 17. By seeking from 105 starting points (*Appendix g*) the best local maximum was found at extract volume of 0.301 % (v/v) and concentration of 44.14 (g/ml) %, at this condition the time of charge is at 3.62 hours as illustrated by the ramp Figure 4.67.

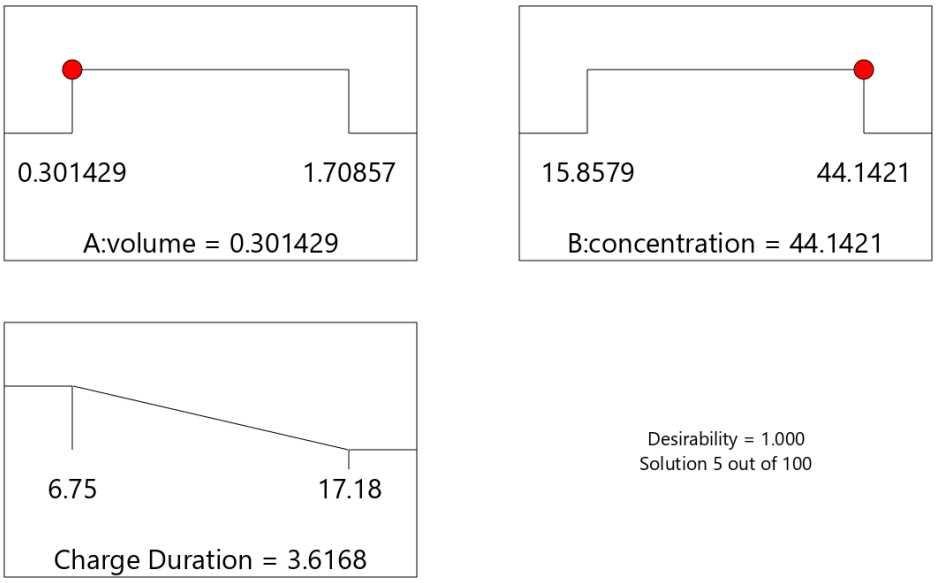

Figure 4.67: Desirability ramp of minimizing charge capacity using Blackjack additive.

4.4.1.2 Discharge capacity

4.4.1.2.1 Analysis

Table 17 displays the results of a one-way analysis of variance (ANOVA) for the charge cycle. The model is not significant in comparison to the noise, according to the model's F-value of 2.89. The probability of noise causing an F-value this large is 38.40%. With a P-value of 0.384, no meaningful model terms are present.

Table 17: ANOVA for linear model for *Bidens Pilosa* discharge cycle.

Source	Sum of Squares	df	Mean Square	F-value	p-value	
Model	6.05	2	3.02	2.89	0.384	not significant
A-volume	0.2829	1	0.2829	0.2704	0.6947	
B-concentration	4.25	1	4.25	4.06	0.2933	
Residual	1.05	1	1.05			
Cor Total	7.09	3				

According to the fit statistic presented in Table 18, the overall mean, with a predicted R2 value of -1.654, may be a better predictor of the discharge cycle response than the existing model, . In some circumstances, a higher order model might potentially be

more accurate. An inadequate signal is indicated by a ratio of 3.83, making this model inappropriate for navigating the design space.

Table 18: Fit statistic for *Bidens Pilosa* discharge cycle

Std. Dev.	1.02		R^2	0.8526
Mean	3.44		Adjusted R^2	0.5577
C.V. %	29.78		Predicted R^2	-1.654
			Adeq Precision	3.8305

The following linear model reveals how the individual variables affected the battery electrochemical processes during the first charge cycle, where X_1 represents volume and X_2 for concentration: $Y = 2.73 + 0.41\,X_1 - 1.57\,X_2$

Shown in Figure 4.68 is a response surface model plot for the first charge cycle of the electrolyte solution with Blackjack additive shows a linear relationship between concentration and discharge duration.

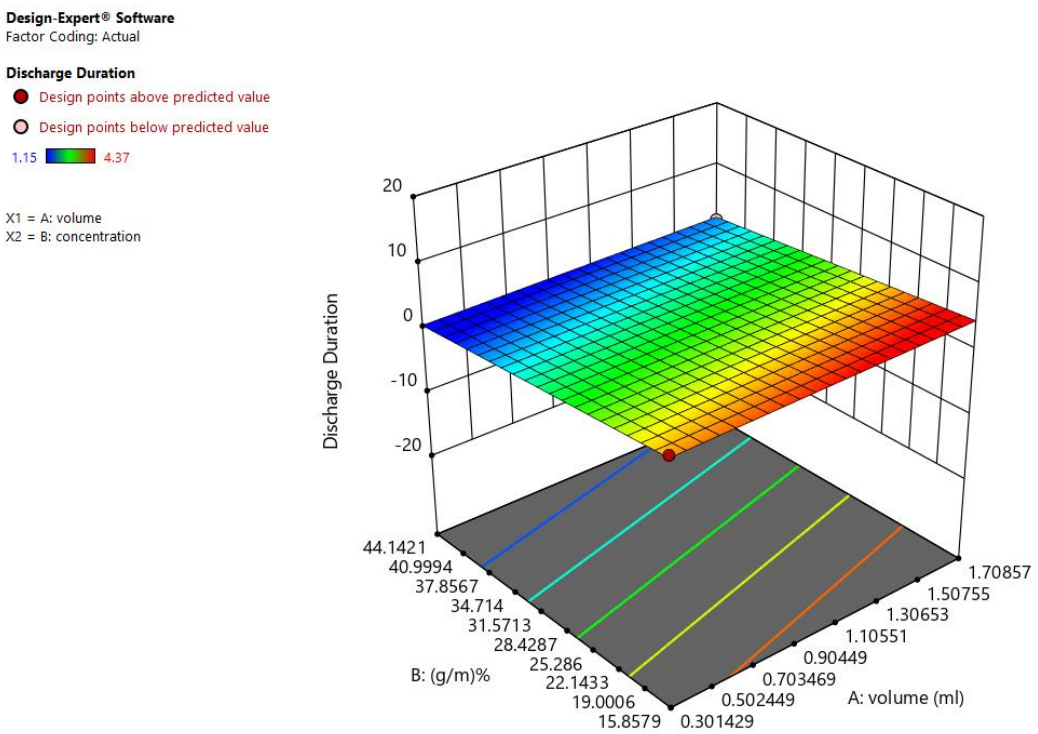

Figure 4.68: surface model plot for the first discharge cycle of the electrolyte solution with Blackjack additive.

4.4.1.2.2 Numerical optimization

A numerical optimization procedure using desirability function with the objective of maximizing utilization of battery active components thus increasing discharge duration by maintaining the dependent variables of volume and concentration within the specified ranges of the experiment design. By seeking from 105 starting points the optimum value was found at extract volume of 1.7 % (v/v) and concentration of 15.85 (g/ml) % from 94 possible solutions shown in *Appendix h*. At this point the duration of discharge was 4.71 hours.

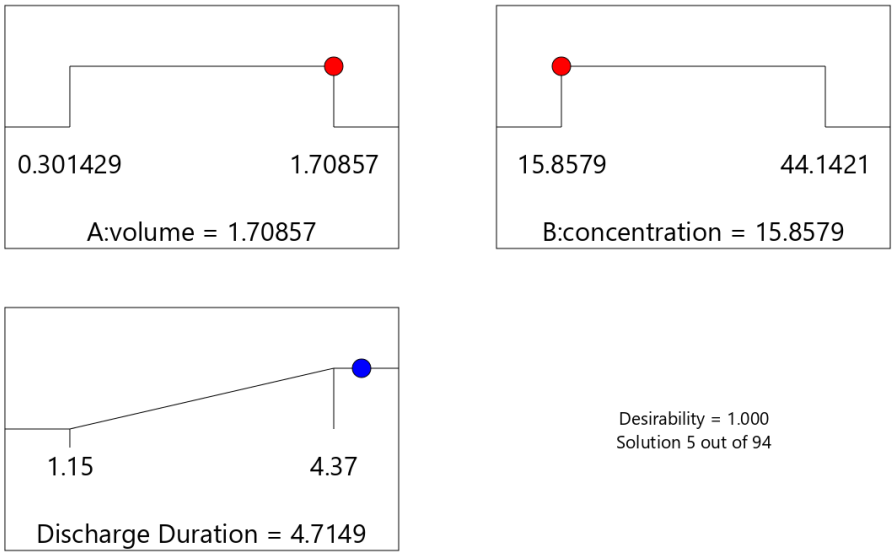

Figure 4.69: Desirability ramp of maximizing discharge capacity using Blackjack additive.

4.4.2 *Hibiscus Sabdariffa* additive experiments

4.4.2.1 Charge cycle

4.4.2.1.1 Analysis

Table 19 displays the results of a one-way analysis of variance (ANOVA) for the charge cycle. The model is not significant in comparison to the noise, according to the model

F-value of 0.54. An F-value this large could result from noise in 69.24% of cases. The P-value of 0.6924 indicates that there are no significant model terms.

Table 19: ANOVA for linear model for Roselle charge cycle.

Source	Sum of Squares	df	Mean Square	F-value	p-value	
Model	0.8968	2	0.4484	0.543	0.6924	not significant
A-volume	0.0719	1	0.0719	0.0871	0.8173	
B-concentration	0.1972	1	0.1972	0.2388	0.7106	
Residual	0.8258	1	0.8258			
Cor Total	1.72	3				

According to the predicted R^2 in Table 20, the overall mean might be a more accurate predictor of the response than the current model. This model cannot be used to explore the design space since the adequate Precision ratio of 1.38 suggests an insufficient signal.

Table 201: Fit statistic for Roselle charge cycle

Std. Dev.	0.9088		R^2	0.5206
Mean	17.54		Adjusted R^2	-0.4382
C.V. %	5.18		Predicted R^2	-7.629
			Adeq Precision	1.3825

The following linear model reveals how the individual variables affected the battery electrochemical processes during the first charge cycle, where X_1 represents volume and X_2 represents concentration; $Y = 17.59 + 0.205\,X_1 + 0.34\,X_2$

A response surface plot for the first charge cycle of the electrolyte solution with Roselle additive in Figure 4.70 shows a linear relationship between concentration and charge duration

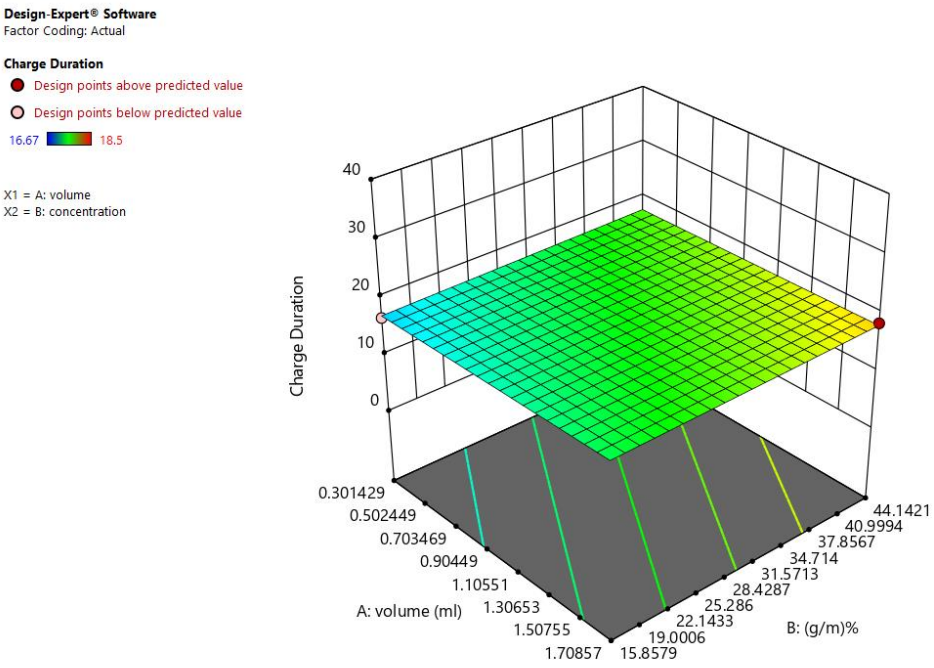

Figure 4.70: Response surface plot for Roselle charge cycle

4.4.2.1.2 Numerical optimization

By seeking from 105 starting points the best local minimum was found using a desirability function at extract volume of 0.301 %(v/v) and concentration of 15.86 (g/ml) % from possible solutions in *Appendix i* At this condition the estimated duration of charge is at 17.01 hours as illustrated by the ramp Figure 4.71

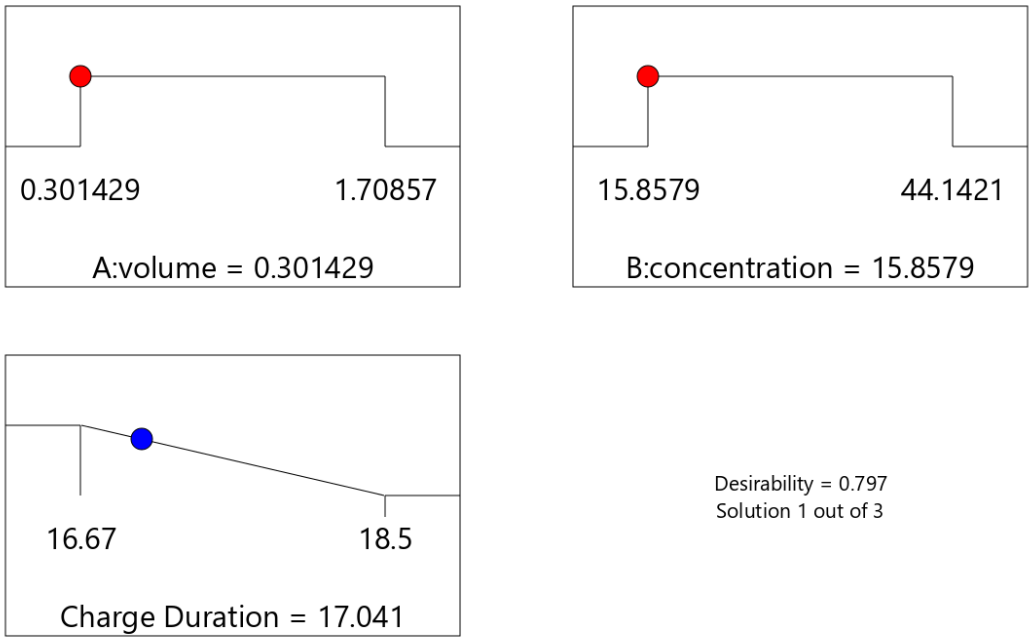

Figure 4.71: Desirability ramp for maximizing charge capacity using Roselle additive.

4.4.2.2 Discharge cycle

4.4.2.2.1 Analysis

Table 21 displays the results of a one-way analysis of variance (ANOVA) for the charge cycle. The model is not significant in comparison to the noise, according to the model's F-value of 48.44. An F-value of this size has a 10.11% possibility of being caused by noise. Model terms are not significant, as indicated by the P-value of 0.1011.

Table 212: ANOVA for linear model for Roselle discharge cycle

Source	Sum of Squares	Df	Mean Square	F-value	p-value	Conclusion
Model	0.5497	2	0.2748	48.44	0.1011	not significant
A-volume	0.0348	1	0.0348	6.13	0.2443	
B-concentration	0.1361	1	0.1361	23.99	0.1282	
Residual	0.0057	1	0.0057			
Cor Total	0.5553	3				

The fit statistic in Table 22 shows a predicted R^2 of 0.8161 which is in reasonable agreement with the adjusted R^2 of 0.9693 by a difference of less than 0.2. The ratio of 13.007, which is more than 4 and denotes an appropriate signal, is the desired adequate precision for the discharge capacity response for Roselle, and this model can be utilized to navigate the design space.

Table 22: Fit statistic for Roselle discharge cycle

Std. Dev.	0.0753		R^2	0.9898
Mean	4.22		Adjusted R^2	0.9693
C.V. %	1.78		Predicted R^2	0.8161
			Adeq Precision	13.0071

The following linear model reveals how the individual variables affected the battery electrochemical processes during the first discharge cycle, where X_1 represents volume and X_2 represents concentration: $Y = 4.17 - 0.143\,X_1 - 0.282\,X_2$

A response surface plot for the first discharge cycle of the electrolyte solutions with Roselle additive shows a linear relationship between concentration and charge duration.

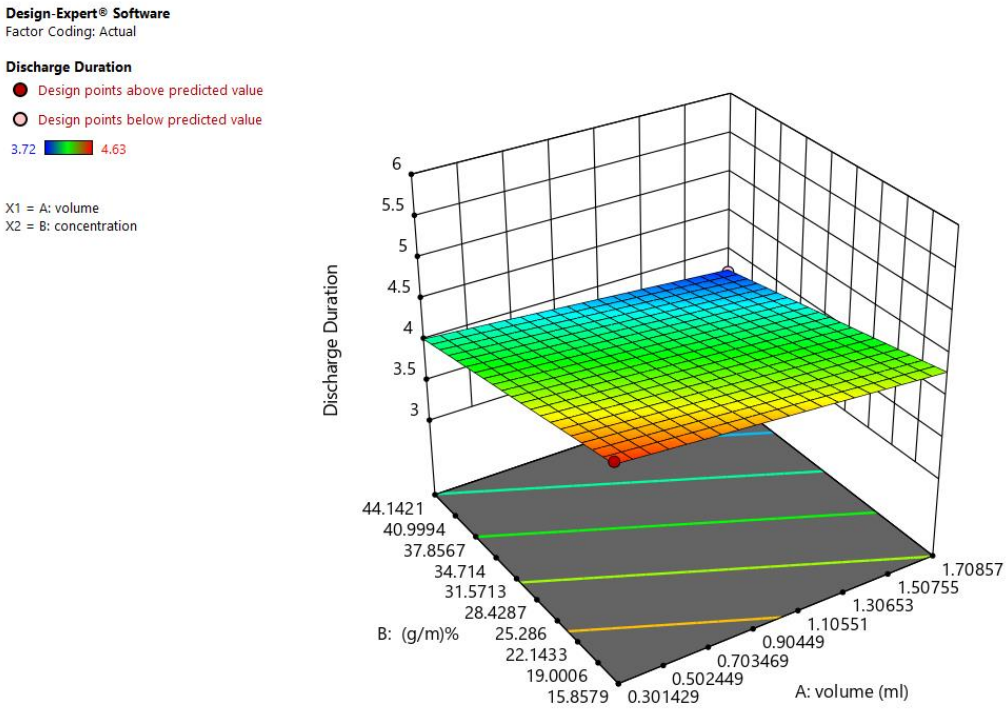

Figure 4.72: Response surface plot for Roselle discharge cycle

4.4.2.2.2 Numerical optimization

By seeking from 105 starting points the optimum value (Figure 4.73) was found at extract volume of 0.301% (v/v) and concentration of 15.86 (g/ml) % from 6 possible solutions shown in *Appendix j*.

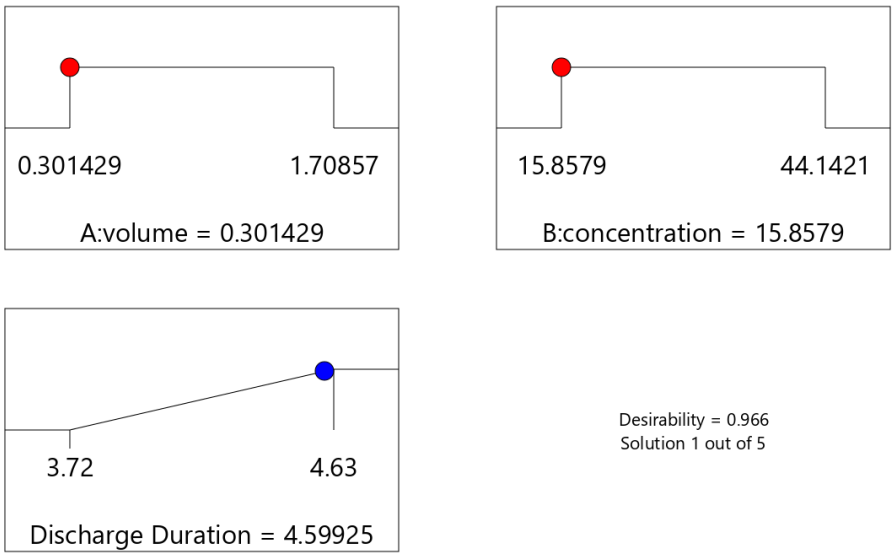

Figure 4.73: Desirability ramp for maximizing discharge capacity using Roselle additive.

CHAPTER 5: CONCLUSION AND RECOMMENDATIONS

5.1 Conclusion

The results gathered have led to the following conclusions:

1. Electrolyte additive developed from *Hibiscus Sabdariffa*'s calyces was subjected to phytochemical analysis which identified various bioactive components that influenced battery performance, these included saponins, tannins, carboxylic acids, and flavonoids. It was also revealed that electrolyte additive developed from *Bidens Pilosa* leaf extract contained a variety of secondary metabolites, such as saponins and tannins.
2. To establish the electrochemical effect of active groups (Saponins, tannins, etc.) in plant extract additive and on cell potential, it was shown that presence of plant extract additives does not affect the variation of the optimum concentration (specific gravity) of the dilute sulfuric acid (H_2SO_4) during charge/discharge cycles such that it is maintained between the empirically tested 1.10 g/cm³ and 1.28 g/cm³.
3. Variation of discharge rates indicates that formation and dissolution of lead sulfate precipitate is affected by the presence of plant bio-active compounds adsorbed on the electrode surface. The migration and diffusion of electrons and hydrogen ions released at the cathode are improved or restricted by the porosity of the lead sulfate layer that forms.
4. A numerical optimization procedure determined the following quantity and concentration of plant extracts for optimum battery performance; 0.301 %(v/v) and concentration of 15.86 (g/ml) % for the Roselle additive, 1.7%(v/v) and concentration of 15.85 (g/ml) % of blackjack additive to obtain the shortest

charge cycle and 1.7 %(v/v) and concentration of 15.85 (g/ml) % of blackjack additive to maximize duration on discharge.

5. The difference in results obtained in Roselle and Blackjack additive is because of the difference in quantity of phytochemicals depot in respective plant material. Variables like different soil chemistry, rainfall, topography, and climate that have an impact on how plants interact with their surroundings affect the concentration of bioactive substances in plant leaves, which in turn affects the observed effect of plant extracts additive in the battery electrolyte solution.
6. This study investigates a novel approach that uses of plant extracts as additive to the electrolyte of the Lead acid battery. The results show the varied effect of electrolyte additives derived from natural plant extracts, on electrochemical performance of the Lead-Acid Battery

5.2 Recommendations

1. Additional experiment runs should be done to understand battery discharge capacity performance for additive volume and concentration determined as optimum by the numerical optimization procedure.
2. Investigate the effect of natural plant extract additive on other important battery parameters such as cycle life of the Battery and other common mechanisms of failure such as corrosion of plates, positive-plate expansion, water loss and acid Stratification.
3. Surface characterization and analyses should be performed to determine the microstructure and morphology of the plant extracts, particle size and distribution and physical adsorption to/on active materials.

4. Extracting the phytochemicals using other solvents should be performed to assess effect of different yields of total phenolic (tannins) and total glycosidic compound contents on battery capacity.
5. Plant extracts should be incorporated in lead-acid battery technology as alternative electrolytes to improve the battery discharge capacity whilst minimizing usage of chemical based conventional electrolytes and advancing the push towards truly sustainable storage.

REFERENCES

Abd Aziz, N. A., Hasham, R., Sarmidi, M. R., Suhaimi, S. H., & Idris, M. K. H. (2021). A review on extraction techniques and therapeutic value of polar bioactives from Asian medicinal herbs: Case study on Orthosiphon aristatus, Eurycoma longifolia and Andrographis paniculata. *Saudi Pharmaceutical Journal*, *29*(2), 143–165. https://doi.org/10.1016/j.jsps.2020.12.016

Abubakar, A. R., & Haque, M. (2020). Preparation of Medicinal Plants: Basic Extraction and Fractionation Procedures for Experimental Purposes. *Journal of Pharmacy & Bioallied Sciences*, *12*(1), 1–10. https://doi.org/10.4103/jpbs.JPBS_175_19

Ajayi, S. O., Ademosun, T. O., Okoro, E. R., Ajanaku, C. O., Mordi, R. C., & Ajanaku, K. O. (2019). Corrosion Inhibitory properties of *Bidens Pilosa* Plant Extract on Mild Steel in Acidic Media. *Journal of Physics: Conference Series*, *1378*, 042005. https://doi.org/10.1088/1742-6596/1378/4/042005

Al Hadi, A. Muh. R., Ekaputri, C., & Reza, M. (2019). Estimating the state of charge on lead acid battery using the open circuit voltage method. *Journal of Physics: Conference Series*, *1367*(1), 012077. https://doi.org/10.1088/1742-6596/1367/1/012077

Al-Hashimi, A. G. (2012). *Antioxidant and antibacterial activities of Hibiscus Sabdariffa L. extracts*. 6.

Armand, M., Grugeon, S., Vezin, H., Laruelle, S., Ribière, P., Poizot, P., & Tarascon, J.-M. (2009). Conjugated dicarboxylate anodes for Li-ion batteries. *Nature Materials*, *8*(2), 120–125. https://doi.org/10.1038/nmat2372

Armand, M., & Tarascon, J.-M. (2008). Building better batteries. *Nature*, *451*(7179), 652–657. https://doi.org/10.1038/451652a

Asian Development Bank. (2018). *Handbook on Battery Energy Storage System* (0 ed.). Asian Development Bank. https://doi.org/10.22617/TCS189791-2

Auwal, M. S., Saka, S., Mairiga, I. A., Sanda, K. A., Shuaibu, A., & Ibrahim, A. (2014). Preliminary phytochemical and elemental analysis of aqueous and fractionated pod extracts of Acacia nilotica (Thorn mimosa). *Veterinary Research Forum : An International Quarterly Journal*, *5*(2), 95–100.

Bartolome, A. P., Villaseñor, I. M., & Yang, W.-C. (2013). *Bidens Pilosa* L. (Asteraceae): Botanical Properties, Traditional Uses, Phytochemistry, and Pharmacology. *Evidence-Based Complementary and Alternative Medicine*, *2013*, 1–51. https://doi.org/10.1155/2013/340215

Bhattacharya, A., & Basumallick, I. N. (2003). Effect of mixed additives on lead–acid battery electrolyte. *Journal of Power Sources*, *113*(2), 382–387. https://doi.org/10.1016/S0378-7753(02)00552-9

Boden, D. P. (2004). Comparison of methods for adding expander to lead-acid battery plates—Advantages and disadvantages. *Journal of Power Sources*, *133*(1), 47–51. https://doi.org/10.1016/j.jpowsour.2003.12.006

BU-201: How does the Lead Acid Battery Work? (2010, September 26). Battery University. https://batteryuniversity.com/article/bu-201-how-does-the-lead-acid-battery-work

Catherino, H. A., Feres, F. F., & Trinidad, F. (2004). Sulfation in lead–acid batteries. *Journal of Power Sources*, *129*(1), 113–120. https://doi.org/10.1016/j.jpowsour.2003.11.003

Chalasani, S. (1998). *Water loss in valve regulated batteries*. 79–84. https://doi.org/10.1109/INTLEC.1998.793481

Chen, Z., Li, J., Yu, J., Wu, L., Zhou, S., Rao, Y., & Cao, J. (2022). The critical role of aluminum sulfate as electrolyte additive on the electrochemical performance of lead-acid battery. *Electrochimica Acta*, *407*, 139877. https://doi.org/10.1016/j.electacta.2022.139877

Chiang, L.-C., Chang, J.-S., Chen, C.-C., Ng, L.-T., & Lin, C.-C. (2003). Anti-Herpes simplex virus activity of *Bidens Pilosa* and Houttuynia cordata. *The American Journal of Chinese Medicine*, *31*(3), 355–362. https://doi.org/10.1142/S0192415X03001090

Deepti, D. J., & Ramanarayanan, V. (2006). State of charge of lead acid battery. *2006 India International Conference on Power Electronics*, 89–93. https://doi.org/10.1109/IICPE.2006.4685347

Deng, Q., Pei, J., Fan, C., Ma, J., Cao, B., Li, C., Jin, Y., Wang, L., & Li, J. (2017). Potassium salts of para-aromatic dicarboxylates as the highly efficient organic anodes for low-cost K-ion batteries. *Nano Energy*, *33*, 350–355. https://doi.org/10.1016/j.nanoen.2017.01.016

Denholm, P., Ela, E., Kirby, B., & Milligan, M. (2010). The Role of Energy Storage with Renewable Electricity Generation. *Technical Report*, 61.

Dietz, H., Dittmar, L., Ohms, D., Radwan, M., & Wiesener, K. (1992). Noble metal-free catalysts for the hydrogen/oxygen recombination in sealed lead/acid batteries using immobilized electrolytes. *Journal of Power Sources*, *40*(1), 175–186. https://doi.org/10.1016/0378-7753(92)80050-L

Eftekhari, A., & Kim, D.-W. (2017). Cathode materials for lithium–sulfur batteries: A practical perspective. *Journal of Materials Chemistry A*, *5*(34), 17734–17776. https://doi.org/10.1039/C7TA00799J

El-Rahman, H. A. A., Salih, S. A., & Mokhtar, A. A. (2011). *Role of phosphoric acid on the corrosion performance of Pb-1.7%Sb grid of lead-acid batteries*. 8.

Exide Industries. (2022). *Battery Maintenance Tips from Exide Industries*.. https://www.exideindustries.com/products/industrial-batteries/battery-tips.aspx

Ezeonwumelu, J., Julius, A., Muhoho, C., Ajayi, A., Oyewale, A., Tanayen, J., Balogun, S., Ibrahim, A., Adzu, B., Adiukwu, P., Oloro, J., Kiplagat, D., Goji, T., Okoruwa, G., Onchweri, A., & Reddy, M. (2011). Biochemical and Histological Studies of Aqueous Extract of *Bidens Pilosa* Leaves from Ugandan Rift Valley in Rats. *British Journal of Pharmacology and Toxicology*, *2*, 302–309.

Fraga-Corral, M., García-Oliveira, P., Pereira, A. G., Lourenço-Lopes, C., Jimenez-Lopez, C., Prieto, M. A., & Simal-Gandara, J. (2020). Technological Application of Tannin-Based Extracts. *Molecules*, *25*(3), 614. https://doi.org/10.3390/molecules25030614

Garche, J., Döring, H., & Wiesener, K. (1991). Influence of phosphoric acid on both the electrochemistry and the operating behaviour of the lead/acid system. *Journal of Power Sources*, *33*(1), 213–220. https://doi.org/10.1016/0378-7753(91)85060-A

Ghufron, M., Istiroyah, Perwita, C. A., Masruroh, Khairati, N., Ramadhan, F. R., Setiawan, Y. E., & Pranata, K. B. (2020). Influence of electrolyte concentration on static and dynamic Lead-Acid battery. *Journal of Physics: Conference Series*, *1595*, 012012. https://doi.org/10.1088/1742-6596/1595/1/012012

Goodenough, J. B., Abruna, H. D., & Buchanan, M. V. (2007). *Basic Research Needs for Electrical Energy Storage. Report of the Basic Energy Sciences Workshop on Electrical Energy Storage, April 2-4, 2007* (935429; p. 935429). https://doi.org/10.2172/935429

Graham, N., Gang, F., Fowler, G., & Watts, M. (2008). Characterisation and coagulation performance of a tannin-based cationic polymer: A preliminary assessment. *Colloids and Surfaces A: Physicochemical and Engineering Aspects*, *327*(1), 9–16. https://doi.org/10.1016/j.colsurfa.2008.05.045

H. Hamed, H., H. Zainulabdeen, I., Sh. Raheem, S., & E. Mohammed, A. (2018). A Comparison Study of Performance Efficiency of Lead-Acid Batteries Available in the Iraqi Markets. *International Journal of Engineering & Technology*, *7*(4.37), 150. https://doi.org/10.14419/ijet.v7i4.37.24091

Hammerstone, J. F., Lazarus, S. A., & Schmitz, H. H. (2000). Procyanidin Content and Variation in Some Commonly Consumed Foods. *The Journal of Nutrition*, *130*(8), 2086S-2092S. https://doi.org/10.1093/jn/130.8.2086S

Hong, J., Lee, M., Lee, B., Seo, D.-H., Park, C. B., & Kang, K. (2014). Biologically inspired pteridine redox centres for rechargeable batteries. *Nature Communications*, *5*(1), 5335. https://doi.org/10.1038/ncomms6335

IEEE, S. B. C. (2020). *IEEE Recommended Practice for Maintenance, Testing, and Replacement of Vented Lead-Acid Batteries for Stationary Applications*. IEEE. https://doi.org/10.1109/IEEESTD.2021.9373055

IRENA. (2015). *Battery Storage for Renewables: Market Status and Technology Outlook*. https://www.irena.org/publications/2015/Jan/Battery-Storage-for-Renewables-Market-Status-and-Technology-Outlook

Kareru, P. G., Keriko, J. M., Gachanja, A. N., & Kenji, G. M. (2007). Direct Detection of Triterpenoid Saponins in Medicinal Plants. *African Journal of Traditional, Complementary, and Alternative Medicines*, *5*(1), 56–60.

Karimi, M. A., Karami, H., & Mahdipour, M. (2006). Sodium sulfate as an efficient additive of negative paste for lead-acid batteries. *Journal of Power Sources*, *160*(2), 1414–1419. https://doi.org/10.1016/j.jpowsour.2006.03.036

Kimura, T., Ishiguro, A., Andou, Y., & Fujita, K. (2000). Effect of electrochemically oxidized carbon colloid on lead acid batteries. *Journal of Power Sources*, *85*(1), 149–156. https://doi.org/10.1016/S0378-7753(99)00394-8

Kitaronka, Sefu. (2022). *Lead-Acid Battery*. 768887 Bytes. https://doi.org/10.6084/M9.FIGSHARE.19115057

Kore, K. B., Tandale, P. U., Rondiya, S. R., Jathar, S. B., Bade, B. R., Nasane, M. P., Barma, S. V., Nilegave, D. S., Kurhe, N. V., Jadkar, S. R., & Funde, A. M. (2021). *Charge—Discharge cycle performance of lead acid battery for energy storage application*. 040002. https://doi.org/10.1063/5.0043346

Kregiel, D., Berlowska, J., Witonska, I., Antolak, H., Proestos, C., Babic, M., & Zhang, L. B. and B. (2017). Saponin-Based, Biological-Active Surfactants from Plants. In *Application and Characterization of Surfactants*. IntechOpen. https://doi.org/10.5772/68062

Kurzweil, P. (2010). Gaston Planté and his invention of the lead-acid battery-The genesis of the first practical rechargeable battery. *Journal of Power Sources*, *195*, 4424–4434. https://doi.org/10.1016/j.jpowsour.2009.12.126

Leahy, M. J., Connolly, D., & Buckley, D. N. (2010). Wind energy storage technologies. In *WIT Transactions on State of the Art in Science and Engineering* (1st ed., Vol. 1, pp. 661–714). WIT Press. https://doi.org/10.2495/978-1-84564-205-1/21

Lecce, D. D., Verrelli, R., & Hassoun, J. (2017). Lithium-ion batteries for sustainable energy storage: Recent advances towards new cell configurations. *Green Chemistry*, *19*(15), 3442–3467. https://doi.org/10.1039/C7GC01328K

Lee, B., Ko, Y., Kwon, G., Lee, S., Ku, K., Kim, J., & Kang, K. (2018). Exploiting Biological Systems: Toward Eco-Friendly and High-Efficiency Rechargeable Batteries. *Joule*, *2*(1), 61–75. https://doi.org/10.1016/j.joule.2017.10.013

Lee, J., & Park, M. J. (2017). Tattooing Dye as a Green Electrode Material for Lithium Batteries. *Advanced Energy Materials*, *7*(12), 1602279. https://doi.org/10.1002/aenm.201602279

Liedel, C. (2020). Sustainable Battery Materials from Biomass. *Chemsuschem*, *13*(9), 2110–2141. https://doi.org/10.1002/cssc.201903577

Linden, D., Beard, K. W., & Reddy, T. B. (Eds.). (2019). *Linden's handbook of batteries* (Fifth edition). McGraw-Hill.

Linden, D., & Reddy, T. B. (Eds.). (2002). *Handbook of batteries* (3rd ed). McGraw-Hill.

Liu, S., Sun, Y., Li, J., Dong, J., & Bian, Q. (2017). Preparation of Herbal Medicine: Er-Xian Decoction and Er-Xian-containing Serum for In Vivo and In Vitro Experiments. *Journal of Visualized Experiments*, *123*, 55654. https://doi.org/10.3791/55654

Mauger, A., & Julien, C. M. (2017). Critical review on lithium-ion batteries: Are they safe? Sustainable? *Ionics*, *23*(8), 1933–1947. https://doi.org/10.1007/s11581-017-2177-8

Meethale Kunnambath, P., & Thirumalaisamy, S. (2015). Characterization and Utilization of Tannin Extract for the Selective Adsorption of Ni (II) Ions from Water. *Journal of Chemistry*, *2015*, e498359. https://doi.org/10.1155/2015/498359

Megateli, R. M., Idir, G., & Arab, A. H. (2015). Study of the variation of the specific gravity of the electrolyte during charge/discharge cycling of a lead acid battery. *2015 3rd International Conference on Control, Engineering & Information Technology (CEIT)*, 1–4. https://doi.org/10.1109/CEIT.2015.7232980

Meissner, E. (1997). Phosphoric acid as an electrolyte additive for lead/acid batteries in electric-vehicle applications. *Journal of Power Sources*, *67*(1), 135–150. https://doi.org/10.1016/S0378-7753(97)02506-8

Miroshnikov, M., Kato, K., Babu, G., Thangavel, N. K., Mahankali, K., Hohenstein, E., Wang, H., Satapathy, S., Divya, K. P., Asare, H., Ajayan, P. M., Arava, L. M. R., & John, G. (2019). Made From Henna! A Fast-Charging, High-Capacity, and Recyclable Tetrakislawsone Cathode Material for Lithium Ion Batteries. *ACS Sustainable Chemistry & Engineering*, *7*(16), 13836–13844. https://doi.org/10.1021/acssuschemeng.9b01800

MIT, E. V. T. (2008). *A Guide to Understanding Battery Specifications*. 3.

Mugford, S. T., & Osbourn, A. (2012). Saponin Synthesis and Function. In T. J. Bach & M. Rohmer (Eds.), *Isoprenoid Synthesis in Plants and Microorganisms* (pp. 405–424). Springer New York. https://doi.org/10.1007/978-1-4614-4063-5_28

Mukhopadhyay, A., Hamel, J., Katahira, R., & Zhu, H. (2018). Metal-Free Aqueous Flow Battery with Novel Ultrafiltered Lignin as Electrolyte. *ACS Sustainable Chemistry & Engineering*, *6*(4), 5394–5400. https://doi.org/10.1021/acssuschemeng.8b00221

Musei, N. N., Onu, C. E., Ihuaku, K. I., & Igbokwe, P. K. (2021). Effects of Lithium Sulfate and Zinc Sulfate Additives on the Cycle Life and Efficiency of Lead Acid Batteries. *ACS Omega*. https://doi.org/10.1021/acsomega.0c05831

Oguzie, E. E. (2008). Evaluation of the inhibitive effect of some plant extracts on the acid corrosion of mild steel. *Corrosion Science*, *50*(11), 2993–2998. https://doi.org/10.1016/j.corsci.2008.08.004

Oliveira, F. Q., Andrade-Neto, V., Krettli, A. U., & Brandão, M. G. L. (2004). New evidences of antimalarial activity of *Bidens Pilosa* roots extract correlated with polyacetylene and flavonoids. *Journal of Ethnopharmacology*, *93*(1), 39–42. https://doi.org/10.1016/j.jep.2004.03.026

Oluyele, O., Falowo, D. E., Oladunmoye, M. K., Owoyemi, O. O., & Olotu, E. J. (2020). Effects of *Bidens Pilosa* (L) Extract on Haematological Parameters of Swiss Albino Rats Orogastrically Dosed with Escherichia coli O157:H7. *European Journal of Medical and Health Sciences*, *2*(2), Article 2. https://doi.org/10.24018/ejmed.2020.2.2.236

Onu, C. E., Musei, N. N., & Igbokwe, P. K. (2021). *Exploring the Additive Effects of Aluminium and Potassium Sulfates in Enhancing the Charge Cycle of Lead Acid Batteries*. 10.

Ordoñez, J., Gago, E. J., & Girard, A. (2016). Processes and technologies for the recycling and recovery of spent lithium-ion batteries. *Renewable and Sustainable Energy Reviews*, *60*, 195–205. https://doi.org/10.1016/j.rser.2015.12.363

Owoyemi, O., & Oladunmoye, M. K. (2017). *Phytochemical Screening and Antibacterial Activities of Bidens Pilosa L. and Tridax procumbens L. on Skin Pathogens*. *8*, 24–46.

Pacôme, O. A., Bernard, D. N., Sékou, D., Allico, D., David, N. J., Mongomaké, K., & Hilaire, K. T. (2014). *Phytochemical and Antioxidant Activity of Roselle (Hibiscus Sabdariffa L*. 13.

Paglietti, A. (2016). Electrolyte Additive Concentration for Maximum Energy Storage in Lead-Acid Batteries. *Batteries*, *2*(4), Article 4. https://doi.org/10.3390/batteries2040036

Pavlov, D. (2011). *Lead-Acid Batteries: Science and Technology*. Elsevier.

Pavlov, D. (2017a). Additives to the Pastes for Positive and Negative Battery Plates. In *Lead-Acid Batteries: Science and Technology* (pp. 335–379). Elsevier. https://doi.org/10.1016/B978-0-444-59552-2.00007-9

Pavlov, D. (2017b). Fundamentals of Lead–Acid Batteries. In *Lead-Acid Batteries: Science and Technology* (pp. 33–129). Elsevier. https://doi.org/10.1016/B978-0-444-59552-2.00002-X

Pavlov, D. (2017c). H 2 SO 4 Electrolyte—An Active Material in the Lead–Acid Cell. In *Lead-Acid Batteries: Science and Technology* (pp. 133–167). Elsevier. https://doi.org/10.1016/B978-0-444-59552-2.00003-1

Pavlov, D., Naidenov, V., & Ruevski, S. (2006). Influence of H2SO4 concentration on lead-acid battery performance. *Journal of Power Sources*, *161*(1), 658–665. https://doi.org/10.1016/j.jpowsour.2006.03.081

Pavlov, D., Petkova, G., & Rogachev, T. (2008). Influence of H2SO4 concentration on the performance of lead-acid battery negative plates. *Journal of Power Sources*, *175*(1), 586–594. https://doi.org/10.1016/j.jpowsour.2007.09.015

Perry, R. H., & Green, D. W. (Eds.). (2008). *Perry's chemical engineers' handbook* (8th ed). McGraw-Hill.

Petkova, G., Nikolov, P., & Pavlov, D. (2006). Influence of polymer additive on the performance of lead-acid battery negative plates. *Journal of Power Sources*, *158*(2), 841–845. https://doi.org/10.1016/j.jpowsour.2005.11.033

Posada, J. O. G., Rennie, A. J. R., Villar, S. P., Martins, V. L., Marinaccio, J., Barnes, A., Glover, C. F., Worsley, D. A., & Hall, P. J. (2017). Aqueous batteries as grid scale energy storage solutions. *Renewable and Sustainable Energy Reviews*, *68*, 1174–1182. https://doi.org/10.1016/j.rser.2016.02.024

Rand, D. A. J., & Moseley, P. T. (2015). Energy Storage with Lead–Acid Batteries. In *Electrochemical Energy Storage for Renewable Sources and Grid Balancing* (pp. 201–222). Elsevier. https://doi.org/10.1016/B978-0-444-62616-5.00013-9

Redl, K., Breu, W., Davis, B., & Bauer, R. (1994). Anti-inflammatory active polyacetylenes from Bidens campylotheca. *Planta Medica*, *60*(1), 58–62. https://doi.org/10.1055/s-2006-959409

Riaz, G., & Chopra, R. (2018). A review on phytochemistry and therapeutic uses of *Hibiscus Sabdariffa* L. *Biomedicine & Pharmacotherapy*, *102*, 575–586. https://doi.org/10.1016/j.biopha.2018.03.023

Sadhukhan, B., Mondal, N., & Chattoraj, S. (2016). Optimisation using central composite design (CCD) and the desirability function for sorption of methylene blue from aqueous solution onto Lemna major. *Karbala International Journal of Modern Science*, *2*. https://doi.org/10.1016/j.kijoms.2016.03.005

Sauer, D. U. (2009). BATTERIES | Charge–Discharge Curves. In *Encyclopedia of Electrochemical Power Sources* (pp. 443–451). Elsevier. https://doi.org/10.1016/B978-044452745-5.00052-6

Shaikh, J. R., & Patil, M. (2020). Qualitative tests for preliminary phytochemical screening: An overview. *International Journal of Chemical Studies*, *8*(2), 603–608. https://doi.org/10.22271/chemi.2020.v8.i2i.8834

Silva, F. L., Fischer, D. C. H., Tavares, J. F., Silva, M. S., de Athayde-Filho, P. F., & Barbosa-Filho, J. M. (2011). Compilation of secondary metabolites from *Bidens Pilosa* L. *Molecules (Basel, Switzerland)*, *16*(2), 1070–1102. https://doi.org/10.3390/molecules16021070

Son, E. J., Kim, J. H., Kim, K., & Park, C. B. (2016). Quinone and its derivatives for energy harvesting and storage materials. *Journal of Materials Chemistry A*, *4*(29), 11179–11202. https://doi.org/10.1039/C6TA03123D

Stanimirova, R., Marinova, K., Tcholakova, S., Denkov, N. D., Stoyanov, S., & Pelan, E. (2011). Surface Rheology of Saponin Adsorption Layers. *Langmuir*, *27*(20), 12486–12498. https://doi.org/10.1021/la202860u

Stéphane, F. F. Y., Jules, B. K. J., Batiha, G. E.-S., Ali, I., & Bruno, L. N. (2021). Extraction of Bioactive Compounds from Medicinal Plants and Herbs. In *Natural Medicinal Plants*. IntechOpen. https://doi.org/10.5772/intechopen.98602

Tan, S. L. J., & Webster, R. D. (2012). Electrochemically Induced Chemically Reversible Proton-Coupled Electron Transfer Reactions of Riboflavin (Vitamin B2). *Journal of the American Chemical Society*, *134*(13), 5954–5964. https://doi.org/10.1021/ja300191u

Tiwari, P., Kumar, B., Kaur, M., Kaur, G., & Kaur, H. (2011). *Phytochemical-screening-and-extraction-a-review.pdf*. Internationale Pharmaceutica Sciencia.

Torcheux, L., & Lailler, P. (2001). A new electrolyte formulation for low cost cycling lead acid batteries. *Journal of Power Sources*, *95*(1), 248–254. https://doi.org/10.1016/S0378-7753(00)00621-2

Vetter, M., & Rohr, L. (2014). Lithium-Ion Batteries for Storage of Renewable Energies and Electric Grid Backup. In *Lithium-Ion Batteries* (pp. 293–309). Elsevier. https://doi.org/10.1016/B978-0-444-59513-3.00013-3

Waag, W., & Sauer, D. U. (2009). Secondary Batteries – Lead– Acid Systems | State-of-Charge/Health. In *Encyclopedia of Electrochemical Power Sources* (pp. 793–804). Elsevier. https://doi.org/10.1016/B978-044452745-5.00149-0

Wagner, R., & Sauer, D. U. (2001). Charge strategies for valve-regulated lead/acid batteries in solar power applications. *Journal of Power Sources*, *95*(1), 141–152. https://doi.org/10.1016/S0378-7753(00)00614-5

Wang, H., Li, F., Zhu, B., Guo, L., Yang, Y., Hao, R., Wang, H., Liu, Y., Wang, W., Guo, X., & Chen, X. (2016). Flexible Integrated Electrical Cables Based on Biocomposites for Synchronous Energy Transmission and Storage. *Advanced Functional Materials*, *26*(20), 3472–3479. https://doi.org/10.1002/adfm.201600014

Wang, H., Yang, Y., & Guo, L. (2017). Renewable-Biomolecule-Based Electrochemical Energy-Storage Materials. *Advanced Energy Materials*, *7*(23), 1700663. https://doi.org/10.1002/aenm.201700663

Wang, S., Fan, Y., Stroe, D.-I., Fernandez, C., Yu, C., Cao, W., & Chen, Z. (2021). Chapter 1—Lithium-ion battery characteristics and applications. In S. Wang, Y. Fan, D.-I. Stroe, C. Fernandez, C. Yu, W. Cao, & Z. Chen (Eds.), *Battery System Modeling* (pp. 1–46). Elsevier. https://doi.org/10.1016/B978-0-323-90472-8.00003-2

Wu, Z., Liu, Y., Deng, C., Zhao, H., Zhao, R., & Chen, H. (2020). The critical role of boric acid as electrolyte additive on the electrochemical performance of lead-acid battery. *Journal of Energy Storage*, *27*, 101076. https://doi.org/10.1016/j.est.2019.101076

Xuan, T. D., & Khanh, T. D. (2016). Chemistry and pharmacology of *Bidens Pilosa*: An overview. *Journal of Pharmaceutical Investigation*, *46*(2), 91–132. https://doi.org/10.1007/s40005-016-0231-6

Yin, C.-Y. (2010). Emerging usage of plant-based coagulants for water and wastewater treatment. *Process Biochemistry*, *45*(9), 1437–1444. https://doi.org/10.1016/j.procbio.2010.05.030

Yu, P., & O'Keefe, T. J. (2002). Evaluation of Lead Anode Reactions in Acid Sulfate Electrolytes: II. Manganese Reactions. *Journal of The Electrochemical Society*, *149*(5), A558. https://doi.org/10.1149/1.1464882

Zhang, B., Zhong, J., Li, W., Dai, Z., Zhang, B., & Cheng, Z. (2010). Transformation of inert PbSO4 deposit on the negative electrode of a lead-acid battery into its active state. *Journal of Power Sources*, *195*(13), 4338–4343. https://doi.org/10.1016/j.jpowsour.2010.01.038

APPENDICES

Appendix A: Calyces of *Hibiscus Sabdariffa*

Appendix B: Sample of Bidens Pilosa

Appendix C: Decoction process of Roselle

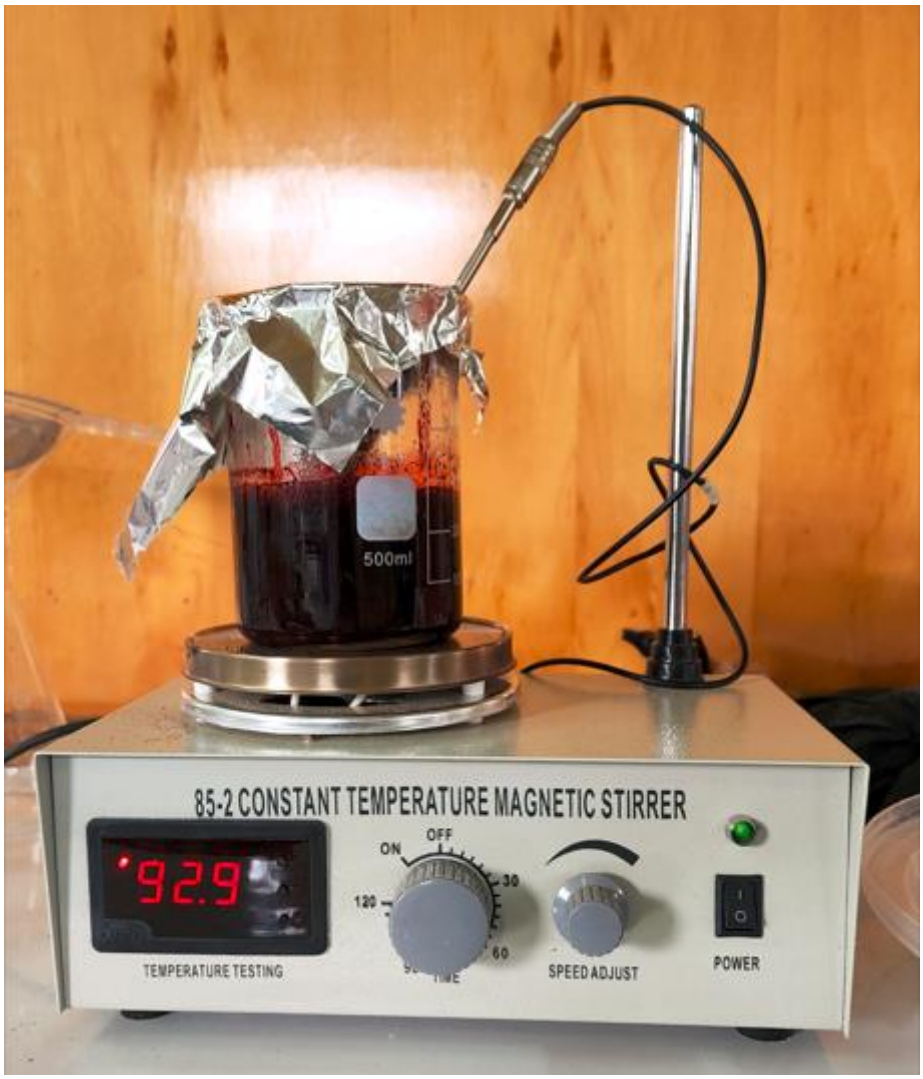

Appendix D: Design table (Randomized)

Factor	Name	Units	Minimum	Maximum	Coded Low	Coded High
A	Volume	(ml)	0.01	2	-1 ↔ 0.30	+1 ↔ 1.71
b	Conc	(g/ml) %	10	50	-1 ↔ 15.86	+1 ↔ 44.14

Std	Group	Run	Volume	Concentration
18	1	1	0	0
17	1	2	0	0
19	1	3	0	0
2	2	4	1	-1
1	2	5	-1	-1
8	3	6	0	-1.41421356
9	3	7	0	-1.41421356
4	4	8	1	1
3	4	9	-1	1
6	5	10	0	0
7	5	11	0	0
5	5	12	0	0
12	6	13	-1.414214	0
13	6	14	1.4142136	0
10	7	15	0	1.414213562
11	7	16	0	1.414213562
15	8	17	0	0
16	8	18	0	0
14	8	19	0	0

Appendix E: Factor settings (Randomized)

Std	Group	Run	Volume (ml)	Conc (g/ml) %
18	1	1	1.005	30
17	1	2	1.005	30
19	1	3	1.005	30
2	2	4	1.70857	15.8579
1	2	5	0.301429	15.8579
8	3	6	1.005	10
9	3	7	1.005	10
4	4	8	1.70857	44.1421
3	4	9	0.301429	44.1421
6	5	10	1.005	30
7	5	11	1.005	30
5	5	12	1.005	30
12	6	13	0.01	30
13	6	14	2	30
10	7	15	1.005	50
11	7	16	1.005	50
15	8	17	1.005	30
16	8	18	1.005	30
14	8	19	1.005	30

Appendix F: (a) charge cycle setup (b) discharge cycle setup

(a)

(b)

Appendix G: Specific gravity measurement using a float hydrometer.

Appendix H: Charge cycle optimum solutions for blackjack extract

Number	volume	concentration	Charge Duration	Desirability
5	0.301	44.142	3.617	1
50	0.344	44.04	3.775	1
17	0.381	44.022	3.886	1
42	0.51	43.732	4.36	1
71	0.425	42.516	4.575	1
84	0.488	42.823	4.639	1
55	0.471	42.681	4.644	1
31	0.368	41.392	4.835	1
91	0.513	42.343	4.89	1
51	0.398	41.375	4.925	1
89	0.308	40.674	4.934	1
26	0.388	41.233	4.95	1
52	0.406	41.293	4.979	1
72	0.697	43.016	5.158	1
22	0.669	42.681	5.205	1
74	0.724	43.025	5.23	1
100	0.654	42.493	5.232	1
59	0.4	40.524	5.249	1
73	0.723	42.896	5.276	1
85	0.353	40.097	5.278	1
18	0.575	41.756	5.284	1
7	0.486	41.069	5.29	1
34	0.491	40.966	5.342	1
69	0.419	40.371	5.361	1
43	0.895	43.968	5.363	1
35	0.732	42.629	5.401	1
28	0.906	43.93	5.407	1
15	0.868	43.536	5.449	1
47	0.747	42.509	5.49	1
78	0.902	43.676	5.49	1
98	0.761	42.587	5.5	1
44	0.968	44.136	5.508	1
4	0.398	39.811	5.511	1
96	0.792	42.782	5.516	1
95	0.912	43.603	5.546	1
8	0.715	42.099	5.553	1
56	0.838	42.974	5.573	1
16	0.795	42.607	5.588	1
25	0.936	43.612	5.612	1
93	0.482	40.019	5.672	1
38	0.437	39.531	5.726	1
99	1.009	43.845	5.73	1
46	0.569	40.499	5.737	1
82	0.848	42.599	5.743	1

53	0.758	41.778	5.795	1
29	0.893	42.771	5.805	1
67	0.975	43.386	5.808	1
68	0.941	43.083	5.825	1
97	0.56	40.161	5.838	1
63	0.386	38.815	5.849	1
10	1.005	43.461	5.864	1
58	0.461	39.288	5.884	1
60	1.072	43.898	5.89	1
40	1.11	44.135	5.908	1
90	1.026	43.457	5.923	1
2	1.084	43.789	5.965	1
33	1.121	44.041	5.975	1
87	0.856	42.031	5.977	1
11	1.093	43.724	6.014	1
66	0.667	40.412	6.048	1
32	1.16	44.129	6.054	1
62	1.116	43.784	6.057	1
37	0.47	38.839	6.079	1
94	0.857	41.662	6.119	1
9	1.079	43.268	6.146	1
92	0.998	42.573	6.176	1
41	0.591	39.494	6.177	1
80	1.113	43.344	6.214	1
54	0.795	40.928	6.217	1
65	0.893	41.636	6.229	1
48	0.743	40.49	6.233	1
14	1.206	43.93	6.259	1
6	0.538	38.837	6.271	1
57	0.563	39.018	6.275	1
49	0.976	42.1	6.291	1
81	0.957	41.945	6.295	1
61	0.913	41.542	6.32	1
27	0.86	41.118	6.328	1
24	1.153	43.329	6.332	1
20	0.789	40.566	6.334	1
79	1.216	43.554	6.427	1
1	1.082	42.534	6.428	1
75	1.183	43.26	6.443	1
39	0.533	38.334	6.446	1
19	1.058	42.251	6.465	1
36	1.195	43.156	6.515	1
83	0.748	39.681	6.551	1
12	1.297	43.816	6.558	1
76	1.199	42.954	6.602	1
23	1.211	42.991	6.623	1
21	1.101	42.153	6.626	1
45	0.395	36.806	6.628	1

64	0.895	40.576	6.632	1
30	1.216	42.986	6.639	1
70	1.172	42.611	6.655	1
88	0.857	40.195	6.667	1
13	0.989	41.122	6.693	1
77	1.098	41.863	6.725	1
86	1.374	43.947	6.727	1
3	1.313	43.435	6.745	1

Appendix I: Discharge cycle optimum solutions for blackjack extract

Number	volume	concentration	Discharge Duration	Desirability
1	1.564	17.773	4.418	1
2	1.314	16.454	4.421	1
3	1.5	16.145	4.562	1
4	1.535	16.101	4.588	1
5	1.709	15.858	4.715	1
6	1.51	16.976	4.476	1
7	1.476	17.324	4.417	1
8	1.501	17.291	4.436	1
9	1.257	16.49	4.384	1
10	1.358	16.884	4.398	1
11	1.594	16.478	4.58	1
12	1.665	17.825	4.471	1
13	1.331	16.243	4.454	1
14	1.646	17.455	4.501	1
15	1.583	16.502	4.571	1
16	1.593	16.365	4.592	1
17	1.536	17.417	4.442	1
18	1.693	16.426	4.643	1
19	1.545	16.87	4.508	1
20	1.703	17.002	4.584	1
21	1.35	16.346	4.453	1
22	1.663	18.571	4.387	1
23	1.282	16.137	4.438	1
24	1.354	15.957	4.499	1
25	1.131	15.948	4.371	1
26	1.512	17.172	4.455	1
27	1.545	18.071	4.374	1
28	1.375	17.164	4.377	1
29	1.612	18.438	4.372	1
30	1.659	16.304	4.637	1
31	1.471	16.802	4.473	1
32	1.431	16.144	4.523	1
33	1.523	16.009	4.591	1
34	1.472	16.654	4.49	1
35	1.602	17.555	4.464	1
36	1.577	17.719	4.432	1
37	1.239	16.354	4.389	1
38	1.322	16.273	4.445	1
39	1.563	15.864	4.63	1
40	1.178	15.909	4.403	1
41	1.481	16.387	4.525	1
42	1.183	16.096	4.385	1
43	1.402	16.629	4.452	1
44	1.638	17.077	4.539	1
45	1.385	16.03	4.509	1
46	1.311	16.801	4.381	1
47	1.4	16.157	4.503	1

48	1.573	16.929	4.518	1
49	1.226	16.007	4.42	1
50	1.416	16.869	4.433	1
51	1.481	17.46	4.405	1
52	1.525	15.882	4.606	1
53	1.665	16.91	4.573	1
54	1.65	16.703	4.587	1
55	1.171	16.011	4.388	1
56	1.65	17.585	4.489	1
57	1.574	17.87	4.413	1
58	1.575	16.183	4.601	1
59	1.415	16.103	4.518	1
60	1.645	16.51	4.605	1
61	1.205	15.986	4.41	1
62	1.216	15.94	4.421	1
63	1.443	17.356	4.395	1
64	1.564	16.969	4.508	1
65	1.389	16.462	4.463	1
66	1.271	16.445	4.397	1
67	1.305	16.706	4.388	1
68	1.628	16.193	4.631	1
69	1.461	16.561	4.494	1
70	1.226	16.435	4.372	1
71	1.196	16.15	4.386	1
72	1.29	16.353	4.418	1
73	1.6	16.945	4.531	1
74	1.141	15.951	4.377	1
75	1.547	16.3	4.572	1
76	1.303	16.815	4.374	1
77	1.526	16.123	4.58	1
78	1.255	16.24	4.41	1
79	1.317	16.664	4.399	1
80	1.307	16.068	4.46	1
81	1.602	17.063	4.519	1
82	1.386	15.862	4.528	1
83	1.53	17.106	4.473	1
84	1.518	17.203	4.455	1
85	1.491	17.078	4.454	1
86	1.256	16.127	4.424	1
87	1.341	16.789	4.399	1
88	1.394	16.835	4.425	1
89	1.626	17.711	4.461	1
90	1.575	17.551	4.449	1
91	1.498	16.576	4.513	1
92	1.536	16.941	4.495	1
93	1.16	16.098	4.372	1
94	1.65	18.214	4.419	1

Appendix J: Charge cycle optimum solutions for Roselle extract

Number	volume	concentration	Charge Duration	Desirability
1	0.301	15.858	17.041	0.797
2	0.301	16.056	17.046	0.795
3	0.387	15.858	17.066	0.784

Appendix K: Discharge cycle optimum solutions for Roselle extract

Number	volume	concentration	Discharge Duration	Desirability
1	0.301	15.858	4.599	0.966
2	0.307	15.858	4.598	0.965
3	0.325	15.858	4.594	0.961
4	0.301	16.154	4.593	0.96
5	0.301	16.573	4.585	0.951
6	1.251	15.858	4.407	0.755

Appendix L: Plagiarism Similarity Index

OPTIMIZATION OF THE LEAD-ACID BATTERY DISCHARGE CAPACITY USING ALTERNATIVE ELECTROLYTES FROM NATURAL PLANT EXTRACTS.

by Vitumbiko Nundwe

Submission date: 09-Mar-2023 10:14AM (UTC+0100)
Submission ID: 2032875643
File name: Vitumbiko_Nundwe__MSc_Thesis_Correction_Final.docx (3.31M)
Word count: 21103
Character count: 119344

OPTIMIZATION OF THE LEAD-ACID BATTERY DISCHARGE CAPACITY USING ALTERNATIVE ELECTROLYTES FROM NATURAL PLANT EXTRACTS.

ORIGINALITY REPORT

17%	12%	12%	4%
SIMILARITY INDEX	INTERNET SOURCES	PUBLICATIONS	STUDENT PAPERS

PRIMARY SOURCES

1	cora.ucc.ie Internet Source	2%
2	Detchko Pavlov. "Fundamentals of Lead–Acid Batteries", Elsevier BV, 2017 Publication	1%
3	coek.info Internet Source	1%
4	ir.mu.ac.ke:8080 Internet Source	1%
5	www.researchgate.net Internet Source	1%
6	Zhixing Cao, Rui Chen, Libin Xu, Xinyi Zhou, Xiaoming Fu, Weimin Zhong, Ramon Grima. "Efficient and scalable prediction of spatio-temporal stochastic gene expression in cells and tissues using graph neural networks", Cold Spring Harbor Laboratory, 2023 Publication	1%